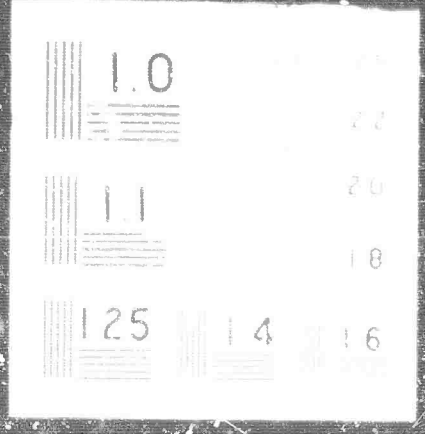

TI REPORT NO.
08-65-121

Final Technical Summary Report

For

New High Temperature Infrared Transmitting Glasses

1 May 1962 through 31 July 1965

Office of Naval Research Contract No. 3810(00)

in cooperation with
Advanced Research Projects Agency
Department of Defense

ARPA Order Number 269
Program Code 5730

30 September 1965

Prepared by

A. Ray Hilton
Texas Instruments Incorporated
13500 North Central Expressway
Dallas, Texas 75205

TI REPORT NO.
08-65-121

Final Technical Summary Report

For

New High Temperature Infrared Transmitting Glasses

1 May 1962 through 31 July 1965

Office of Naval Research Contract No. 3810(00)

in cooperation with
Advanced Research Projects Agency
Department of Defense

ARPA Order Number 269
Program Code 5730

30 September 1965

Prepared by

A. Ray Hilton
Texas Instruments Incorporated
13500 North Central Expressway
Dallas, Texas 75205

BLANK PAGE

FINAL TECHNICAL SUMMARY REPORT

FOR

NEW HIGH TEMPERATURE INFRARED TRANSMITTING GLASSES

TABLE OF CONTENTS

TABLE OF CONTENTS
(continued)

TABLE OF CONTENTS
(continued)

APPENDIXES

LIST OF FIGURES

LIST OF FIGURES
(continued)

LIST OF FIGURES
(continued)

LIST OF TABLES

LIST OF TABLES
(continued)

ABSTRACT

Results obtained in the qualitative evaluation of glasses from seven IVA-VA-VIA ternary systems as high temperature infrared window materials are given. Four-component glasses formed from two ternary systems were prepared and characterized. The pertinent physical properties of non-oxide chalcogenide glasses are summarized. Several specific glass compositions were fabricated in large pieces so that their optical and related physical properties could be accurately measured. The properties of a glass are determined by their constituent elements. The ratios between the constituent elements, and thus the location of the glass-forming region, are found to depend on the binary compounds which form between the constituent elements.

The physical and the chemical nature of non-oxide chalcogenide glasses were investigated using infrared spectroscopy, x-ray diffraction, and mass spectrometry as structural tools. It was found the materials were covalently bonded solids and their refractive indexes could be predicted using a molar refraction approach. The source of most unwanted absorption for wavelengths below 25 microns was attributed to the presence of trace amounts of metallic oxides. Infrared absorption and x-ray diffraction results indicate the group IVA elements silicon and germanium form zigzag chains with the chalcogens, while the group VA element arsenic tends to form pyramidal-type molecules. The chains lead to a stronger, harder glass than the pyramidal arrangements. In Si-As-Te and Ge-As-Te glasses, mass spectrometry results indicate the presence of free or loosely bonded arsenic, arsenic bonded to tellurium, and arsenic bonded to silicon and germanium.

A. Ray Hilton

A. RAY HILTON, Project Manager
Central Analytical Chemistry Facility

P. F. Kane.

P. F. KANE, Manager
Central Analytical Chemistry Facility

BLANK PAGE

FINAL TECHNICAL SUMMARY REPORT

FOR

NEW HIGH TEMPERATURE INFRARED TRANSMITTING GLASSES

Office of Naval Research Contract No. 3810(00)

in cooperation with Advanced Research Projects Agency

I. INTRODUCTION

The investigation of non-oxide chalcogenide glasses as infrared optical materials began in 1950 when R. Frerichs[1,2] rediscovered As_2S_3 glass. Since then, infrared transmitting glasses have been the subject of a number of investigations in this country,[3-7] in England,[8-11] and in Russia.[12-14] The investigation under way at Texas Instruments for more than three years has concentrated on ternary glass systems containing one component from the group IVA elements (Si or Ge), one from the group VA elements (P, As, or Sb), and a chalcogen (S, Se, or Te). Glasses from eight ternary elemental systems[15,16] have been evaluated. Many useful glass compositions were found, but none had the combination of excellent infrared transmission in the 8 to 14 micron region and a high softening point (~500°C), the ultimate goal of the program.

Glasses containing at least four constituent elements were studied in the second phase of the program. Compositions selected represented a blend of two ternary systems. The effects of a single constituent element on the physical properties of a glass were measured from glasses blended between two ternary systems differing by only one constituent element. It was found that the magnitude of the effect depended on how important the element was to the structure of the glass. Large pieces of the most promising optical materials were fabricated and their properties quantitatively measured. As a group, the materials were still physically weak and soft, with poor thermal characteristics.

Apparently, a change in approach was needed for further improvements. In the third and final phase of the program, the essentially experimental approach was abandoned for a more basic program aimed at developing an understanding of the strucutural nature of the non-oxide chalcogenide glasses.

Specifically, the molecular arrangements in glasses from the Si-As-Te and Ge-As-Te systems were studied from physical measurements based on infrared spectroscopy, x-ray diffraction, and mass spectrometry.

II. QUALITATIVE EVALUATION OF GLASSES FROM THE IVA-VA-VIA TERNARY SYSTEM

A. Experimental Procedure

1. Materials Preparation

A large number of samples must be prepared to determine the glass-forming composition region of a three-component system, and a standard method of preparation must be followed.

In this experimental program all samples were prepared from chemicals of at least reagent grade purity. The various compositions were weighed and sealed in quartz vials while under less than 1 micron pressure. Each vial was placed in a rocking furnace and slowly raised to a temperature of 1000 to 1100°C. The mixtures were left in the furnace as homogeneous melts and allowed to react and mix from 16 to 40 hours. Glasses were formed by quenching the samples to room temperature while in air. Usually a sample could be identified as glass or crystalline by visual examination, but x-ray diffraction was used if there was any doubt concerning a particular composition. Samples suitable for optical evaluation and softening point determination were cut from the glass pieces. The optical samples were polished to produce plane and parallel sides.

2. Softening Point

The standard ASTM method for determining softening points of oxide glasses was impractical for these materials. Instead, a simple apparatus such as the one shown in Figure 1, was used to measure a "relative softening point." The relative value was obtained when the sample in the chamber softened enough to move the quartz rod resting on the sample, which in turn produced a movement of the indicator. Glasses of known softening point were found to give "relative values" that were somewhat lower (as much as 100°C) than those obtained by the standard ASTM method. This "relative value" is a fairly accurate measure of the useful temperature of the glass.

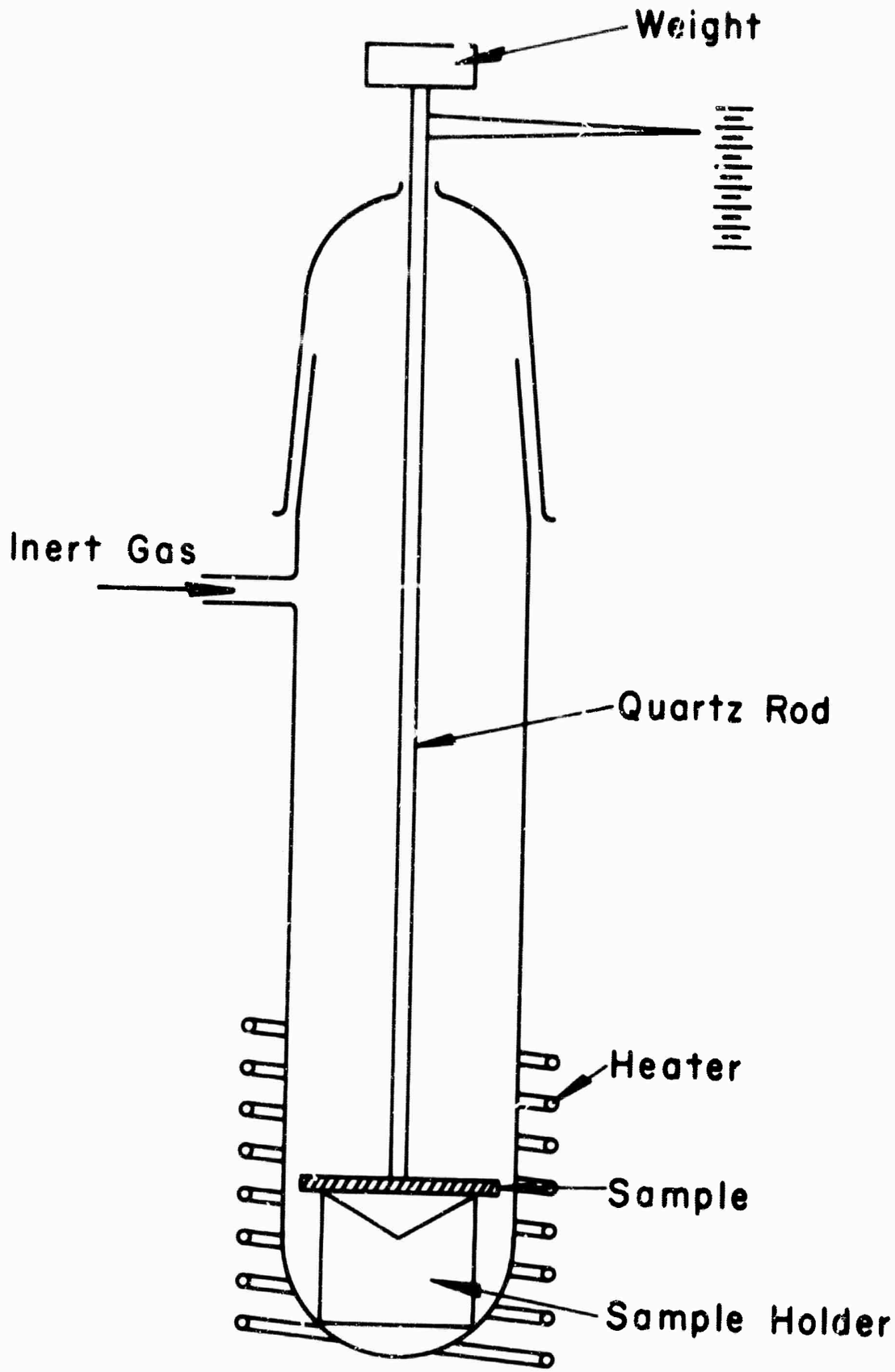

Figure 1 Softening Point Apparatus

3. Optical Properties

The infrared transmission (T) was usually measured from 2.5 to 25 microns wavelength. Samples were 1 to 3 mm thick. Reflectivity (R) was measured from samples cut from the rounded end of the glass piece to eliminate back reflections in the transparent region. A qualitative estimate of the refractive index (n) and the absorption coefficient (α) could be obtained by solving the simplified equation

$$T = (1-R)^2 e^{-\alpha x},$$

where x is the thickness in centimeters

and $$R \approx \frac{(n-1)^2}{(n+1)^2} .$$

Precise optical constants were obtained by using a precise measurement of refractive index, a measurement possible only when the material is very transparent to the infrared and can be fabricated in large prisms or optical wedges. The refractive index can then be measured accurately to four or five significant numbers using the external attachment designed and built for use with our infrared spectrophotometer. A schematic of the attachment is shown in Figure 2. The instrument acts as a monochromatic source of light, and the detection system of the instrument tells when the sample (in prism form) is rotated at the proper angle for the refracted ray to travel back through the slit system. The refractive index is calculated from the angle readings. Such measurements were carried out on a silicon prism and produced five-number agreement with the literature values.

Precise refractive index values as a function of wavelength can be used to calculate the reflectivity (at normal incidence) accurately. Measured transmission values obtained from samples cut from the prism were used to calculate the absorption coefficient from the more exact equation[17]

$$T = \frac{(1-R)^2 e^{-\alpha x}}{1-R^2 e^{-2\alpha x}} .$$

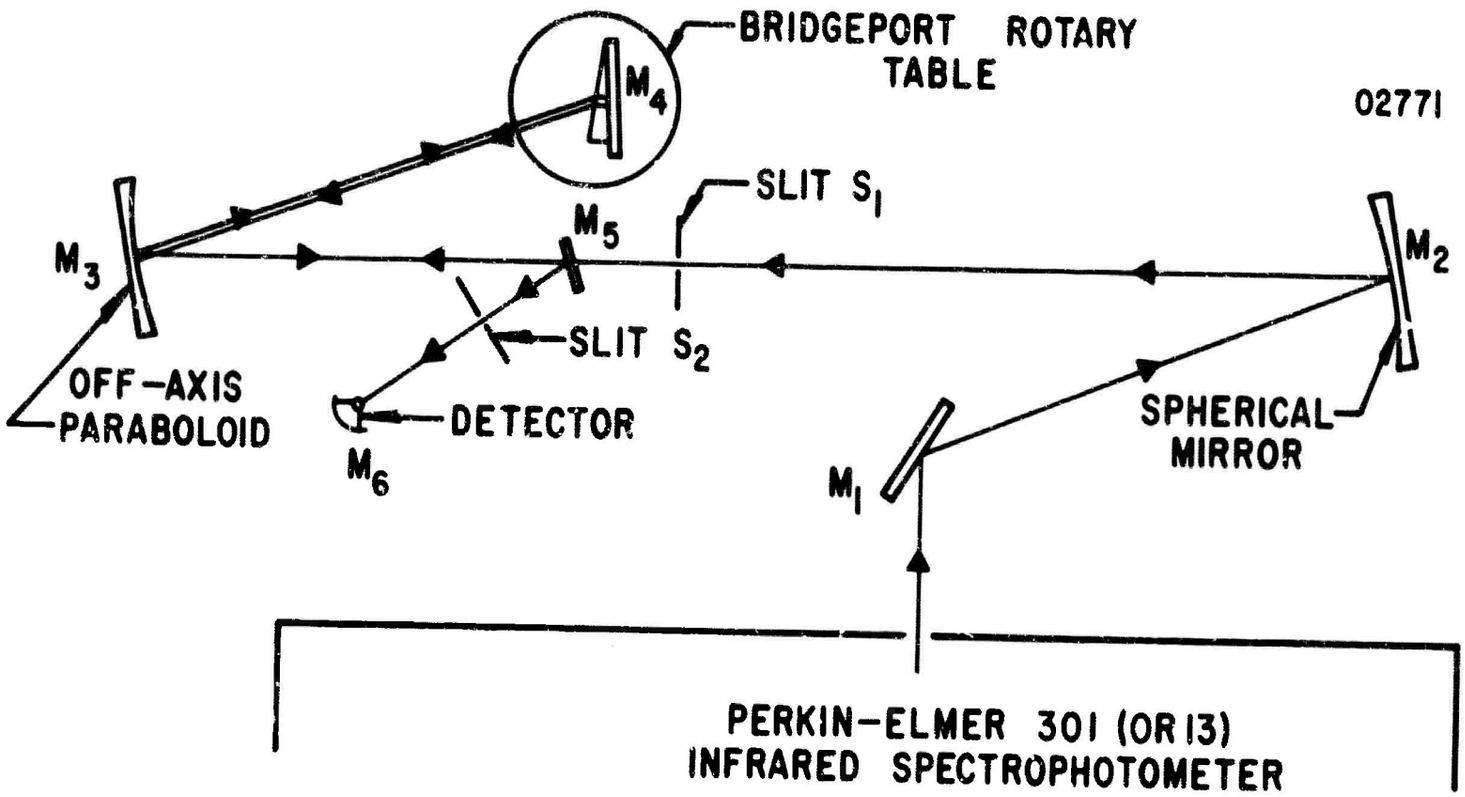

Figure 2 Apparatus for Determining Refractive Index of Infrared Glasses

The calculation was programmed and performed using a digital computer. The normal method of calculating optical constants using transmission measurements obtained from samples of varying thickness was not used because the samples were not homogeneous.

4. Related Properties

a. Hardness

Measurements were made using a Leitz microhardness tester. Values are recorded on the Knoop scale.

b. Thermal Coefficient of Expansion

Measurements were made using a Brinkman Dilatometer. Value are given in in./in.°C.

c. Resistivity and Dielectric Constant

Resistivity and dielectric constant were measured on several samples using a General Radio type 716C capacitance bridge. Aluminum electrodes were evaporated onto the glass surfaces. In some cases, gold or aluminum was evaporated onto the samples and only the resistivity measured using a Keithley 610A electrometer.

d. Physical Strength

The measured values of Young's modulus, shear modulus, and bulk modulus are strongly dependent on sample size and perfection. Suitable glass samples for these measurements were not available; accordingly, only the tensile strength measurement was attempted on a few samples, using a Tinius-Olsen tensile tester.

B. Results

1. Silicon-Antimony-Sulfur Glass System

The results obtained from 36 samples of varying composition are shown in Table I. Samples which formed glasses are marked with an asterisk. Softening points and comments concerning the nature of each sample are given. In the composition diagram in Figure 3 the glass-forming region of the Si-Sb-S system is outlined with solid lines. The dotted lines enclose a composition region in which a homogeneous glass is formed over an immiscible metallic phase. Emission spectroscopic analysis showed the homogeneous glass was silicon-rich; the metallic phase was antimony containing 1-10 percent silicon.

Attempts to form glasses in higher silicon percent regions were made using a Glo-bar rocking furnace capable of obtaining temperatures up to 1400°C. However, at the higher temperatures the reaction mixture reacted with the quartz, resulting in a blow-out of the vial and, of course, failure of the furnace.

TABLE I

All the glasses reacted readily with the atmosphere and gave off hydrogen sulfide. They varied in appearance from dark red to metallic, but when exposed to the atmosphere, all reacted with moisture and were gradually covered with a film. Only one composition showed any appreciable infrared transmission. The results indicate the Si-Sb-S system will produce no optical materials of practical importance.

2. Silicon-Antimony-Selenium Glass System

Results obtained from 42 samples of different composition are given in Table II. Samples that formed glasses are marked with an asterisk. The measured softening points ranged from a maximum of 490°C to a minimum of 163°C for 85 percent selenium glass.

Every sample was found to react somewhat with the atmosphere and give off hydrogen selenide. The degree of reactivity with the atomosphere for each sample is also noted in the table. Some samples were stable with respect to the

TABLE I

The Si-Sb-S System

Sample Number	Atom % Si	Sb	S	Softening Point (°C)	Remarks
10	43	15	42		Incomplete reaction
10A	43	15	42		Incomplete reaction
*11	20	20	60	225	Red, porous, 30-hour reaction, metallic phase present
*11A	20	20	60	150	Porous, 3-hour reaction
*11B	20	20	60	450	48-hour reaction, x-ray shot, IR transmission run
*11C	20	20	60	265	Metallic phase present
12	37	3	60		Exploded
12A	30	10	60		Exploded
*13	10	30	60	280	IR transmission run
*13A	15	35	50	425	Metallic phase
14	65	10	25		Slight reaction at 600°C
14A	40	10	50		Mixture very viscous at 1000°C, crystalline
*15	20	40	40	385	
15A	15	73	12		Crystalline metallic phase present, slight reaction at 600°C
16	23	31	46		Crystalline metallic phase
16A	30	20	50		Plastic phase formed over crystalline metallic phase
17	10	65	25		Metallic phase with soft yellow crystals
17A	10	10	80		Orange plastic phase
*19	15	15	70	415	
19A	30	15	55		Very slight reaction, very viscous
20	25	15	60		Yellow plastic phase with metallic phase
*20A	15	25	60	325	Metallic phase
*21	15	30	55	350	Metallic phase
21A	30	15	55		#19A was crushed and resealed, exploded
21B	30	15	55		Reacted at 1400°C, the quartz broke down and burst
*22	20	25	55	525	Quenched slowly, nonuniform, metallic phase
*22A	15	25	60	285	Quenched slowly, porous, uniform glass
*23	20	15	65	180	Turned orange in air
*23A	5	25	70	225	A lower crystalline phase
*24	15	20	65	250	
*42A	10	20	70	235	
*25	5	20	75	200	Excess sulfur present
*25A	10	15	75	255	Excess sulfur present
*26A	25	20	55	250	Nonuniform
27	25	25	50		Reacted at 1250°C, reacted with quartz tube, burst

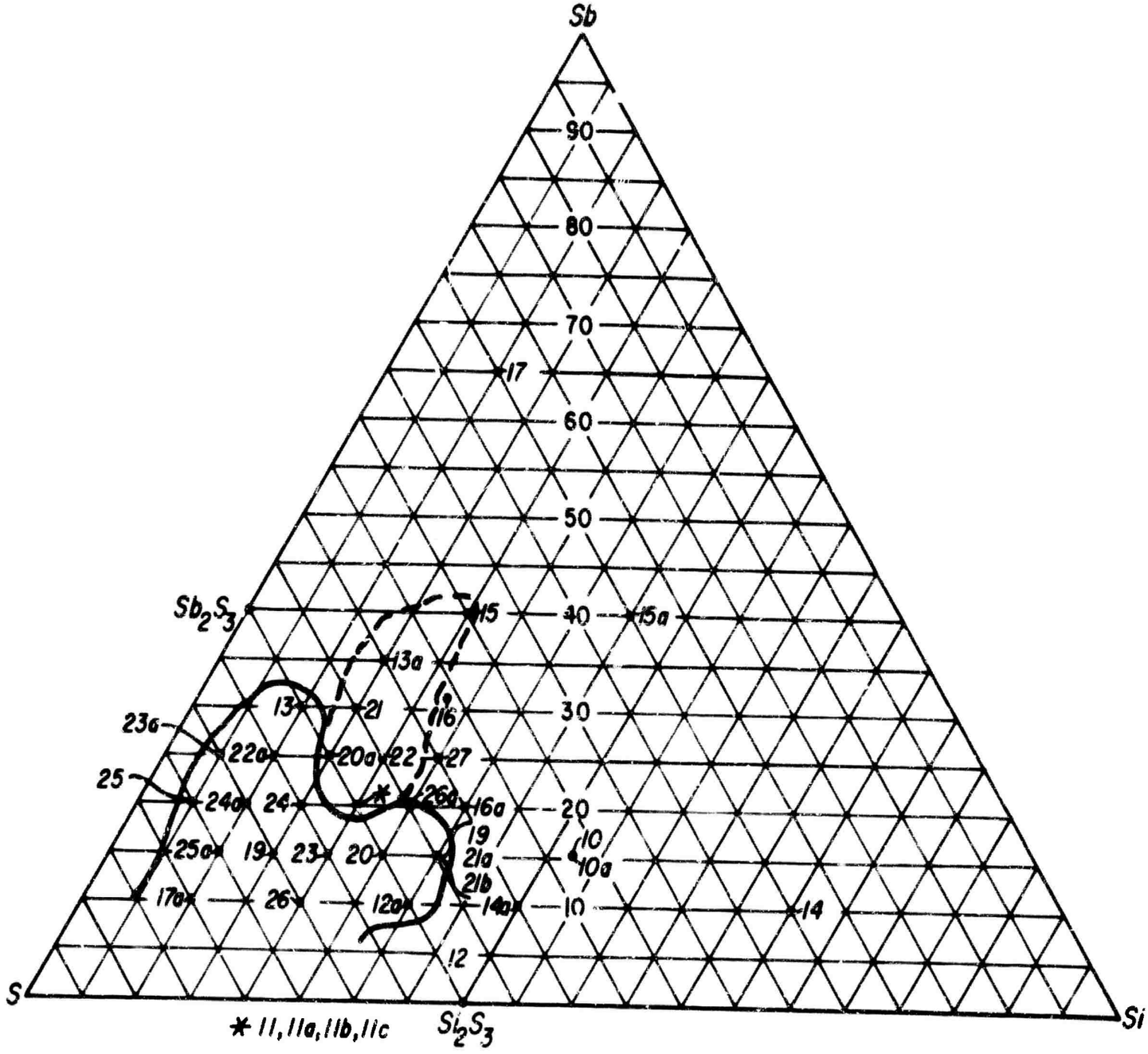

Figure 3 Si-Sb-S Glass Composition Diagram

TABLE II

The Si-Sb-Se System

Sample Number	Atom % Si	Sb	S	Softening Point (°C)	Remarks
*1	20	20	60	450	Slight odor H_2Se, stable glass, unreactive
2	26.7	13.3	60		Crystalline
*3	13.3	26.7	60	240	Slight odor H_2Se, stable glass, unreactive
4	20	25	55		Crystalline
*5	20	15	65	300	Slight odor H_2Se, stable glass, unreactive
*6	15	20	65	235	Slight odor H_2Se, stable glass, unreactive
7	25	20	55		Crystalline
*8	15	30	55	290	Slight odor H_2Se, stable glass, unreactive
*9	25	10	65	300	Odor of H_2Se, glass, decomposes
10	30	10	60		Crystalline
*11	10	30	60	295	Slight odor H_2Se, stable glass, unreactive
12	25	25	50		Crystalline
13	15	15	70	200	Slight odor H_2Se, stable glass, unreactive
14	30	15	55		Crystalline
*15	10	20	70	170	H_2Se odor, stable glass, reactive with atmosphere
*16	20	10	70	175	H_2Se odor, stable glass, reactive with atmosphere
17	20	30	50		Crystalline
18	30	20	50		Crystalline
*19	10	25	65	230	H_2Se odor, glass, decomposes
20	15	35	50		Crystalline
21	10	35	55		Crystalline
*22	5	5	90	145	H_2Se odor, stable glass, reactive with atmosphere
*23	25	5	70	240	H_2Se odor, stable glass, reactive with atmosphere
*24	20	5	75	210	Odor of H_2Se, glass, decomposes
*25	15	10	75	200	H_2Se odor, stable glass, reactive with atmosphere
*26	15	5	80	180	H_2Se odor, stable glass, reactive with atmosphere
*27	10	15	75	175	H_2Se odor, stable glass, reactive with atmosphere
*28	10	10	80	185	H_2Se odor, stable glass, reactive with atmosphere
*29	5	25	70	300	H_2Se odor, stable glass, reactive with atmosphere
*30	5	20	75	200	H_2Se odor, stable glass, reactive with atmosphere
31	5	35	60		Crystalline
32	5	30	65		Crystalline
33	5	15	80		Crystalline phase in glass matrix (by x-ray)
*34	5	10	85	134	H_2Se odor, stable glass, reactive with atmosphere
*35	10	5	85	165	Slight odor of H_2Se, stable glass, unreactive
36	10	40	50		Crystalline
37	5	40	55		Crystalline
38	5	45	50		Crystalline
39	30	5	65		Crystalline
40	60	20	20		Crystalline
41	33.3	33.3	33.3		Crystalline
42	20	60	20		Crystalline

atmosphere over long periods of time (weeks), while the surface of others seemed to decompose. All the glasses were badly attacked when heated in atmosphere.

The glass-forming composition region in the silicon-antimony-selenium system is shown by the solid lines in Figure 4. Some compositions of samples in the boundary region were rechecked and are marked by a circle around the composition point. The glass-forming region is substantially smaller than that of the silicon-antimony-sulfur system, and none of these samples showed the glass and metallic two-phase separation found in the other system.

Several glass samples showed good infrared transmission from 3 to 7 microns but all showed strong infrared absorption at 9.5, 12, 15, and 17 microns wavelength. The index of refraction determined by reflectivity measurements varies from 2 to about 3.5, depending on composition. Glasses from the Si-Sb-Se system will not be useful as high temperature optical materials from 8 to 14 microns.

3. The Silicon-Phosphorus-Tellurium Glass System

Results obtained for 39 different compositions in the Si-P-Te system are shown in Table III The glass-forming composition region is enclosed with the solid line in the composition diagram shown in Figure 5. The region is smaller than that of the Si-As-Te system,[15] and only about one-half , one-third of the area produces glasses of good quality, with softening points below 200°C. The absorption coefficient (α cm^{-1}) and index of refraction of three samples are shown in Figure 6. These values were calculated from transmission and reflectivity measurements. Note the slight absorption at 14 microns and the strong absorption at 20 microns (as shown by an increase in α). The same absorption is found in the Si-As-Te glasses. Infrared transmissions of the $SiTe_4$ glass showed absorption bands at 10, 14 and 20 microns. The cause of these three bands is probably the same in all three glass systems.

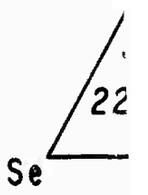

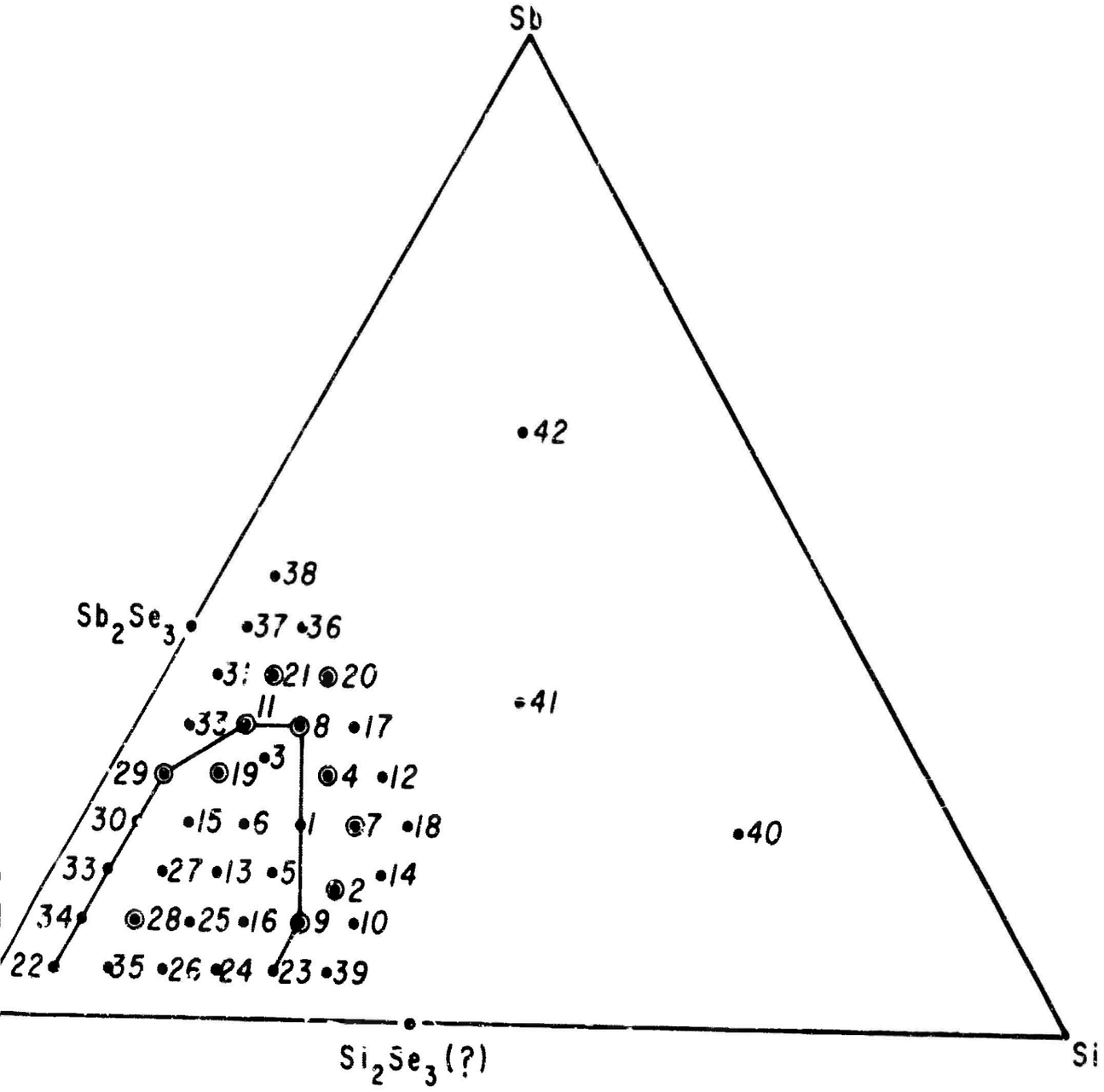

Figure 4 Si-Sb-Se Glass Composition Diagram

TABLE III

TABLE III

The Si-P-Te System

Sample Number	Atom % Si	P	Te	Softening Point (°C)	Remarks
3	20	20	60	190	Stable glass
12	25	25	50		Crystalline
15	40	20	40		Crystalline
16	30	20	50		Unstable glass
19	15	20	65	150	Stable glass, poor IR transmission
20	15	25	60	200	Stable glass, ~ 10% IR transmission
21	20	25	55	185	Stable glass, ~ 10% IR transmission
22	25	20	55	325	Stable glass, poor IR transmission
23	30	25	45		Unstable glass
24	35	20	45	385	Unstable glass
25	35	15	50		Unstable glass
26	30	15	55		Unstable glass
27	25	15	60		Unstable glass
28	20	15	65	250	Stable glass
29	15	15	70	180	Very stable glass, 10% IR transmission
30	10	20	70		Reacted violently with the atmosphere
31	10	25	65		Reacted violently with the atmosphere
32	10	30	60		Reacted violently with the atmosphere
33	15	30	55		Reacted violently with the atmosphere
34	35	25	40		Crystalline, unstable
35	40	15	45		Crystalline, unstable
36	40	10	50		Crystalline, unstable
37	35	10	55		Crystalline, unstable
38	30	10	60	400	Unstable glass
39	25	10	65	300	Stable glass, 10% IR transmission
40	20	10	70	200	Stable glass, 10% IR transmission
41	15	10	75	175	Very good glass, 35% IR transmission
42	15	5	80	160	Very good glass, 35% IR transmission
43	20	5	75	200	Very good glass, 20% IR transmission
47	25	5	70	250	Stable glass
48	30	5	65		Glassy
49	35	5	60		Glassy
50	40	5	55		Crystalline
51	30	0	70		Crystalline
52	25	0	75		Glassy
53	20	0	80		Glassy
54	15	0	85	375	Glassy
55	10	5	85		Crystalline
56	10	10	80		Crystalline

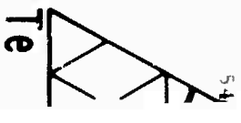

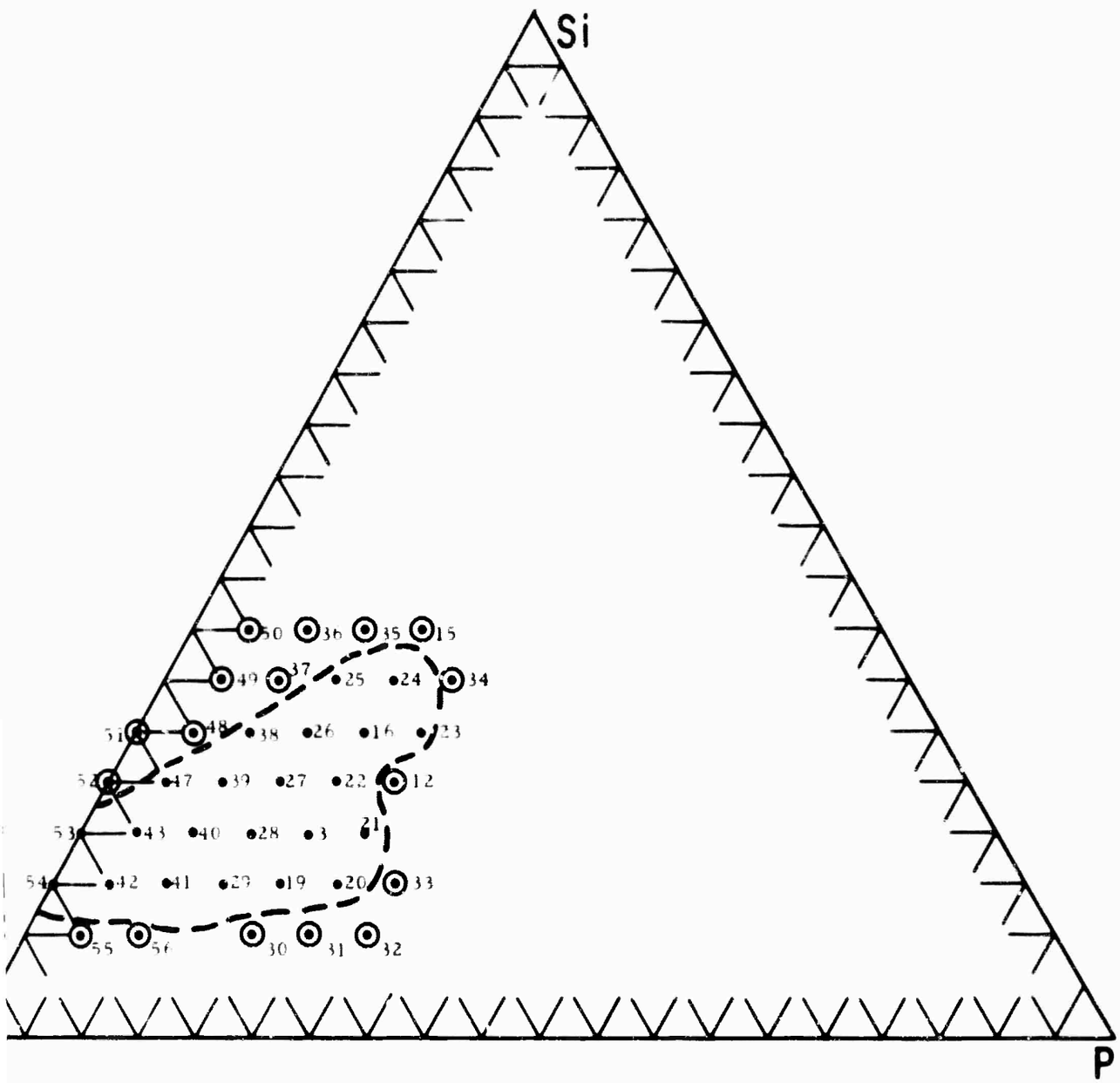

Figure 5 Si-P-Te Glass Composition Diagram

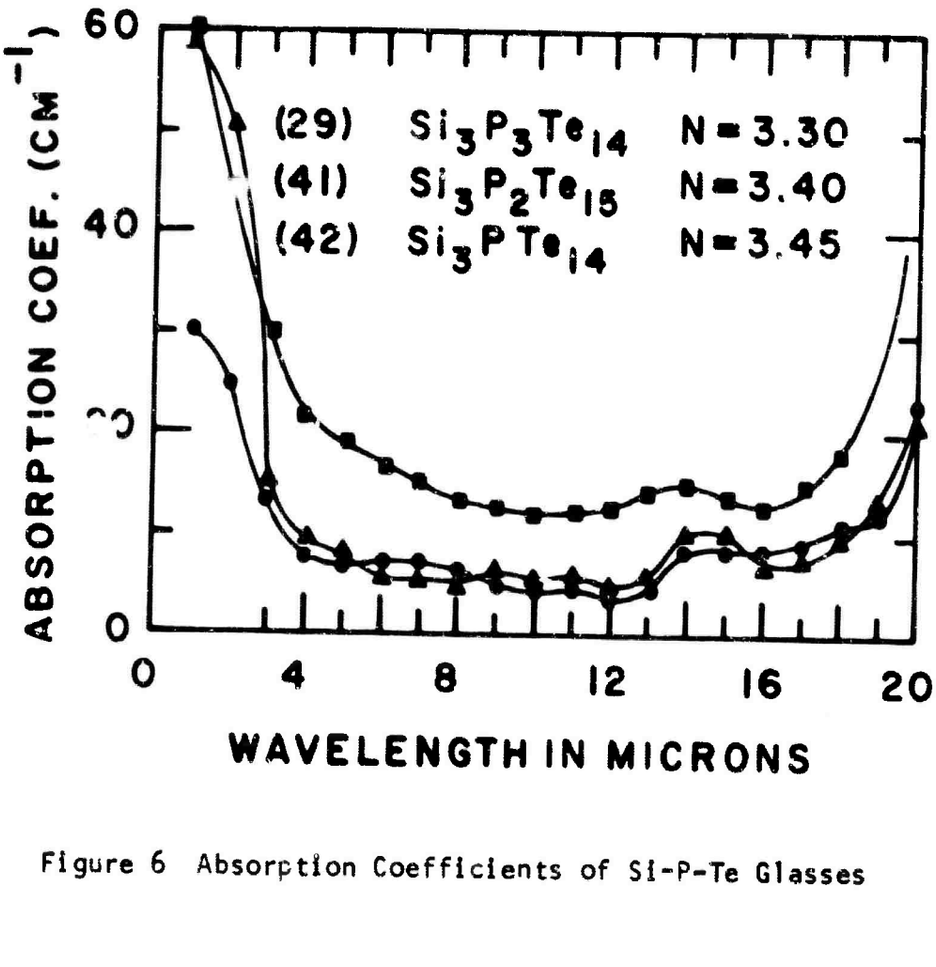

Figure 6 Absorption Coefficients of Si-P-Te Glasses

4. The Germanium-Phosphorus-Sulfur System

The Ge-P-S system has a larger glass-forming region than any other system studied in this investigation. Results obtained from 63 samples of different composition are shown in Table IV. The measured softening points are as high as 520°C, and the glasses show very good transmission in the 3 to 5 micron region. The glass-forming region determined from these composition points is enclosed with the solid line in Figure 7. The dash-dot line encloses the composition region in which glasses show at least 50% transmission in the 3 to 5 micron region (thickness ≥ 1 mm), while the dashed line encloses the region in which the measured softening point is greater than 480°C. The region common to all three (shaded) represents the compositions which should produce the best material for high temperature 3 to 5 micron applications.

Large samples of three promising compositions (68, 101, and 102), two from the shaded region, have been made and studied in detail. Plots of absorption coefficient vs wavelength for the three glasses are given in Figure 8. Note that the refractive indexes of the glasses are not high, 2.1 to 2.3. A non-absorbing, low index glass would not have to be antireflection-coated when used as a window material. The glass containing no phosphorus (#102, Ge_2S_3) shows very good transmission to 12 microns, while the Ge-P-S glasses cut off at about 7 microns. A slight absorption occurs from 3.9 to 4.0 microns. The location of the band varies slightly with composition. As in the case of As_2S_3 glass,[1,2] the band results from dissolved H_2S. Heating samples to a molten state (600°C) while flushing them with an inert gas (argon) substantially reduces the absorption band.

Transmission of all three glasses has been measured while they were exposed to the atomosphere at high temperatures (up to 500°C) for periods of at least one hour. In the region from 1 to 8 microns variations of only ±3% for a 1.5 mm sample were observed during the one-hour period. There was enough instability in the infrared instrument used in making the measurement to account for the change. There was no appreciable change in the transmission of glasses 68, 101, and 102 under these conditions. One sample of 68 was subjected to

TABLE IV

Ge-P-S Glass Samples

Sample No.	Atom. % Ge	P	S	Softening Point (°C)	Remarks
6	20	20	60	500	Stable Glass
7	25	25	50	475	Stable Glass
57	25	15	60	485	Stable Glass
58	25	20	55	510	Stable Glass
59	30	20	50	465	Stable Glass
60	30	25	45	470	Stable Glass
61	25	30	45	465	Stable Glass
62	20	30	50	485	Stable Glass
63	20	25	55	475	Stable Glass
64	15	25	60	470	Stable Glass
65	15	20	65	400	Stable Glass
66	20	15	65	465	Stable Glass
67	25	10	65	490	Stable Glass
68	30	10	60	520	Stable Glass
69	30	15	55	500	Stable Glass
70	35	15	50	425	Stable Glass
71	35	20	45	410	Stable Glass
72	35	25	40	405	Stable Glass
73	30	30	40	420	Stable Glass
74	25	35	40	465	Stable Glass
75	20	35	45	-	Glassy, Two Phase
76	15	35	50	515	Stable Glass
77	15	30	55	510	Stable Glass
78	10	30	60	380	Stable Glass
79	10	25	65	330	Stable Glass
80	10	20	70	275	Stable Glass
81	15	15	70	325	Stable Glass
82	20	10	70	375	Stable Glass
83	25	5	70	400	Stable Glass
84	30	5	65	500	Stable Glass

TABLE IV (Continued)

Sample No.	Atom. % Ge	P	S	Softening Point (°C)	Remarks
86	40	5	55	375	Stable Glass
87	50	5	45	-	Crystalline
88	40	15	45	-	Crystalline
89	40	30	30	-	Stable Glass
90	45	20	35	425	Stable Glass
91	45	5	50	-	Crystalline
92	45	10	45	-	Crystalline
93	50	15	35	455	Stable Glass
94	50	25	25	520	Glassy
95	60	5	35	-	Crystalline
96	60	20	20	-	Crystalline
97	50	35	15	-	Decomposed
98	35	35	30	450	Stable Glass
99	40	10	50	400	Stable Glass
100	35	10	55	420	Stable Glass
101	35	5	60	480	Stable Glass
102	40	-	60	420	Stable Glass
103	40	40	20	450	Stable Glass
104	30	45	25	415	Stable Glass
106	20	45	35	440	Stable Glass
107	40	20	40	380	Stable Glass
108	55	10	35	-	Crystals in Glass
109	55	20	25	-	Crystals in Glass
110	30	55	15	460	Stable Glass
111	10	50	40	520	Stable Glass
112	35	-	65	-	Crystalline
113	10	10	80	285	Stable Glass
114	5	30	65	-	Two Phase Glass
115	15	65	20	-	Exploded on Cooling
135	40	50	10	-	Exploded on Cooling
136	20	55	25	-	Exploded on Cooling
137	15	50	35	-	Crystalline
138	10	40	50	-	Crystalline

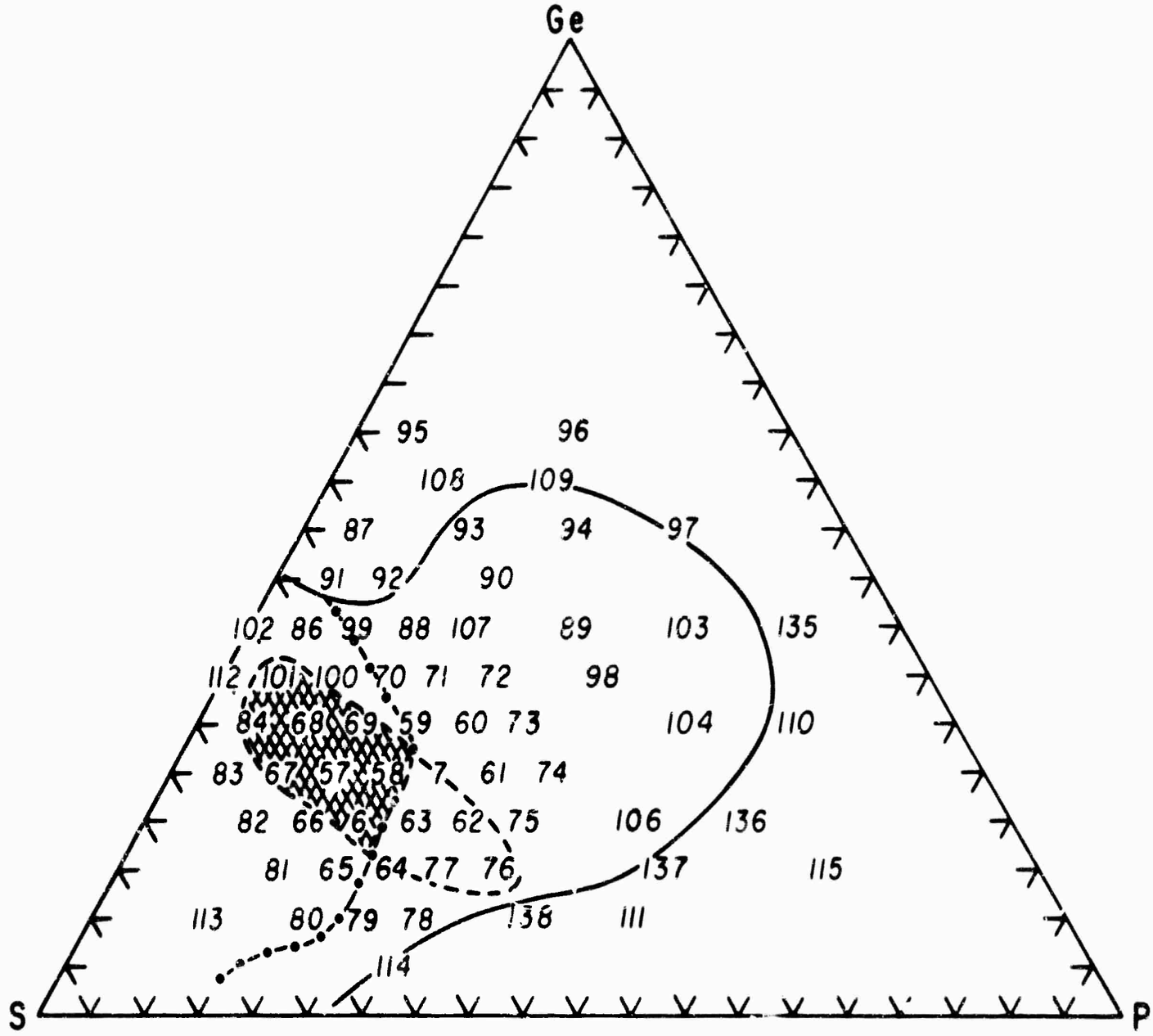

Figure 7 Composition Diagram for Ge-P-S Ternary Glass System

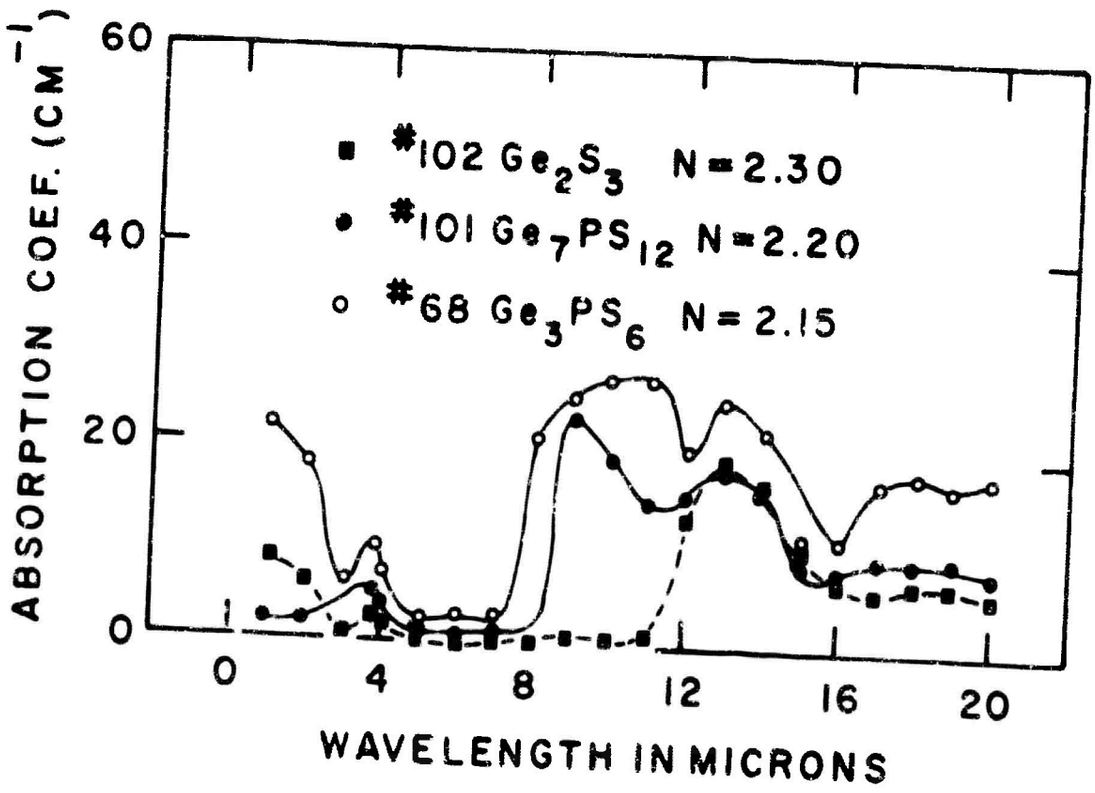

Figure 8 Absorption Coefficients of Ge-P-S Glasses

this test three times with no apparent damage. It is interesting to note that the measured softening point of glass 102 is only 420°C, yet it suffered no damage at 500°C.

5. The Germanium-Phosphorus-Selenium System

Results obtained from 27 compositions are shown in Table V. Softening points are as high as 450°C, and the glasses show good transmission in the 3 to 5 micron region. The glass-forming region determined from these compositions is enclosed by the solid line in Figure 9. The area is substantial compared to other systems but is considerably smaller than that of the Ge-P-S system. The absorption coefficient as a function of wavelength for a typical sample (No.2) is shown in Figure 10. Two samples of Ge-Se glasses (Numbers 129 and 130) containing no phosphorus are also shown. In general, the Ge-P-Se glasses have higher refractive indexes, lower softening points, less chemical stability, and poorer optical quality than Ge-P-S glasses. Their only advantage is that they do not show the 4-micron absorption band; however, when this band is present in other glasses, it can be easily removed. The Ge-P-Se glasses have no practical advantage over the Ge-P-S glasses.

6. The Germanium-Arsenic-Tellurium System

Table VI show results obtained from 46 different compositions. Two glass-forming regions are determined by these composition points, as shown in Figure 11. Both regions lie in a low germanium content region and therefore have low softening points, ranging from 135 to 270°C. Some of the glasses showed two distinct amorphous phases, indicating an immiscible system in this composition region. No attempt was made to study the individual phases.

The infrared transmission of Ge-As-Te glasses is essentially free from absorption bands out to 20 microns. However, all have high refractive indexes (3.0 to 3.5) and low softening points (150°C to 200°C). Refractive index and absorption coefficient as a function of wavelength for three samples are shown in Figure 12. The refractive indexes are the average value for 8 to 14 microns.

TABLE V

Ge-P-Se Glass Samples

Sample No.	Atom. % Ge	P	Se	Softening Point (°C)	Remarks
2	20	20	60	420	Stable Glass
8	20	10	70	300	Stable Glass
9	10	20	70	210	Stable Glass
11	50	25	25	-	Crystalline
116	15	15	70	280	Stable Glass
117	25	10	65	400	Stable Glass
118	25	20	55	450	Stable Glass
119	15	25	60	350	Stable Glass
120	35	10	55	410	Stable Glass
121	35	20	45	-	Crystalline
122	35	30	35	-	Crystalline
123	25	30	45	380	Stable Glass
124	15	35	50	380	Stable Glass
125	45	10	45	-	Crystalline
126	45	20	35	-	Crystalline
127	45	30	25	-	Exploded on Cooling
128	30	40	30	-	Exploded on Cooling
129	25	-	75	300	Stable Glass
130	40	-	60	360	Stable Glass
131	45	5	50	-	Crystalline
132	30	30	40	-	Crystalline
133	20	40	40	-	Decomposes
134	10	40	50	-	Crystals in Glass
139	40	10	50	160	Stable Glass
140	10	35	55	310	Stable Glass
141	5	35	60	180	Stable Glass
142	5	25	70	-	Crystalline

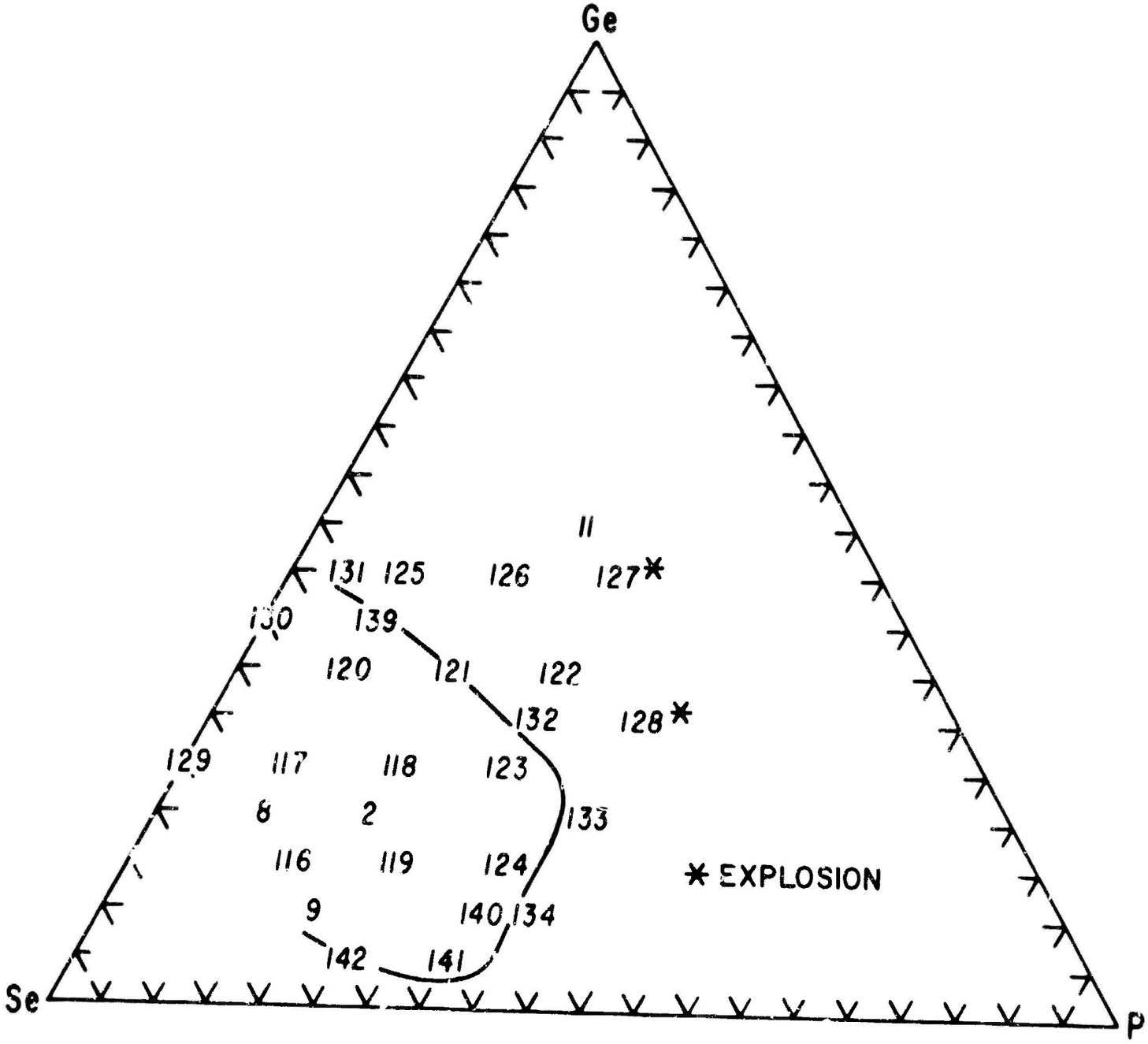

Figure 9 Composition Diagram for Ge-P-Se Terna.y Glass System

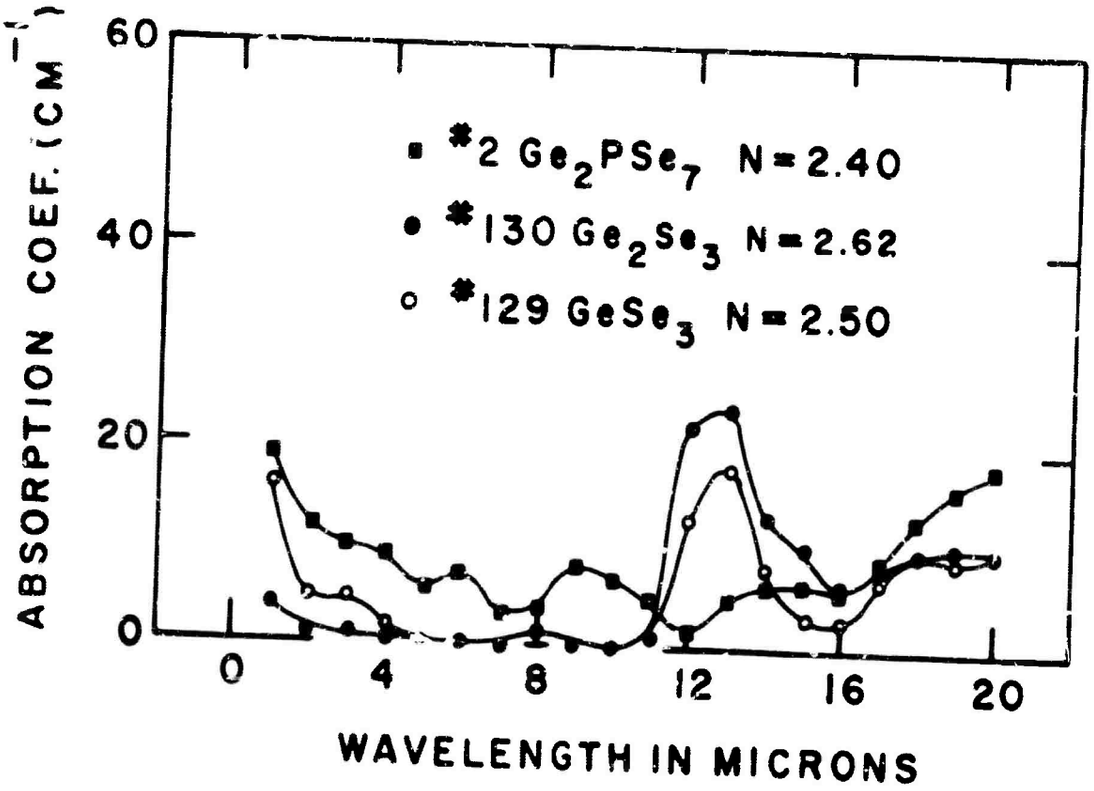

Figure 10 Absorption Coefficients of Ge-P-Se Glasses

TABLE VI

Ge-As-Te Glass Samples

Sample No.	Atom. % Ge	As	Te	Softening Point
143	10	10	80	Two phases
144	20	5	75	—
145	30	5	65	—
146	40	5	55	—
147	40	30	30	—
148	25	35	40	—
149	15	35	50	—
150	5	30	65	Two phases
151	15	25	60	—
152	15	15	70	160°C
153	25	15	60	—
158	10	20	70	135°C
159	10	35	55	—
160	5	45	50	150°C
161	0	40	60	—
162	10	0	30	—
163	20	0	80	—
164	15	45	40	Two phases
165	5	55	40	190°C
166	0	20	80	—
173	15	5	80	Two phases
174	10	15	75	152°C
175	20	45	35	—
176	15	55	30	Two phases
177	10	55	35	230°C
178	10	50	40	250°C
179	5	50	45	185°C
180	5	60	35	200°C
181	10	25	65	164°C

TABLE VI (Continued)

Sample No.	Atom. % Ge	As	Te	Softening Point
182	15	10	75	162°C
183	15	20	65	—
184	10	5	85	—
185	10	60	30	268°C
186	15	50	35	250°C
187	15	60	25	—
188	15	40	45	Two Phases
189	5	10	85	—
190	20	50	30	—
191	10	65	25	235°C
192	5	65	30	205°C
193	20	10	70	—
194	20	15	65	—
195	5	15	80	—
196	20	40	40	—
197	10	40	50	190°C
198	5	40	55	—

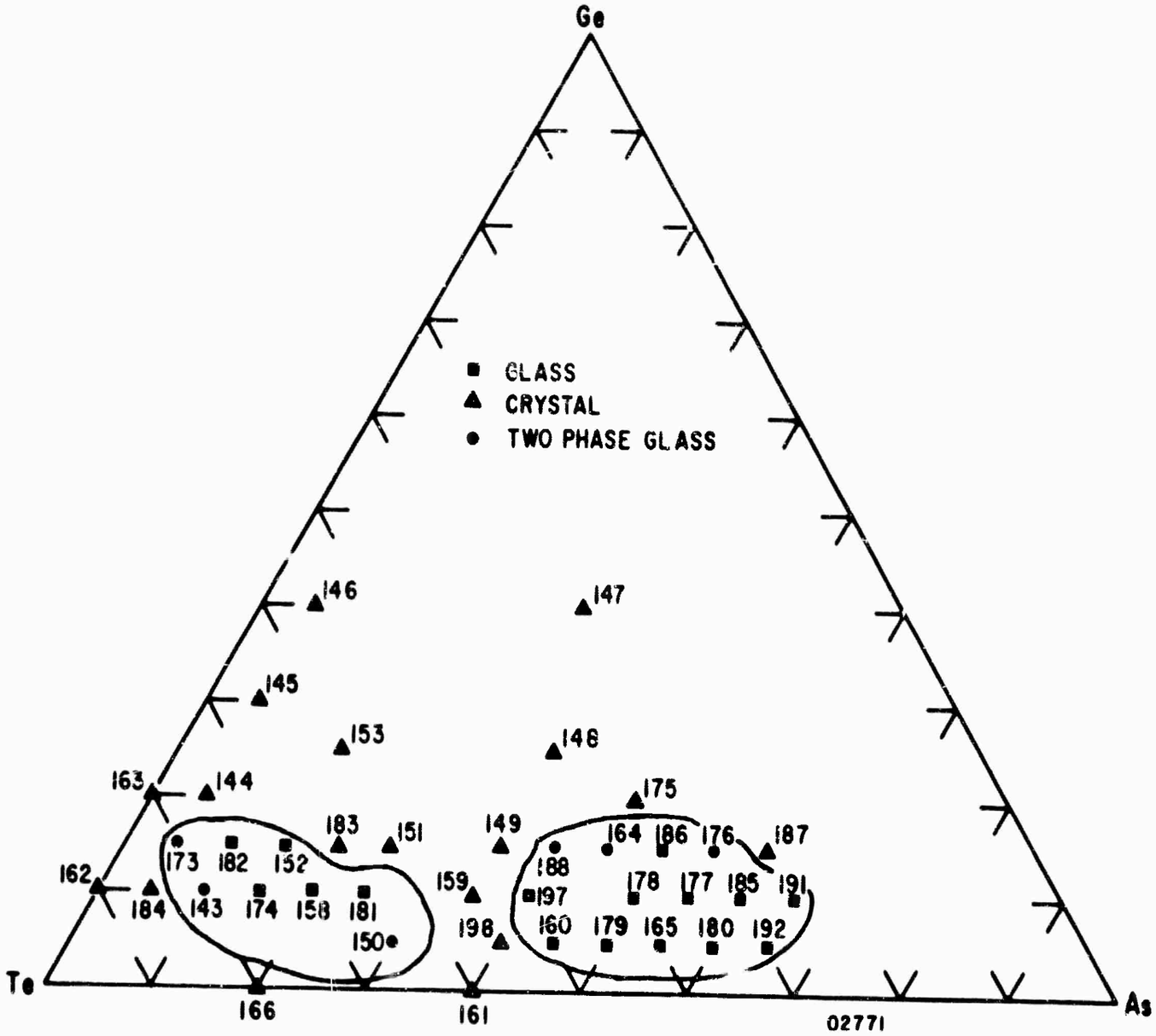

Figure 11 The Ge-As-Te Composition Diagram

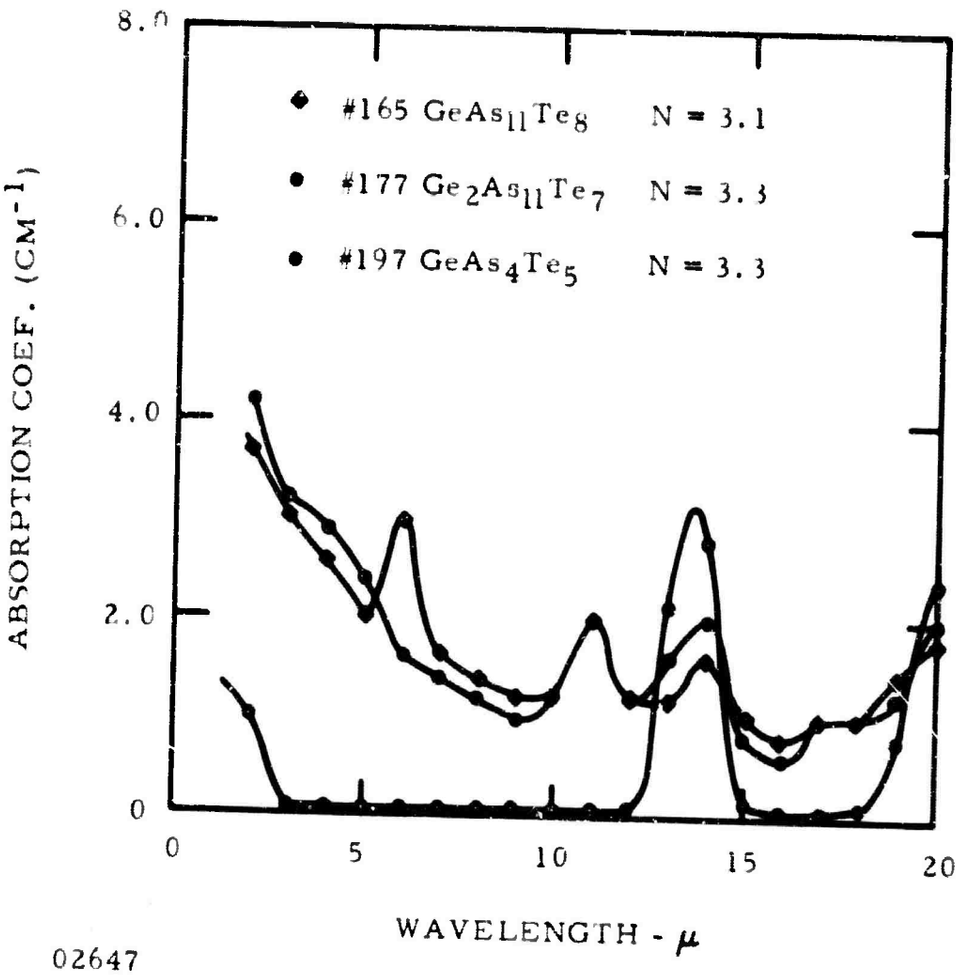

02647

Figure 12 Absorption Coefficients of Some Ge-As-Te Glasses

Absorption coefficients for all three glasses are very low in comparison to other systems. It was necessary to expand the absorption coefficient scale by a factor of 10 to show wavelength variations. The Ge-As-Te system produced glasses freer from absorption bands than any system evaluated thus far. It is unfortunate that the softening points are so low because of the low germanium content.

7. The Germanium-Phosphorus-Tellurium System

Results obtained from 27 samples of different compositions are shown in Table VII. The measured softening points range from 130°C to 390°C. The glass-forming region determined from these composition points is enclosed by the solid line in Figure 13. This glass-forming region may extend further toward the phosphorus-rich region, but because of the high vapor pressures involved, no samples containing more than 30 atomic percent phosphorus were prepared. The chemical stability of some of these glasses was determined and results are shown in Table VIII, along with those for typical Ge-As-Te glasses. Although the Ge-P-Te glasses are somewhat less stable than Ge-As-Te glasses, the results indicate reasonable stability.

A plot of infrared transmission versus wavelength for the Ge-P-Te system is shown in Figure 14. These glasses are essentially free of absorption bands out to 20 microns and show transmission over a greater wavelength range than any glass system previously reported. The refractive indexes, as in the case of the Ge-As-Te glasses, are greater than 3.

8. The Tin-VA-VIA Systems

Results obtained from 19 compositions are shown in Table IX. During sample preparation, several violent explosions occurred at relatively low (< 600°C) temperatures, possibly because of pressure created by very exothermic reactions. Only two compositions produced glass, $SnAsSe_8$ and $SnAsSe_{18}$. The softening points of these glasses were 150°C and 110°C, respectively. Because of the low

TABLE VII

The Ge-P-Te System

Sample No.	Atom. % Ge	P	Te	Softening Point (°C)
199	10	30	60	Exploded
200	15	15	70	145
201	30	10	60	Crystalline
202	25	25	50	Crystalline
203	35	15	50	Exploded
204	25	15	60	Crystalline
205	20	15	75	165
206	10	10	80	Crystalline
207	10	20	70	Crystalline
208	15	20	65	190
209	20	25	55	Crystalline
210	30	20	50	Crystalline
211	20	20	60	Crystalline
212	20	15	65	270
213	25	10	65	390
214	35	0	65	Crystalline
215	15	5	80	Crystalline
216	15	10	75	130
217	25	5	70	Crystalline
218	20	10	70	Crystalline
219	30	5	65	230
220	30	0	70	Crystalline
221	25	0	75	Crystalline
222	20	0	80	Crystalline
223	10	15	75	Crystalline
224	25	5	70	Crystalline
225	27	8	65	Crystalline

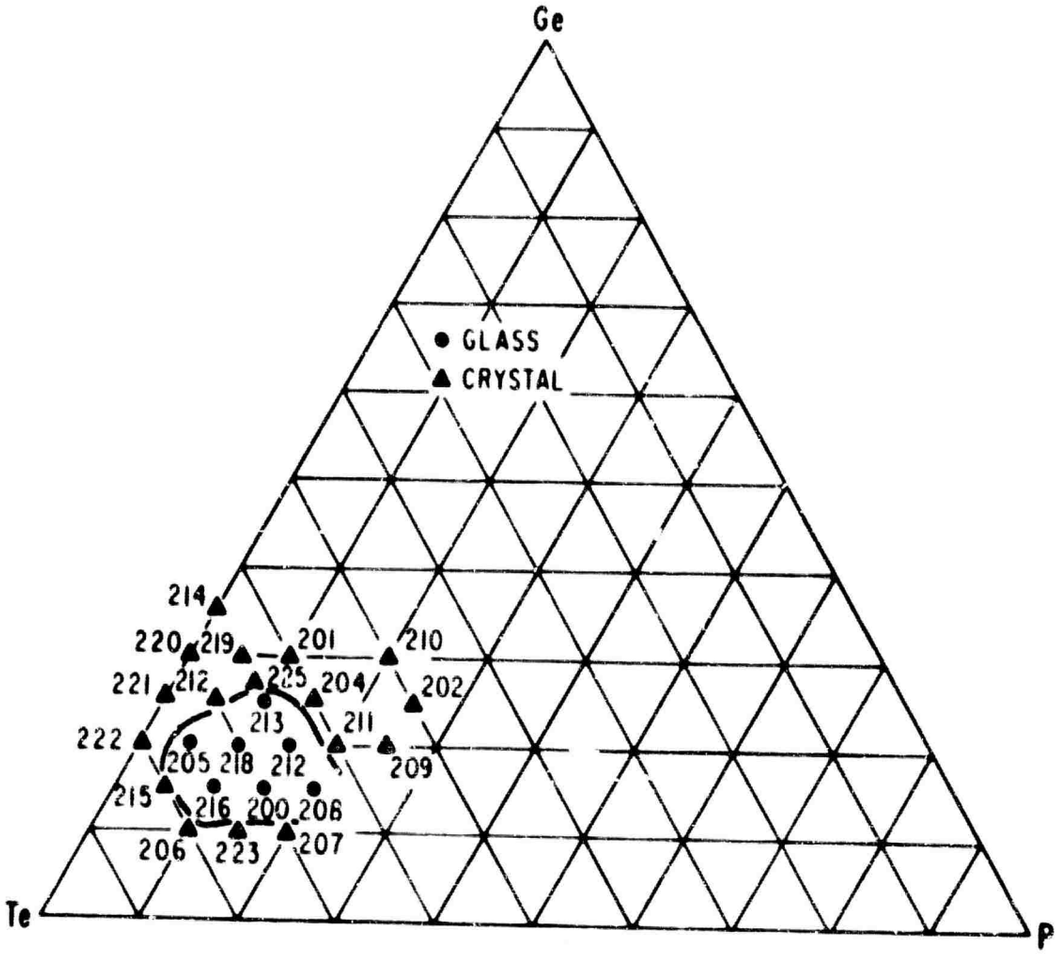

03089

Figure 13 Composition Diagram for Ge-P-Te Glass System

TABLE VIII

Chemical Stability of Ge-P-Te Glass

(Weight Loss, Grams/Gram)

Composition	18 Hours in H_2O at 25°C	1.5 Hours in H_2O at 100°C	20 Hours in HCl - 5%	20 Hours in HNO_3 - 5%	20 Hours in NaOH - 5%
$Ge_3P_3Te_{14}$	0.0003	0.0002	0.0001	0.0083	0.0007
Ge_4PTe_{15}	0.0000	0.0016	0.0009	0.0000	0.0000
$Ge_3P_4Te_{13}$	0.0000	0.0048	0.0007	0.0012	0.0004
$Ge_4P_3Te_{13}$	0.0008	0.0005	0.0012	0.0018	0.0004
$Ge_3P_2Te_{15}$	0.0023	0.0000	0.0023	0.0034	0.0007
$GeAsTe_8$*	0.0001	0.0000	0.0006	0.0001	0.0004
$GeAs_6Te_{13}$*	0.0009	0.0000	0.0002	0.0003	0.0004

* Comparative Values

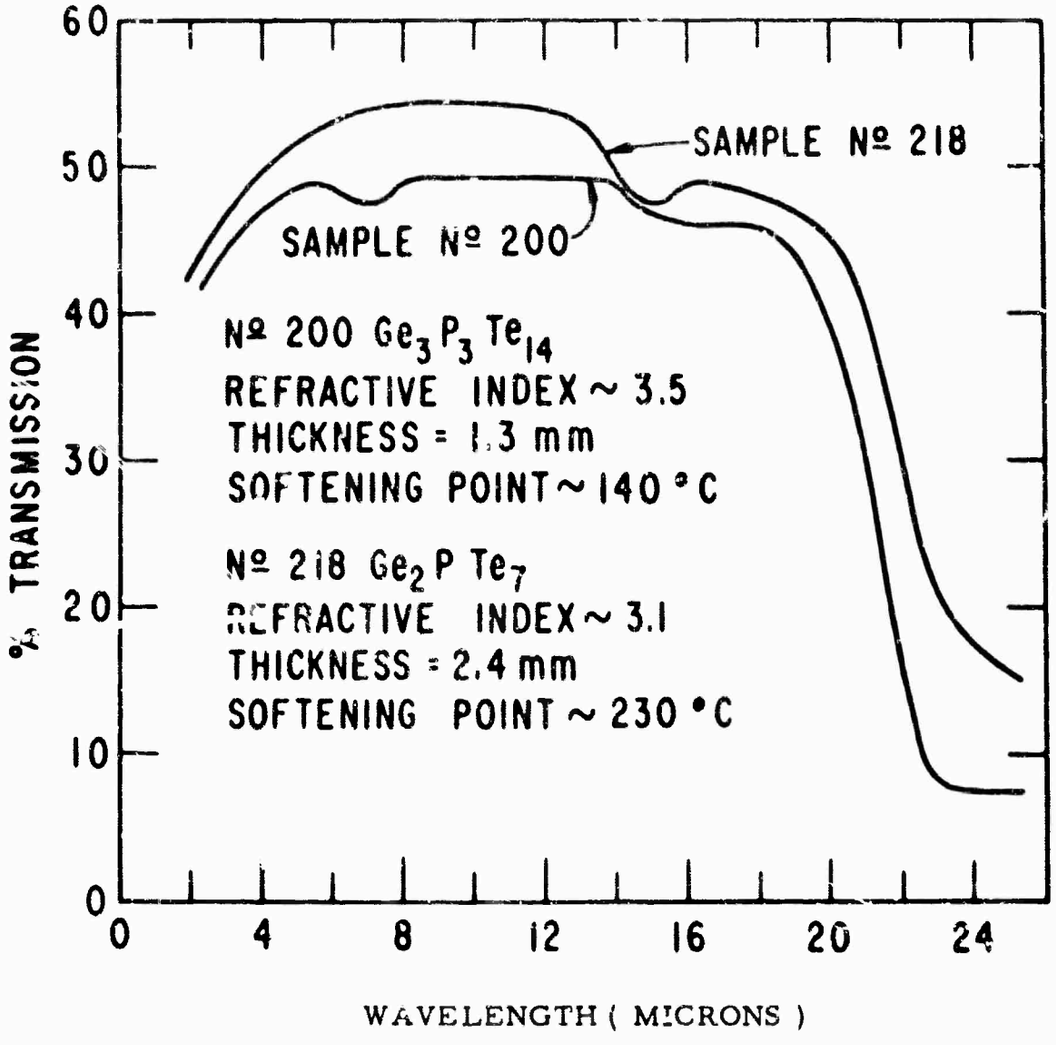

03089

Figure 14 Infrared Transmission of Some Ge-P-Te Glasses

TABLE IX

The Sn-VA-VIA System

Composition	Results
$SnPS_3$	Crystalline
$SnAsS_3$	Crystalline
$SnPSe_3$	Crystalline
$SnAsSe_3$	Crystalline
$SnPTe_3$	Exploded
$SnAsTe_3$	Crystalline
$Sn_3P_2S_{15}$	Crystalline
$Sn_3As_2S_{15}$	Crystalline
SnPS	Exploded
SnAsS	Exploded
$SnPS_{18}$	Exploded
$SnAsS_8$	Exploded
Sn_3AsS_{14}	Crystals in glassy matrix
$Sn_5As_4S_{11}$	Crystalline
$Sn_2As_5S_{13}$	Crystalline
$SnAsSe_8$	Glass - softening point ~ 150°C
$SnAsSe_{18}$	Glass - softening point ~ 110°C
$SnAsTe_8$	Crystalline
$SnAsTe_{18}$	Crystalline

softening points and the difficulty involved in preparing these compositions, work was abandoned on the Sn-VA-VIA glasses in favor of blended glasses.

9. Boron-Arsenic-VIA Systems

Three glass compositions--B_3AsS_6, B_3AsSe_6, and B_3AsTe_6--were prepared in a preliminary study to determine the potential of boron as a glass-former in various chalcogenide systems. The composition containing tellurium did not form a glass; the others were amorphous but were very reactive and decomposed when exposed to the atmosphere. Boron may be useful as a glass modifier, but it does not appear promising as a major glass constituent.

I. Summary of the IVA-VA-VIA Evaluation Results

The qualitative results for the seven ternary systems evaluated under Contract Nonr 3810(00) are given in Table X. Results of the first system evaluated at Texas Instruments are also included. The results for all but the last two systems have been reported in the literature.[15,16]

The maximum softening points indicated for each system are the softening points of the glasses of best optical quality, not the highest softening point obtained. The Si-Sb-S and Si-Sb-Se systems are chemically unstable and have many absorption bands. The Ge-P-S and Ge-P-Se glasses have high softening points and moderate refractive indexes but suffer from strong absorption in the 8 to 14 micron region. The best glasses for 8 to 14 micron application are from the Si-As-Te, Ge-As-Te, and Ge-P-Te systems. The Si-P-Te glasses are very similar to the Si-As-Te but have lower softening points and are not as stable chemically. Glasses from all three systems have high refractive indexes.

TABLE X

General Properties of Best Infrared Transmitting Glasses From Each Ternary System

System	Max. Softening Point	Refractive Index	Absorption	
			3 to 5μ	8 to 14μ
Si-P-Te	180°C	3.4	No	Slight
Si-Sb-Se	270°C	3.3	Yes	Yes
Si-Sb-S	280°C	-	Yes	Yes
Ge-P-Se	420°C	2.4 - 2.6	Slight	Yes
Ge-P-S	520°C	2.0 - 2.3	Very Slight	Yes
Si-As-Te	475°C	2.9 - 3.1	No	Slight
Ge-As-Te	270°C	~3.5	No	Very Slight
Ge-P-Te	380°C	~3.5	No	Very Slight

C. Blended Glasses

Glasses from a particular ternary system are characterized by specific physical and optical properties. These properties can be either enhanced or decreased by carefully blending a specific glass with a different glass system. A specific blend can be obtained by mixing the correct amounts of previously prepared glass or by weighing out the unreacted elements. The latter method has been used predominantly in our program.

Two base glass systems were chosen to study the effects of blending, as shown in Figure 15. The Si-As-Te system was chosen because it has been more fully characterized than the others, and the Ge-As-Te system because of its lack of absorption bands in the desired wavelength region. These two glasses were blended with each other, giving the effect of germanium in the Si-As-Te system, and vice versa. Si-As-Te was then blended with Si-P-Te, Si-Sb-Te, Si-As-Se, and Si-As-S, giving the effects of phosphorus, antimony, selenium, and sulfur on the Si-As-Te system. The Ge-As-Te system was blended with Ge-P-Te, Ge-As-Se, Ge-As-S, and Ge-Sb-Te, giving the effects of phosphorus, selenium, sulfur, and antimony on the Ge-As-Te system.

1. Si-As-Te → Ge-As-Te

Table XI shows the effects on hardness and softening point when germanium was substituted for silicon in various Si-As-Te glasses. In all cases the glass was prepared from the elements in the usual manner. In general, adding germanium caused a slight decrease in the softening point of the glass. This effect is shown graphically in Figure 16. As expected, the glasses with the largest amount of the group IVA element showed the greatest change in softening point. Glasses rich in tellurium, especially the glass with the composition $Si_6As_8Te_{45}$, show little change in softening point or hardness, indicating a structure somewhat different from that of a higher softening, lower tellurium-content glass such as $Si_7As_5Te_8$. This is probably a result of the type of bonding prevalent in the various glasses.

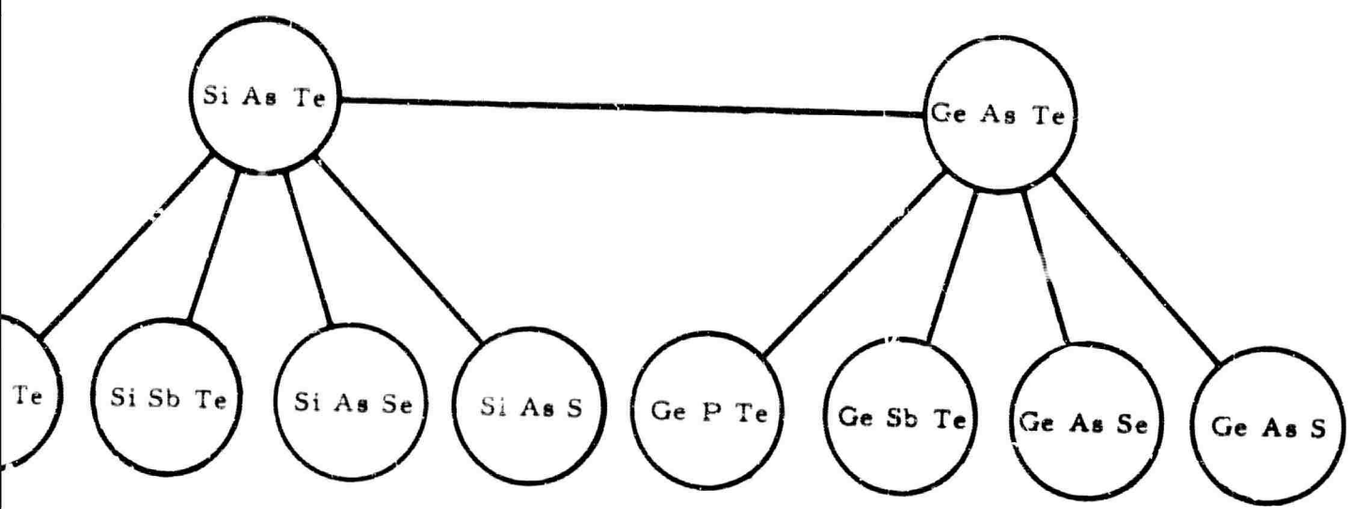

Figure 15 IVA-VA-VIA Glass Blends

TABLE XI

Blended Glasses (Si-As-Te → Ge-As-Te)

Sample No.	Composition	Softening Point (°C)	Hardness (Knoop)
239	$Si_6As_8Te_{26}$	196	108.4
242	$Si_5GeAs_8Te_{26}$	190	126.5
245	$Si_4Ge_2As_8Te_{26}$	124	126.5
248	$Si_3Ge_3As_8Te_{26}$	200	136.8
251	$Si_2Ge_4As_8Te_{26}$	190	127.0
253	$SiGe_5As_8Te_{26}$	180	126.5
255	$Ge_6As_8Te_{26}$	Crystalline	-
258	$Si_6As_9Te_{45}$	160	108.4
260	$Si_5GeAs_9Te_{45}$	136	105.8
261	$Si_4Ge_2As_9Te_{45}$	148	110.9
262	$Si_3Ge_3As_9Te_{45}$	146	108.7
263	$Si_2Ge_4As_9Te_{45}$	148	109.0
264	$SiGe_5As_9Te_{45}$	150	113.4
265	$Ge_6As_9Te_{45}$	162	113.7
240	$Si_5As_5Te_{10}$	310	166.9
266	$Si_4GeAs_5Te_{10}$	290	156.5
267	$Si_3Ge_2As_5Te_{10}$	293	179.0
268	$Si_2Ge_3As_5Te_{10}$	256	151.2
269	$SiGe_4As_5Te_{10}$	Crystalline	-
241	$Si_7As_5Te_8$	434	207.8
244	$Si_6GeAs_5Te_8$	380	195.6
247	$Si_5Ge_2As_5Te_8$	394	198.6
250	$Si_4Ge_3As_5Te_8$	379	195.0
251	$Si_3Ge_4As_5Te_8$	Crystalline	-

030

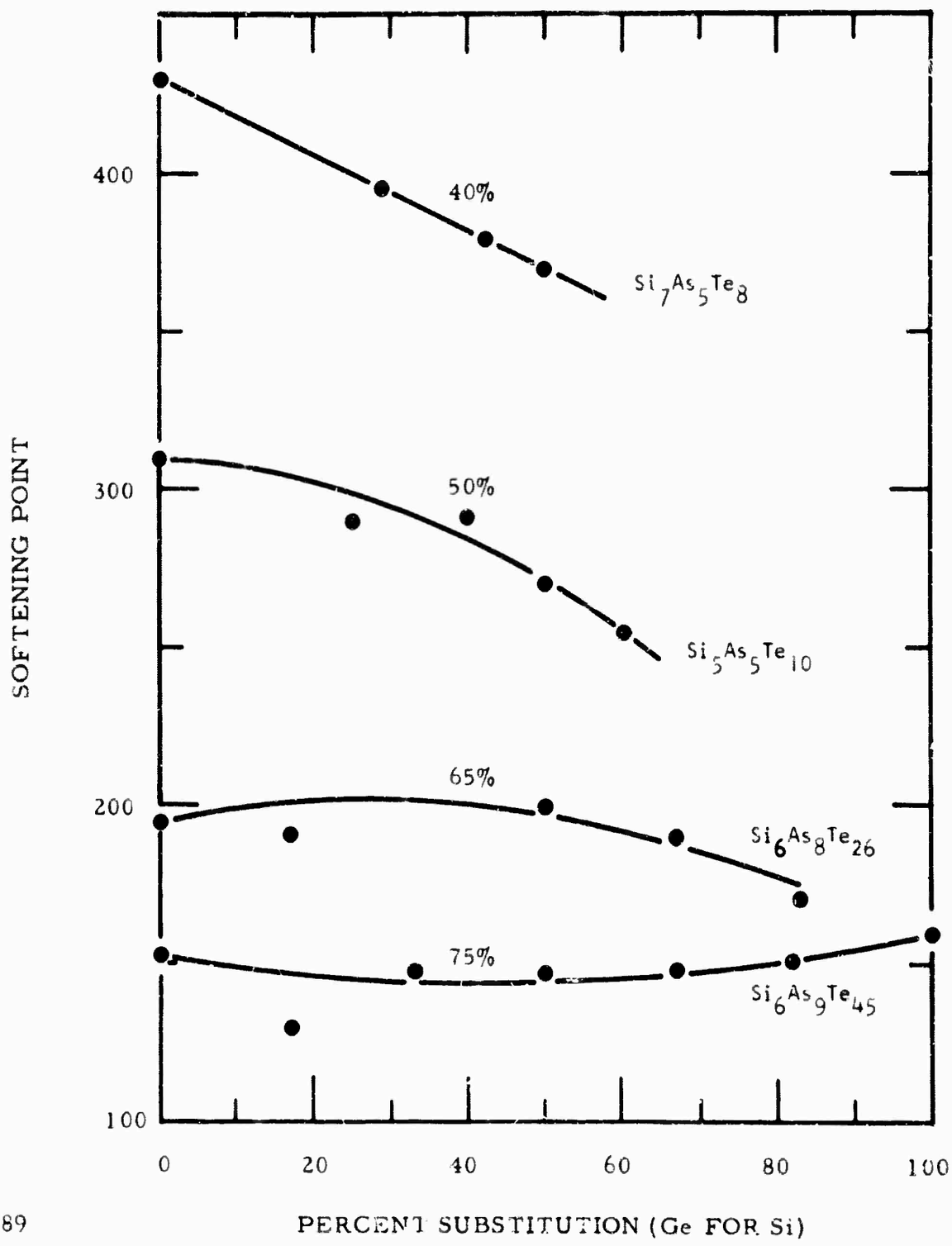

3089

Figure 16 Substitution of Ge for Si in Si-As-Te Glass: Effect on Softening Point

The measured values of hardness and softening points given in Table XI are plotted in Figure 17. Tellurium-rich glass undoubtedly contains Te-Te bonds and thus has a lower softening point. Addition or substitution of a relatively minor element should affect the properties of the glass very little. The low softening glasses are tellurium-rich and should be softer than those containing large amounts of the group IVA elements. Germanium also affects the Si-As-Te system by reducing the absorption coefficient, especially at 10 and 14 microns. This effect is shown in Figure 18. The origin of these bands will be discussed in another section.

2. Si-As-Te → Si-As-S

Table XII shows the softening points obtained when Te is replaced with S in the Si-As-Te system. The softening point is not appreciably lowered until sulfur comprises about one-third of the group VIA elements. The refractive index is also lowered, as expected, by the addition of sulfur. The refractive index for $Si_{37}As_{30}Te_{33}$ is 3.12 at 8 microns, while the refractive index for $Si_{37}As_{30}Te_{18}S_{15}$ is 2.76 at the same wavelength. Sulfur also causes a loss in transmission, particularly at 10 microns. A typical plot of infrared transmission versus wavelength is shown in Figure 19. Replacing only one-tenth of the tellurium with sulfur causes a factor of 4 decrease in transmission at 10 microns. Replacing one-fifth of the tellurium with sulfur causes a loss in transmission by almost a factor of 20.

3. Si-As-Te → Si-As-Se

Table XIII shows the softening points obtained when tellurium is replaced by selenium in the Si-As-Te system. In one family of glasses in which the ratio of tellurium and selenium to the IVA and VA elements was 1 to 1, the softening point increased slightly with an increase in selenium. In another family of glasses the ratio of tellurium and selenium to the IVA and VA elements was 2 to 1, and the softening points decreased slightly. Again, this is an indication of the presence of Te-Te or Te-Se bonds in the group VIA-rich glasses.

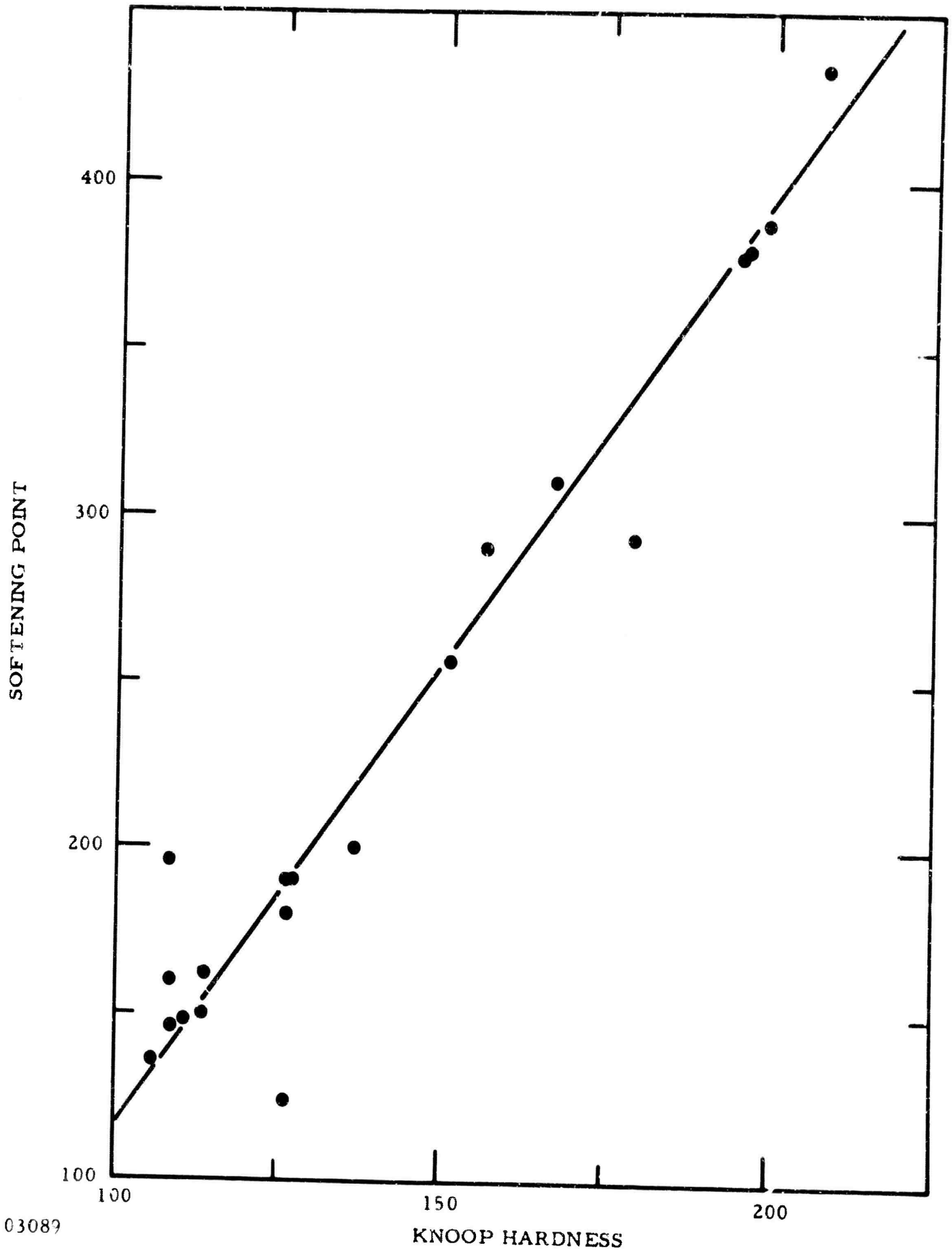

03089

Figure 17 Substitution of Ge for Si in Si-As-Te Glass: Correlation between Knoop Hardness and Softening-Point

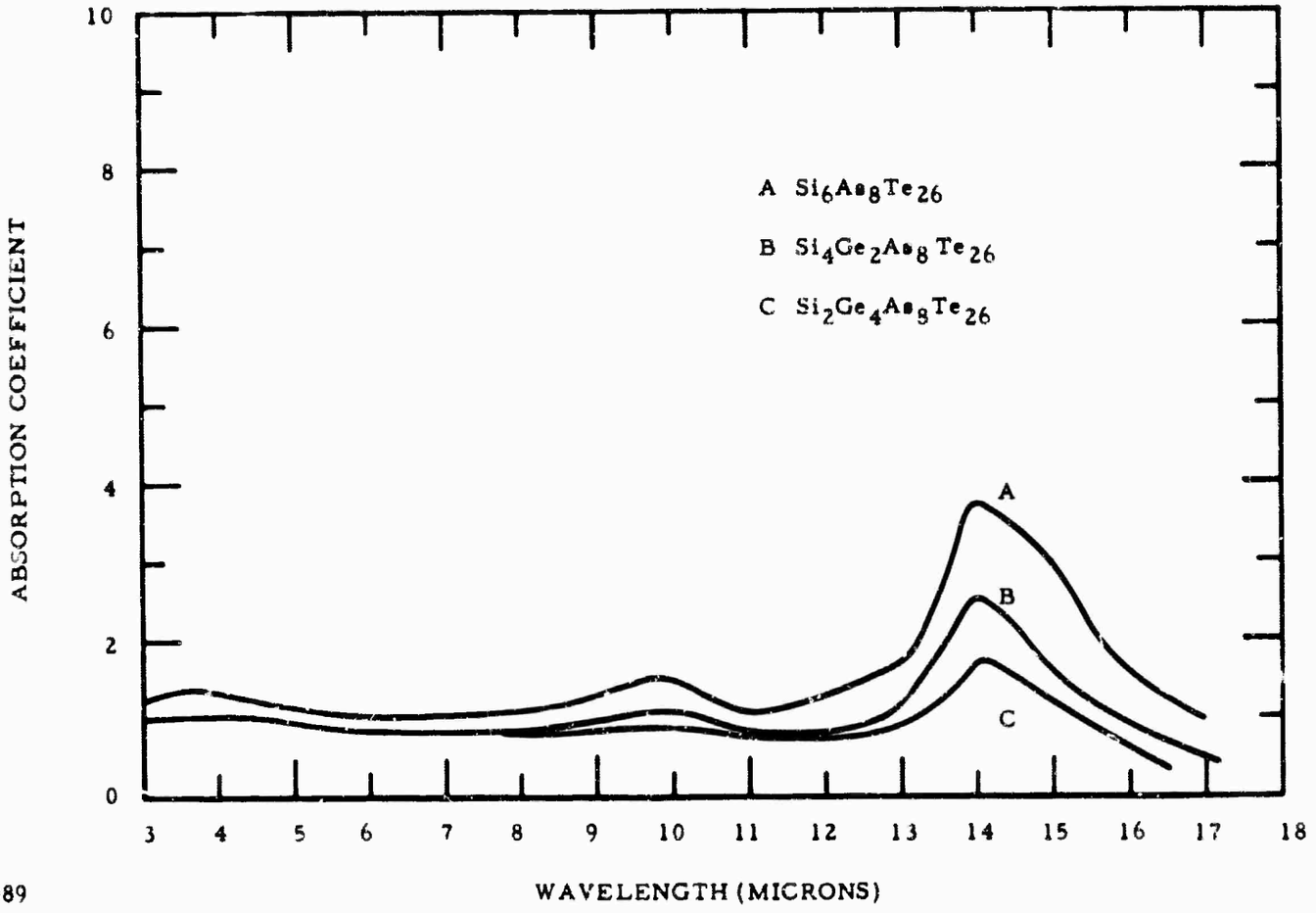

03089

Figure 18 Absorption Coefficient of Si-As-Te – Ge-As-Te Glasses

TABLE XII

The Si-As-Te → Si-As-S System

Sample No.	Composition	Softening Point (°C)
312	$Si_{37}As_{30}Te_{33}$	474
313	$Si_{37}As_{30}Te_{30}S_3$	478
314	$Si_{37}As_{30}Te_{27}S_6$	510
315	$Si_{37}As_{30}Te_{24}S_9$	480
316	$Si_{37}As_{30}Te_{21}S_{12}$	334
317	$Si_{37}As_{30}Te_{18}S_{15}$	294
318	$Si_{37}As_{30}Te_{15}S_{18}$	Reacts with the atmosphere
296	$Si_5As_5Te_{10}$	317
297	$Si_5As_5Te_9S$	300
298	$Si_5As_5Te_8S_2$	276
299	$Si_5As_5Te_7S_3$	Reactive
302	$Si_5As_5Te_6S_4$	170
303	$Si_5As_5Te_5S_5$	140
306	$Si_5As_5Te_4S_6$	198
307	$Si_5As_5Te_3S_7$	Reacts with the atmosphere

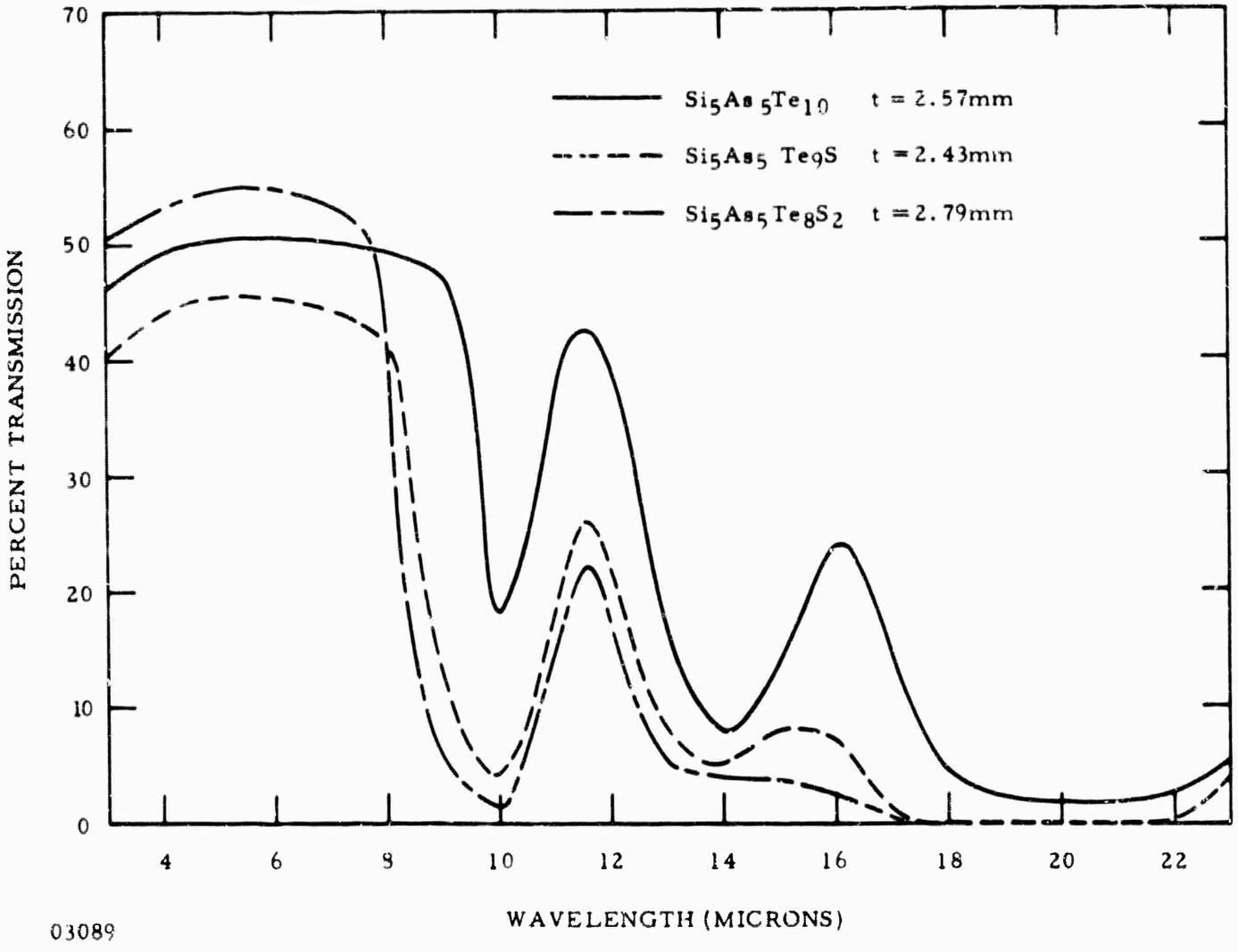

Figure 19 Infrared Transmission of Si-As-Te – Si-As-S Glasses

TABLE XIII

The Si-As-Te → Si-As-Se System

Sample No.	Composition	Softening Point (°C)
353	$Si_{25}As_{25}Te_{50}$	314
359	$Si_{25}As_{25}Te_{49.5}Se_{5}$	311
360	$Si_{25}As_{25}Te_{49}Se$	313
361	$Si_{25}As_{25}Te_{48}Se_{2}$	319
354	$Si_{25}As_{25}Te_{47}Se_{3}$	342
355	$Si_{25}As_{25}Te_{44}Se_{6}$	323
356	$Si_{25}As_{25}Te_{41}Se_{9}$	343
357	$Si_{25}As_{25}Te_{38}Se_{12}$	-
358	$Si_{25}As_{25}Te_{35}Se_{15}$	Too reactive, very brittle
362	$Si_{16.7}As_{16.7}Te_{66.6}$	200
363	$Si_{16.7}As_{16.7}Te_{64.6}Se_{2}$	-
364	$Si_{16.7}As_{16.7}Te_{52.6}Se_{4}$	218
365	$Si_{16.7}As_{16.7}Te_{60.6}Se_{6}$	205
366	$Si_{16.7}As_{16.7}Te_{58.6}Se_{8}$	227
367	$Si_{16.7}As_{16.7}Te_{56.6}Se_{10}$	187
368	$Si_{16.7}As_{16.7}Te_{54.6}Se_{12}$	176
369	$Si_{16.7}As_{16.7}Te_{52.6}Se_{14}$	165
370	$Si_{16.7}As_{16.7}Te_{50.6}Se_{16}$	Too reactive

Infrared transmission was not adversely affected by addition of selenium. Bands are present at 10, 14 and 20 microns, as shown in Figure 20.

4. Si-As-Te → Si-P-Te → Si-Sb-Te

Substituting phosphorus for arsenic caused the silicon to remain unreacted. The base glass, $Si_{15}As_{15}Te_{60}$, and the corresponding Si-P-Te glass were comparable and should have formed an amorphous material. This blend was studied further, but the reason for the unreacted silicon was not determined. Antimony substituted for arsenic in the Si-As-Te system produced little change in softening point and infrared transmission. Results of these two systems are shown in Table XIV.

5. Ge-As-Te → Ge-As-S

When tellurium is replaced by sulfur in the Ge-As-Te system, the softening point increases with an increase in sulfur content, as shown in Table XV. The observed effect was large, even though the ratio of VIA elements to IVA and VA elements was only 0.67. Absorption at 13 microns is increased by addition of sulfur, and the refractive index is lowered. $Ge_4As_{20}Te_{16}$ has a refractive index of 3.57 at 8 microns, and $Ge_4As_{20}Te_{10}S_6$ has 3.12 at the same wavelength. A typical plot of infrared transmission versus wavelength for these two glasses is shown in Figure 21.

6. Ge-As-Te → Ge-As-Se

Table XVI shows how substituting selenium for tellurium affects the softening point in the Ge-As-Te system. In one family of glass, $Ge_{15}As_{15}Te_{70}$, where the group VIA element comprises 70% (atomic) of the composition, the softening point was increased 50% by this substitution. When the group VIA element comprises only 40% (atomic), as in $Ge_{15}As_{45}Te_{40}$, the softening point again was increased by about 50% on almost total substitution of selenium.

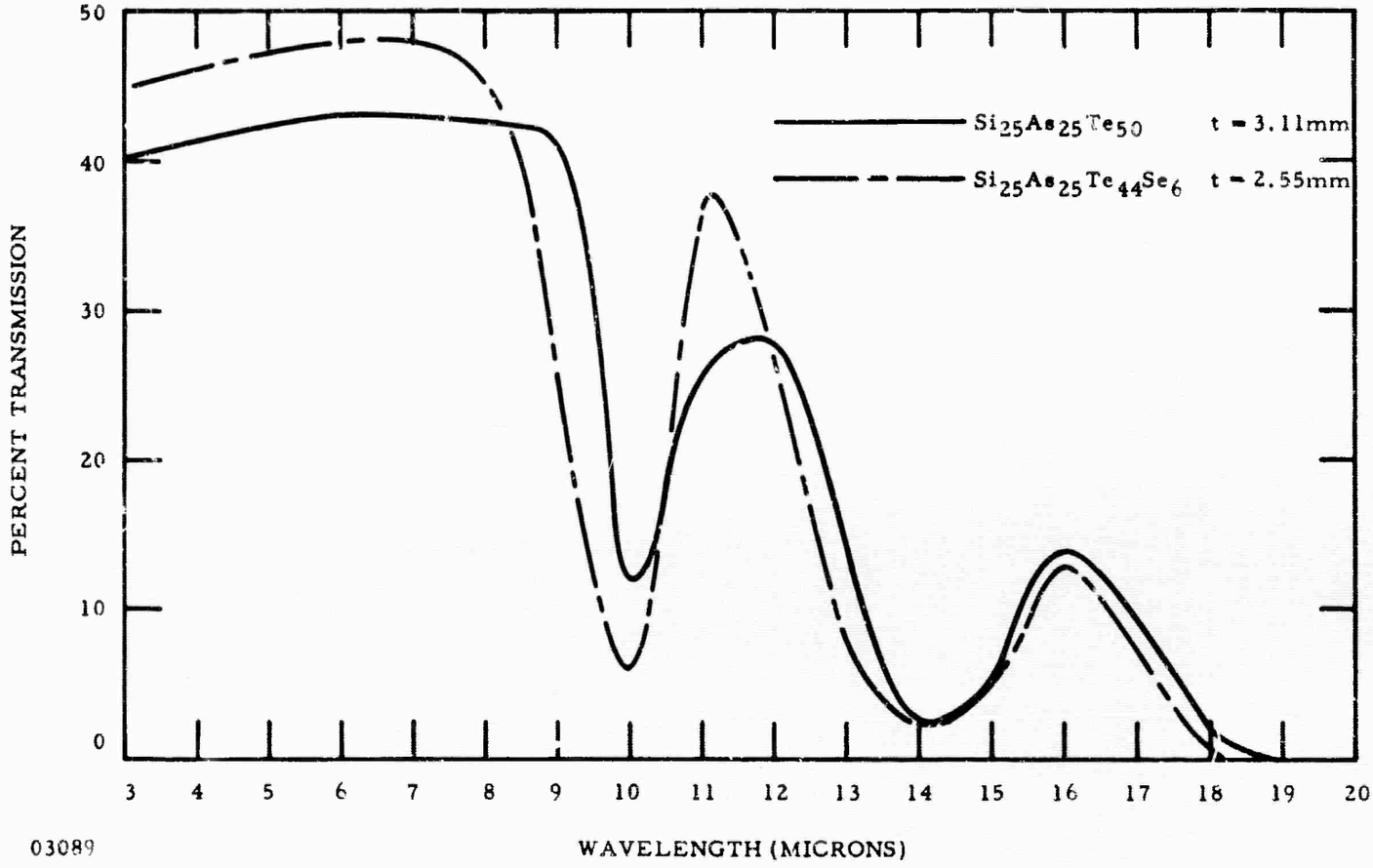

Figure 20 Infrared Transmission of Si-As-Te and Si-As-Te-Se Glass

TABLE XIV

The Si-As-Te → Si-Sb-Te and Si-As-Te → Si-P-Te Systems

Sample No.	Composition	Softening Point (°C)
278	$Si_{14}As_{10}Te_{24}$	341
279	$Si_{14}As_{9}SbTe_{24}$	331
283	$Si_{14}As_{8}Sb_{2}Te_{24}$	334
284	$Si_{14}As_{9}Sb_{3}Te_{24}$	Crystalline
276	$Si_{10}As_{10}Te_{20}$	315
277	$Si_{10}As_{9}SbTe_{20}$	315
280	$Si_{10}As_{8}Sb_{2}Te_{20}$	301
281	$Si_{10}As_{7}Sb_{3}Te_{20}$	300
282	$Si_{10}As_{6}Sb_{4}Te_{20}$	Crystalline
347	$Si_{15}As_{25}Te_{60}$	203
348	$Si_{15}As_{23}P_{2}Te_{60}$	Silicon did not react
349	$Si_{15}As_{21}P_{4}Te_{60}$	Silicon did not react
350	$Si_{15}As_{19}P_{6}Te_{60}$	Silicon did not react
351	$Si_{15}As_{17}P_{8}Te_{60}$	Silicon did not react

TABLE XV

The Ge-As-Te → Ge-As-S System

Sample No.	Composition	Softening Point (°C)
308	$Ge_4As_{20}Te_{16}$	215
309	$Ge_4As_{20}Te_{14}S_2$	223
310	$Ge_4As_{20}Te_{12}S_4$	236
311	$Ge_4As_{20}Te_{10}S_6$	251
318	$Ge_4As_{20}Te_8S_8$	229
319	$Ge_4As_{20}Te_6S_{10}$	280
340	$Ge_4As_{20}Te_4S_{12}$	285
341	$Ge_4As_{20}Te_2S_{14}$	278
342	$Ge_4As_{20}S_{16}$	260

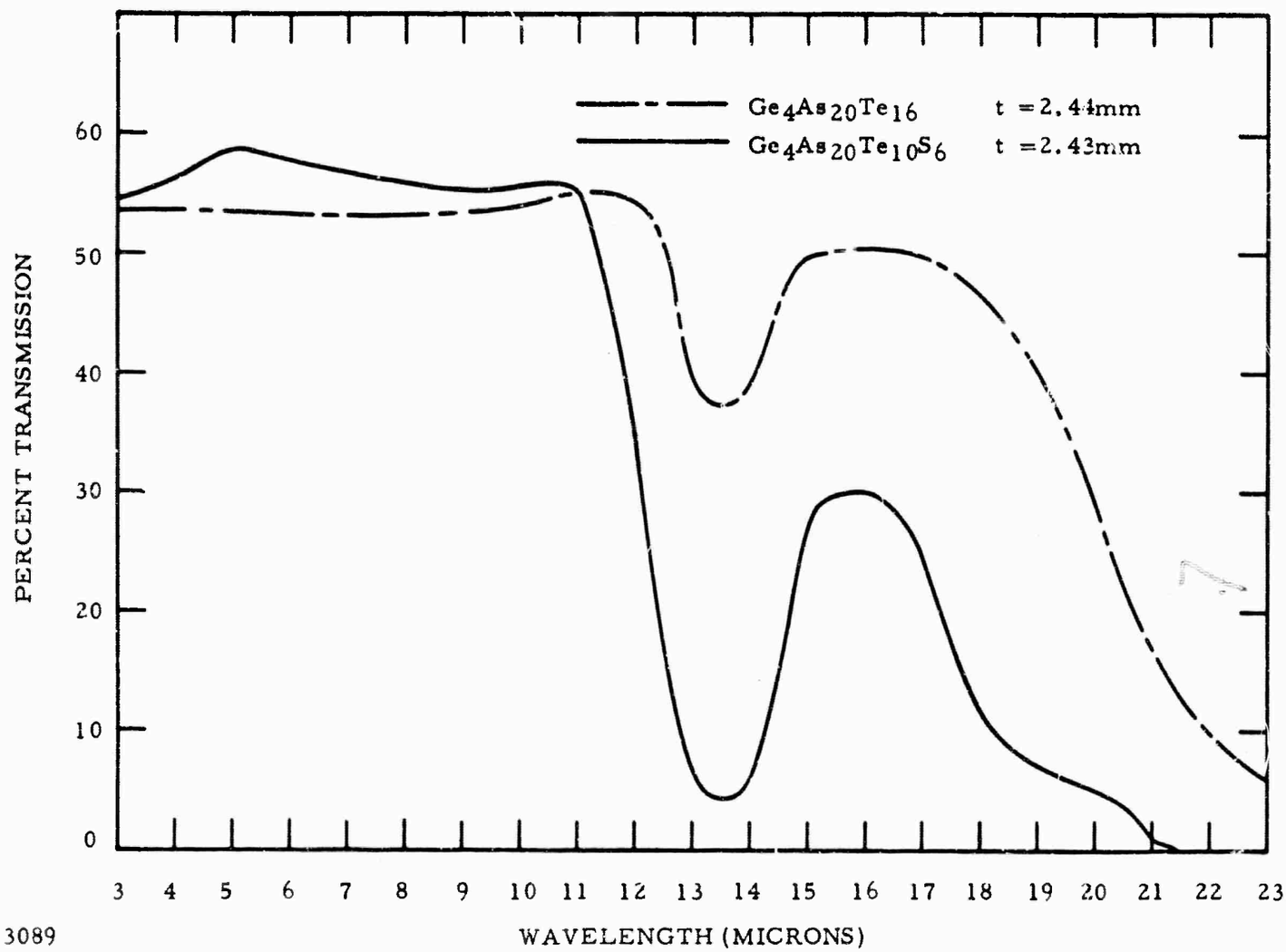

Figure 21 Infrared Transmission of Ge-As-Te and Ge-As-Te-S Glass

TABLE XVI

The Ge-As-Te → Ge-As-Se System

Sample No.	Composition	Softening Point (°C)
320	$Ge_{15}As_{15}Te_{70}$	160
321	$Ge_{15}As_{15}Te_{65}Se_{5}$	194
322	$Ge_{15}As_{15}Te_{60}Se_{10}$	192
323	$Ge_{15}As_{15}Te_{55}Se_{15}$	174
328	$Ge_{15}As_{15}Te_{50}Se_{20}$	192
329	$Ge_{15}As_{15}Te_{45}Se_{25}$	184
330	$Ge_{15}As_{15}Te_{40}Se_{30}$	182
331	$Ge_{15}As_{15}Te_{35}Se_{35}$	210
336	$Ge_{15}As_{15}Te_{30}Se_{40}$	202
337	$Ge_{15}As_{15}Te_{25}Se_{45}$	210
338	$Ge_{15}As_{15}Te_{20}Se_{50}$	206
339	$Ge_{15}As_{15}Te_{15}Se_{55}$	222
344	$Ge_{15}As_{15}Te_{10}Se_{60}$	240
324	$Ge_{15}As_{45}Te_{40}$	247
325	$Ge_{15}As_{45}Te_{35}Se_{5}$	259
326	$Ge_{15}As_{45}Te_{30}Se_{10}$	266
327	$Ge_{15}As_{45}Te_{25}Se_{15}$	283
332	$Ge_{15}As_{45}Te_{20}Se_{20}$	308
333	$Ge_{15}As_{45}Te_{15}Se_{25}$	317
334	$Ge_{15}As_{45}Te_{10}Se_{30}$	322
335	$Ge_{15}As_{45}Te_{5}Se_{35}$	315
343	$Ge_{15}As_{45}Se_{40}$	355

Figure 22 shows change in refractive index as a function of composition for a $Ge_{15}As_{15}Te_{(70-x)}Se_x$ glass. The refractive index is found to change linearly from ~ 3.5 at 8 microns for $Ge_{15}As_{15}Te_{70}$ to 2.9 at 8 microns for $Ge_{15}As_{15}Te_{20}Se_{50}$. A typical plot of infrared transmission as a function of wavelength is shown in Figure 23. The band at 13 microns is reportedly caused by an impurity.[5]

D. General Physical Properties of Non-Oxide Chalcogenide Glasses

1. Softening Points and Hardness

The higher the softening point, the harder the glass. This fact is graphically demonstrated in Figure 24. The measured hardness for about 100 different compositions is plotted against the measured softening point. Many of these glass compositions contained four elements. Even at softening points of 500°C the hardness is not over 250 on the Knoop scale.

2. Thermal Coefficient of Expansion

The higher the softening point, the smaller the thermal coefficient of expansion. Results obtained from about 30 points are plotted in Figure 25. Quantitatively, the relationship is not very clear because the glasses from which these measurements were made are from different systems, and the coefficient of expansion is affected by many factors. As pointed out earlier, small molecules within the glass network can affect such a property.

3. Density

The densities of selenium, tellurium glasses containing silicon, germanium, arsenic, and phosphorus are almost a linear function of the calculated average molecular weight of the glass. The measured densities for 28 glass compositions (a few are sulfur glasses) are plotted against their molecular weights in Figure 26. Many of the samples were small, producing some uncertainty in the density values. The most reliable values were used to form a straight line. These points were the measured densities of large cast Si-As-Te and Ge-As-Te wedges and the

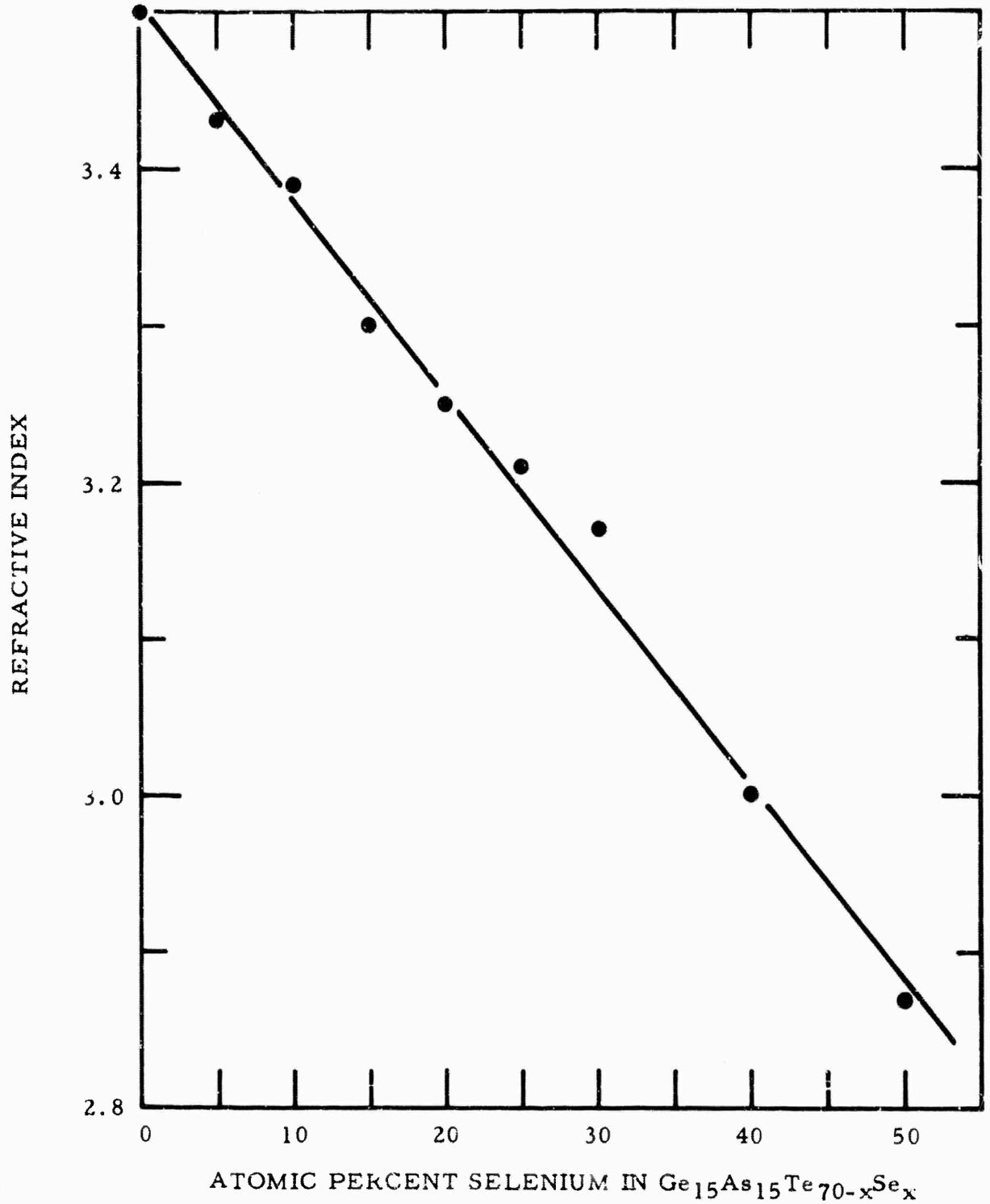

Figure 22 Refractive Index for the $Ge_{15}As_{15}Te_{70} \rightarrow Ge_{15}As_{15}Te_{20}Se_{50}$ System

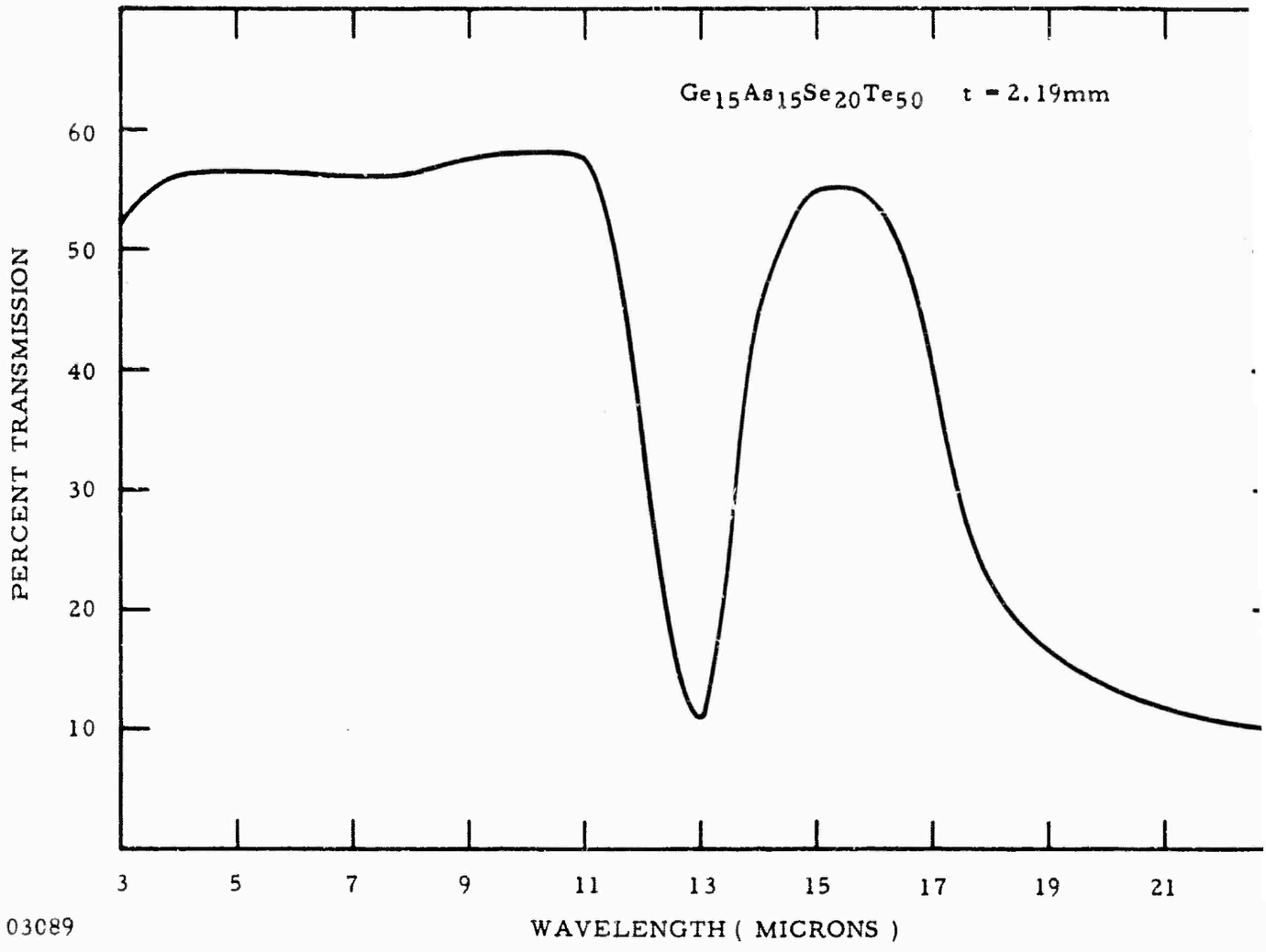

Figure 23 Infrared Transmission of $Ge_{15}As_{15}Se_{20}Te_{50}$

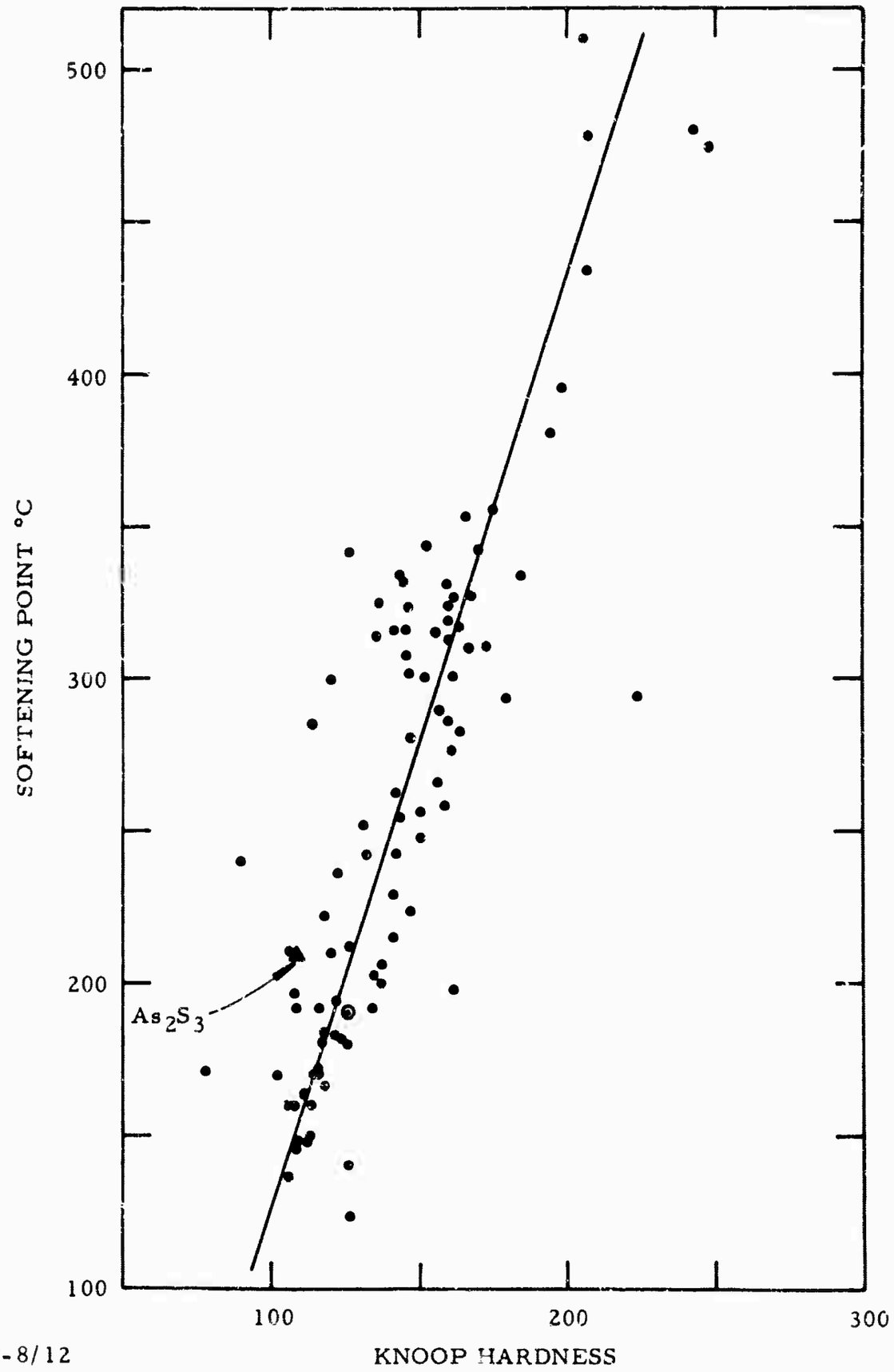

Figure 24 Correlation of Softening Point and Knoop Hardness

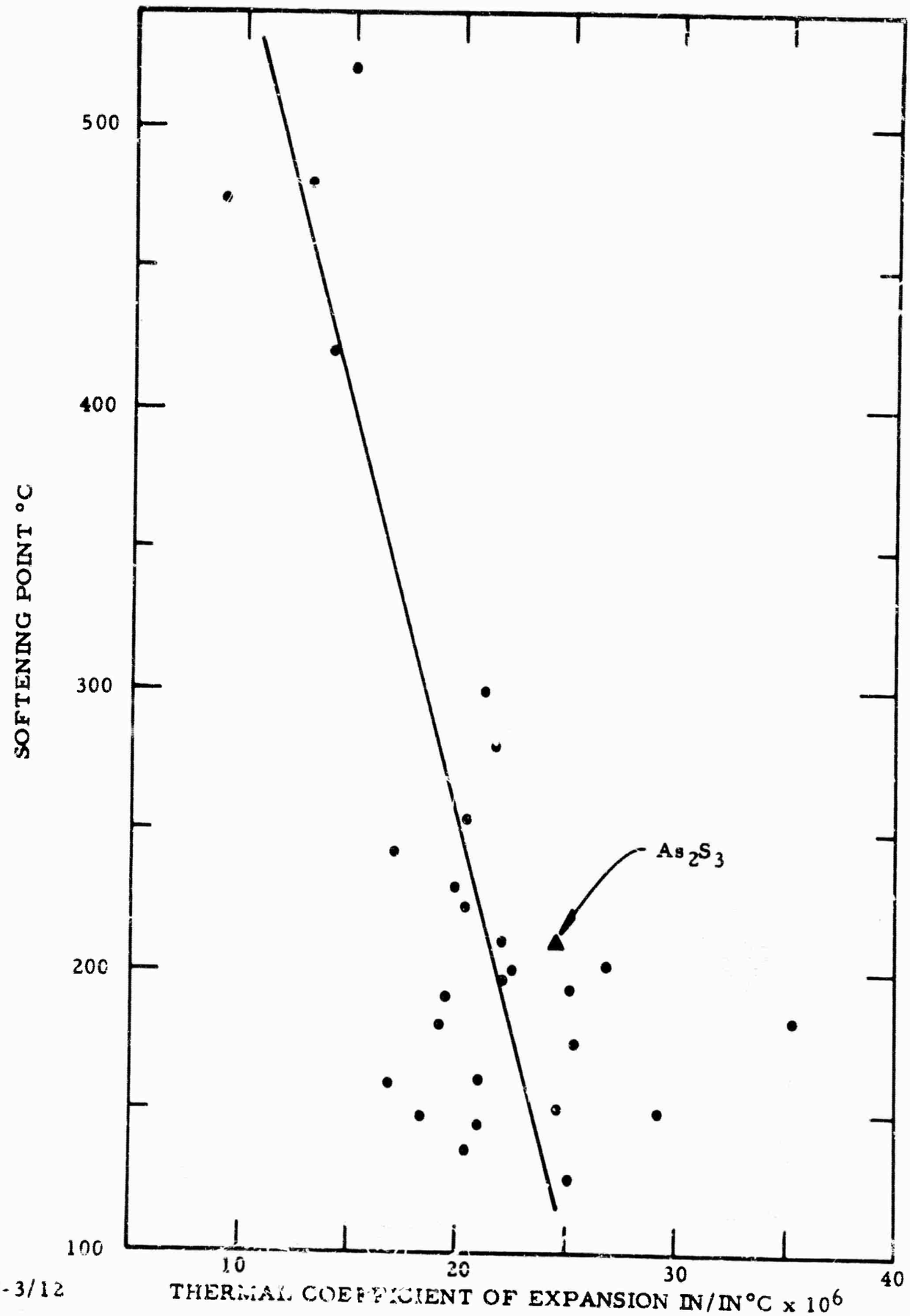

Figure 25 Correlation of Softening Point and Thermal Coefficient of Expansion

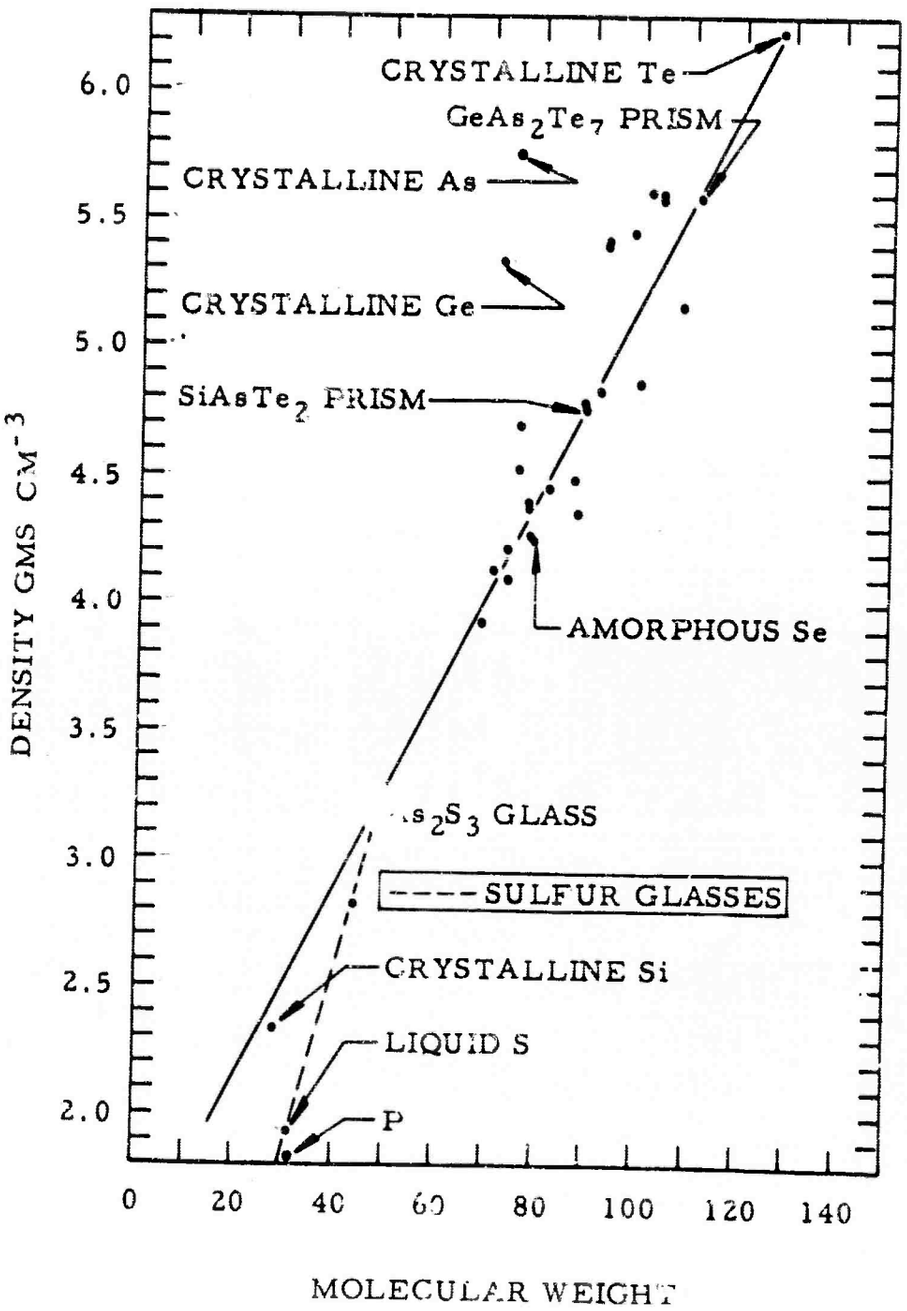

Figure 26 Density Versus Molecular Weight for Non-Oxide Chalcogenide Glasses

literature value for the density of As_2S_3 glass. It is surprising to note that crystalline tellurium, crystalline silicon, and amorphous selenium fall almost on this line. The few points available for sulfur glasses indicate they follow a line of a different slope, shown by dashes in the figure. The density and atomic weights of germanium, arsenic, and yellow phosphorus are plotted for reference.

Many of the measured densities do not fall on the line. Some variations represent errors in the data, some represent real differences in densities. As the percentage of the group IVA and VA elements increases, deviation from the line should increase. The linear relation seems to hold up to a small percentage (around 10%). To verify these results, measured density values for 15 samples of Ge-As-Se glasses reported by Myuller, et al.,[14] were compared with those predicted from the straight line of Figure 26 and the calculated molecular weight. The results are shown in Table XVII. Agreement is -3%.

4. Physical Strength

Attempts to measure the physical strength of glass samples were unsuccessful. Several samples of Ge-As-Te glasses were blended with sulfur and selenium and the tensile strength of the samples measured. The results are shown in Table XVIII. Most of the samples initiated fracture at very low pressure (< 1000 psi), and large scatter was found in the data (± 100%). The smaller values represent fracture due to sample imperfection, and the larger values represent either ultimate tensile strength of the glass or a sample of better perfection. The only conclusion that can be drawn is that these glasses have ultimate tensile strength values of at least 700-1000 psi. Large, almost perfect samples are needed for meaningful measurements.

5. Electrical Properties

The non-oxide chalcogenide glasses are high resistivity semiconductors.[12] Their electrical properties have been investigated extensively.[7,12,15] Although electrical properties were not emphasized in this program, attempts were made to measure the values for several glasses. The results are shown in Table XIX.

TABLE XVI[illegible]

Density of Ge-As-Se Glasses[14]

Glass (Atom%)	Density Measured	Density Calculated	% Error
$As_{35.7}Se_{60.7}Ge_{3.6}$	4.59	4.37	- 4.7
$As_{32.2}Se_{61.3}Ge_{6.5}$	4.57	4.33	- 5.2
$As_{25.0}Se_{62.5}Ge_{12.5}$	4.50	4.29	- 4.6
$As_{18.2}Se_{63.6}Ge_{18.2}$	4.44	4.33	- 2.5
$As_{14.3}Se_{64.3}Ge_{21.4}$	4.37	4.33	- 0.9
$As_{19.3}Se_{58.0}Ge_{22.7}$	4.39	4.33	- 1.4
$As_{27.2}Se_{40.9}Ge_{[illegible]}$	4.58	4.29	- 6.3
$As_{23.9}Se_{52.2}$ [illegible]	4.43	4.31	- 2.7
$As_{19.7}Se_{42.9}Ge_{37.4}$	4.58	4.29	- 6.3
$As_{22.2}Se_{55.6}Ge_{22.2}$	4.41	4.33	- 1.6
$As_{20.0}Se_{60.0}Ge_{20.0}$	4.41	4.33	- 1.6
$As_{26.6}Se_{60.0}Ge_{13.4}$	4.45	4.33	- 2.7
$As_{13.4}Se_{60.0}Ge_{26.6}$	4.37	4.33	- 0.9
$As_{29.6}Se_{55.6}Ge_{14.8}$	4.44	4.33	- 2.5
$As_{14.8}Se_{55.6}Ge_{29.6}$	4.39	4.31	- 1.8

-3% Average Error

TABLE XVIII

Tensile Strength of Some Germanium Glasses

Glass Composition	Ultimate Tensile Strength (psi)
$Ge_4As_{20}Te_6S_{10}$	1030
$Ge_{15}As_{15}Te_{65}Se_5$	500
$Ge_{15}As_{15}Te_{15}Se_{55}$	290* 700
$Ge_{15}As_{15}Te_{10}Se_{60}$	330*
$Ge_{10}As_{50}Te_{40}$	770
$Ge_{10}As_{50}Te_{30}S_{10}$	390* 740

*Fracture initiated by sample defects

TABLE XIX

Dielectric Properties of Some Glasses

Glass	Dielectric Constant	Frequency (cps)	Resistivity (ohm-cm) (300°K)
$Ge_{15}As_{15}Se_{70}$			5×10^{10}
$Si_{15}Sb_{15}S_{70}$			9.6×10^{7}
$Ge_{15}P_{15}Se_{70}$			9.3×10^{10}
$Si_{15}Sb_{35}S_{50}$	14	100	2×10^{9}
$Si_{6}As_{9}Te_{45}$			5×10^{5}
$Ge_{2}As_{3}Te_{15}$			2×10^{7}
$Si_{3}Ge_{2}As_{5}Te_{10}$	24	1kc	1×10^{8}
$Ge_{3}P\ S_{6}$			9×10^{9}
$GeAs_{4}Te_{5}$			5×10^{5}
$Si_{4}As_{3}Te_{3}$			5×10^{9}
$GeAs_{2}Te_{7}$			2.8×10^{4}

A dielectric constant reading was obtained for only two samples. Resistivities vary from 10^4 to 10^{10} ohm-cm.

E. Glasses Characterized in Detail

Optical and related properties of glasses cannot be determined accurately unless large samples are available. During most of this program, exploratory work has been emphasized, and there was not enough time to work out the technical details needed to fabricate a particular glass composition in large, usable pieces. Recently, it became apparent that large plates of infrared transmitting glasses would soon be needed for airborne infrared optical systems manufactured at Texas Instruments. A small sideline effort was organized to try to cast large glass plates. The glasses selected for development were Si-As-Te, Ge-As-Te, and blended glasses of the two systems. The work was funded under Contract No. DA 36-039-AMC-00133(E) with TI's Apparatus division. The successful results of this effort are illustrated in Figure 27, which shows an 8 in. x 10 in. x 1/4 in. glass plate and several prisms.

As part of our present program these glasses were optically and physically characterized. The refractive index was precisely measured using the cast glass prisms and the refractive index attachment for the spectrophotometer already described. The measurements are good to at least four numbers, with some doubt in the fifth (± 0.0003). From the precise index value, reflectivity and the absorption constant were calculated. Results obtained for Si-Ge-As-Te glass, a Si-As-Te glass, and a Ge-As-Te glass are shown in Figures 28-30. Two prisms of Si-Ge-As-Te glass, from different melts made with different starting materials, were measured. The refractive index differences ranged from only 0.0026 at 3 microns to 0.0010 at 8 microns, surprisingly good agreement. With the criterion that an optical material should have an absorption coefficient less than 1 cm^{-1}, the Si-Ge-As-Te glass is good from 2.5 to 12.5 microns, the Si-As-Te good to only about 9 microns, and the Ge-As-Te good from 2.5 to 20 microns. Softening points, deformation points, thermal coefficients of expansion, and hardness of all three glasses are shown in Table XX. Quantitative

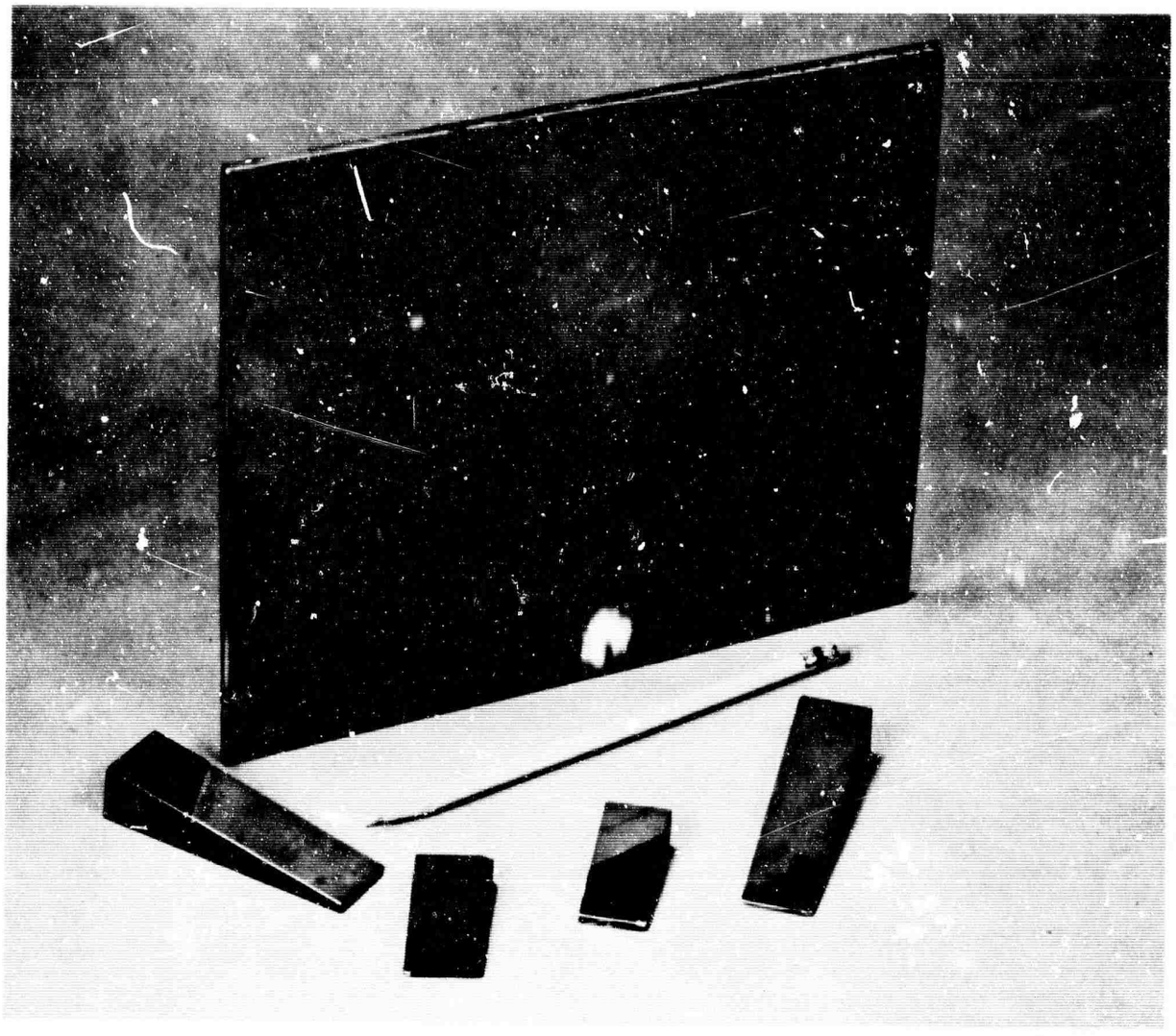

Figure 27 Photograph of Large Prisms and One Plate of Non-Oxide Chalcogenide Glasses

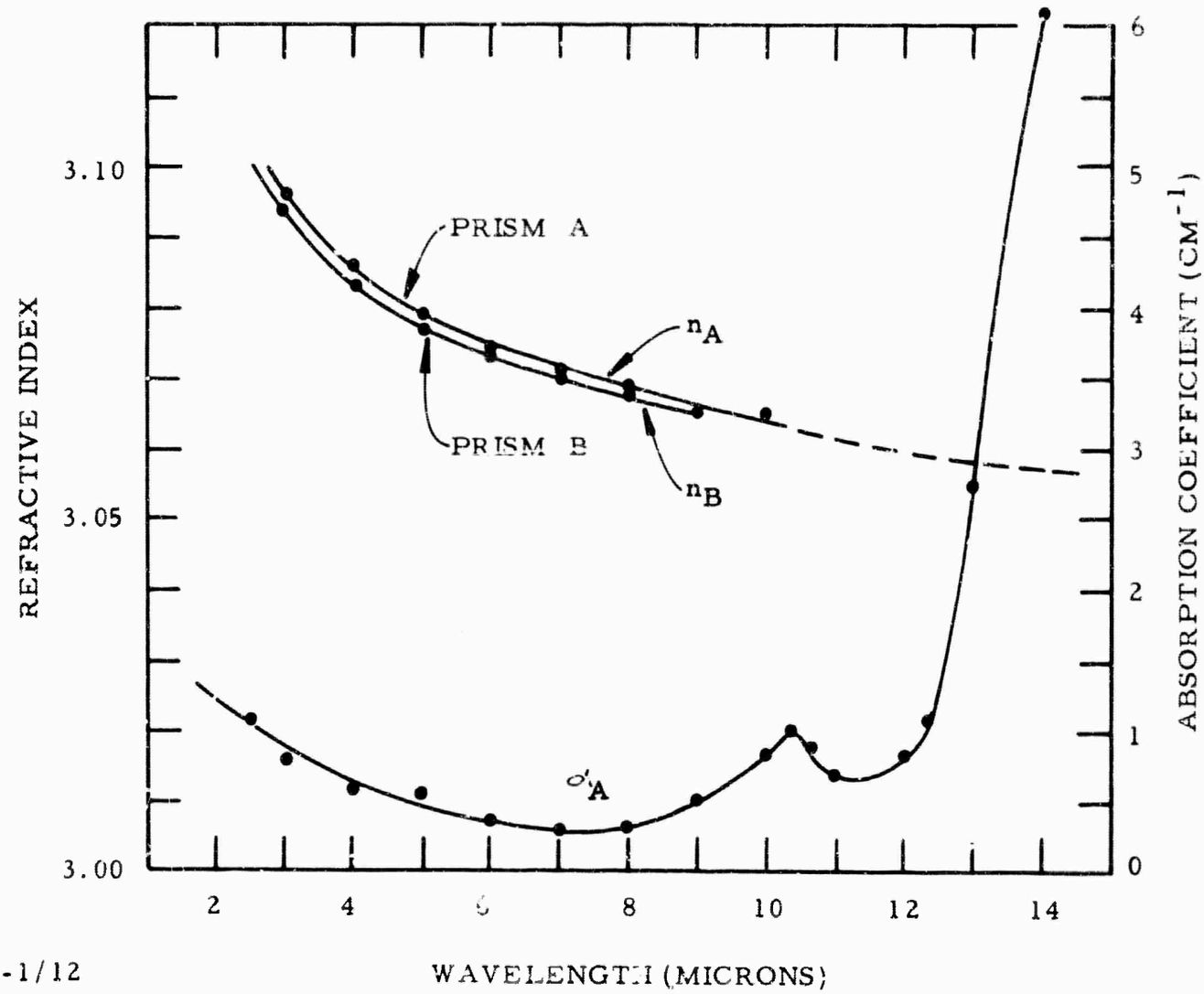

Figure 28 Optical Constants of $Si_2Ge_3As_5Te_{10}$ Glass

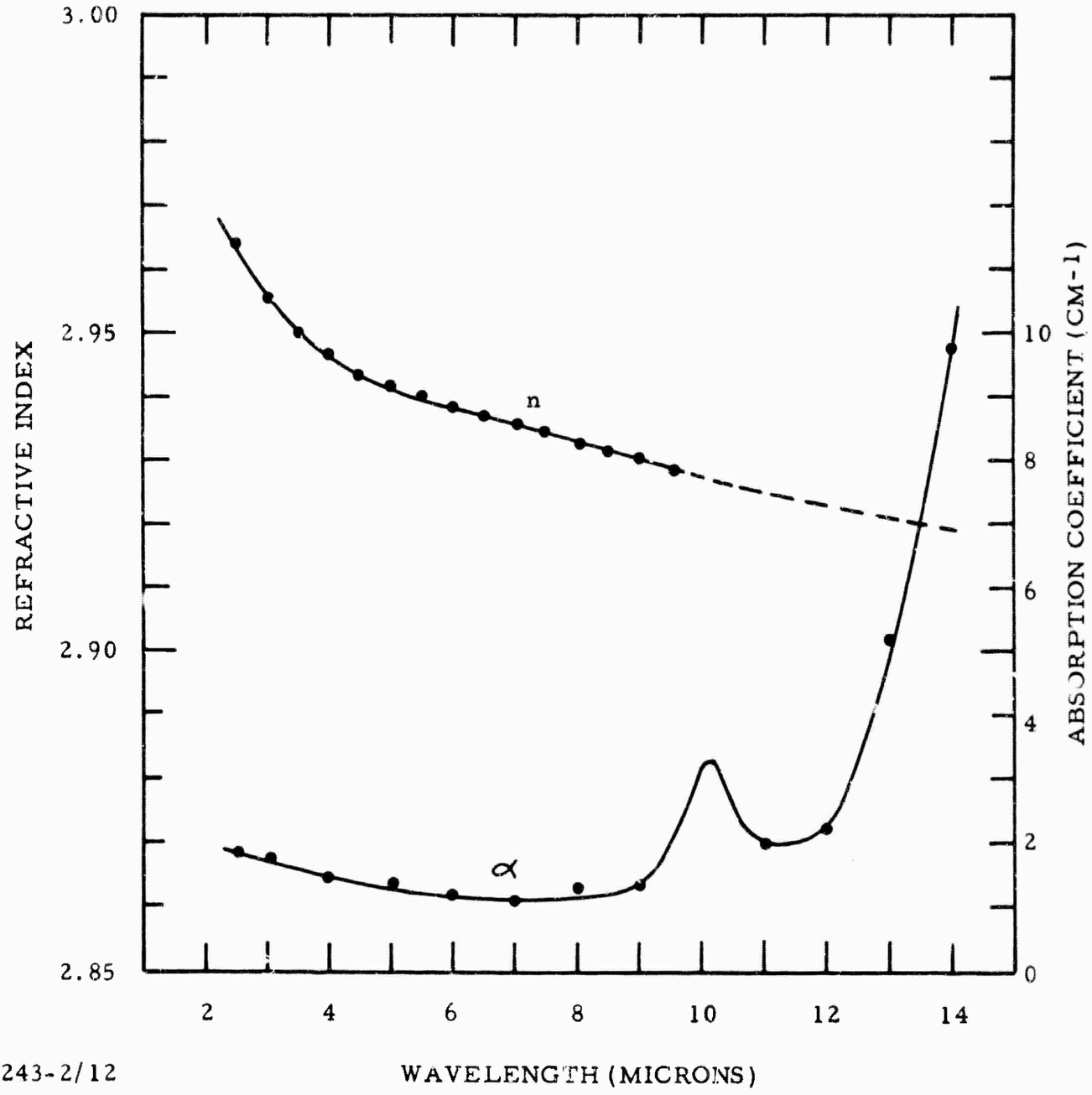

Figure 29 Optical Constants of $SiAsTe_2$ Glass

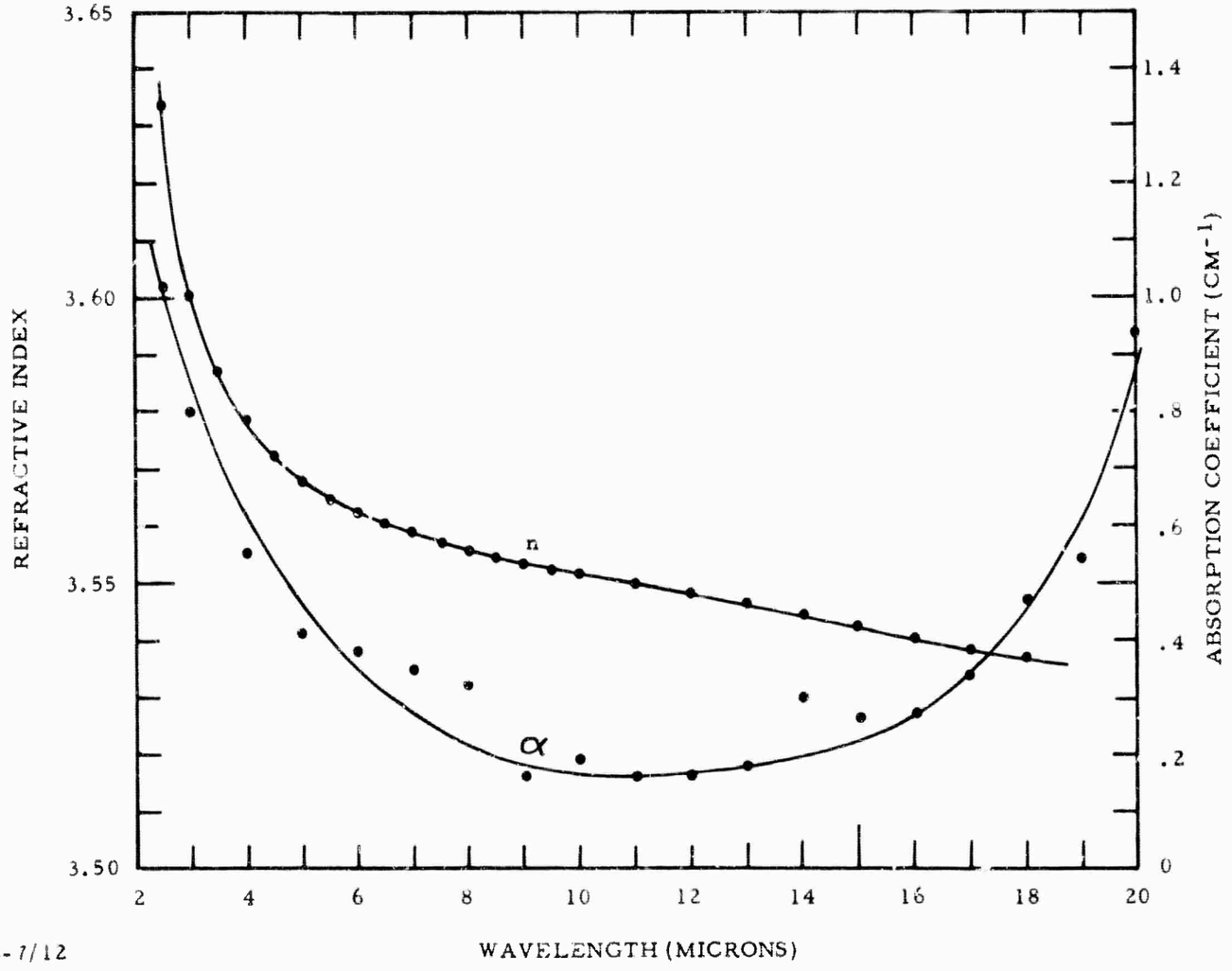

Figure 30 Optical Constants of $GeAs_2Te_7$ Glass

TABLE XX

Physical Constants of Characterized Glasses

Composition	Refractive Index	Softening Point (°C)	Deformation Point (°C)	Thermal Coefficient of Expansion (in./in.°C x 10^6)	Hardness (Knoop scale)
$SiAsTe_2$	2.93	317	250	13	167
$Si_3Ge_2As_5Te_{10}$	3.06	320	284	10	179
$GeAs_2Te_7$	3.55	178	140	18	111
Ge_3PS_6	2.15	520	375	15	185
Ge_7PS_{12}	2.20	480	360	13	179
Ge_2S_3	2.30	420	360	14	179
$Si_6As_4Te_9Sb$	2.95	475	350	9	168

results obtained for several other promising glasses are also included.

Most of the glasses studied in this program have had high refractive indexes, particularly the best optical quality Si-As-Te and Ge-As-Te glasses. Because of large reflection losses caused by the high refractive indexes, transmission of these glasses is greatly reduced. The reflection loss can be significantly reduced by using suitable dielectric reflection coatings, as is done in the high index crystalline materials. The glasses studied take dielectric coatings quite well. The results obtained when a 10-micron quarter-wave coating was applied to a Si-Ge-As-Te glass window are shown in Figure 31. The average transmission in the range 8 to 13 microns was raised to 77% in this sample. The dielectric used was PbF_2.

F. Elemental Effects in Non-Oxide Glasses

The starting point in understanding how individual elements affect the properties of the glasses is their individual tendency toward glass formation. In Figure 32 the glass-forming composition regions of the Ge-P-S, Ge-P-Se, and Ge-P-Te systems and the Si-As-Te, Si-P-Te, Ge-As-Te, and Ge-P-Te systems are compared. If the differences in size of the glass-forming composition areas is taken as a measure of differences in tendency toward glass-forming ability for the different elements, the conclusions are:

Glass Forming Tendency

S > Se > Te

As > P > Sb

Si > Ge > Sn

This conclusion is in agreement with the conclusions of Russian investigators[12] except for the reversal of P and As, which is somewhat puzzling. It has been suggested* that the reversed order of these elements is due to the

* Professor Heinz Krebs, Lehrstuhl für Anorganische Chemie der Technischen Hochschule, Stuttgart, Germany. Visiting Scientist at Texas Instruments, Summer of 1964.

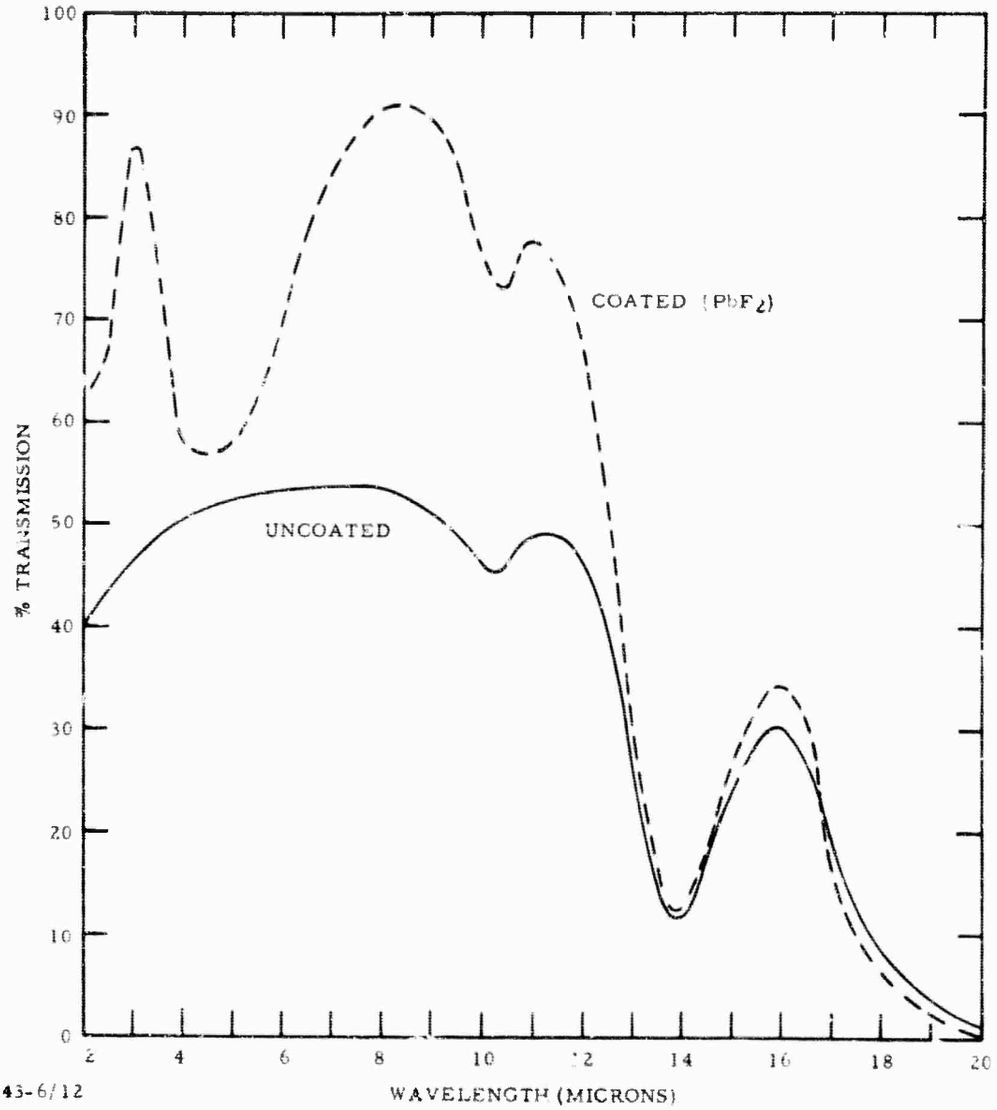

Figure 31 IR Transmission of Cast Si-Ge-As-Te Glass Before and After Coating with PbF_2

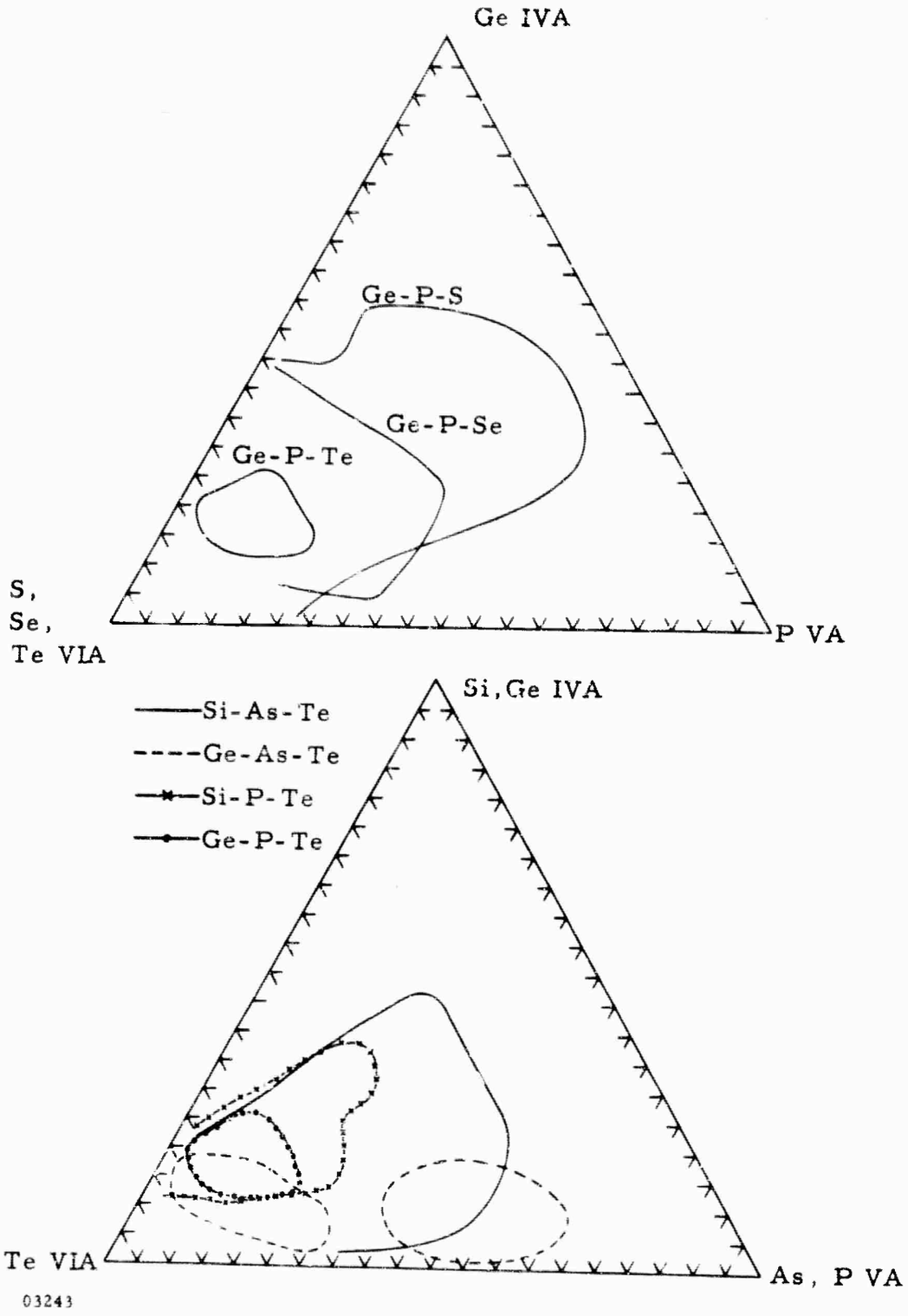

03243

Figure 32 A Comparison of the Glass-Forming Composition Regions of the Ternary Systems

ability of As to form bonds with Si and Ge, while P[18] does not. A discussion of glass formation from the standpoint of classical structural inorganic chemistry is presented in Appendix I.

When one compares the softening points of different glasses, especially those differing only by one constituent element, qualitative conclusions concerning softening points can be drawn. Generally, softening points decrease with increasing atomic weight of the constituent element used. That is:

Softening Points

S > Se > Te

P > As > Sb

Si > Ge > Sn

Obviously, the differences in physical properties of the two types of glasses must lie in the differences in type and strength of their individual chemical bonds. Insight into why these differences are so great can be gained by examining the electronegativities and electronegativity differences for the elements concerned. The values are shown (using the Pauling scale) in Table XXI. Note the electronegativity of oxygen is 3.5 while the next chalcogen, sulfur, is only 2.5, a full unit difference. The values for selenium and tellurium are 2.4 and 2.1, respectively, almost the same as sulfur. Sulfur, selenium, and tellurium are solids. All three elements show a tendency toward forming covalent bonds with themselves in the form of rings and chains (tellurium to a lesser extent). Oxygen is a diatomic gas, not like the other chalcogens at all. If many of the general properties of the non-oxide chalcogens are preserved in the glasses, there is no reason at all to expect them to be similar to oxide glasses.

Electronegativity difference can be taken as a rough measure of the bond energy between two atoms. The larger the difference, the more likely a bond will form. The smaller the difference, the more covalent the nature of the bond. A purely covalent bond has an electronegativity difference of zero

TABLE XXI

Bonding in Chalcogenide Glasses

Pauling Electronegativities:

		O - 3.5
Si - 1.8	P - 2.1	S - 2.5
Ge - 1.8	As - 2.0	Se - 2.4
Sn - 1.8	Sb - 1.9	Te - 2.1

Electronegativity Differences:

Δ	Δ	Δ
Si-O-1.7	P-O-1.4	Si-P-0.3
Si-S-0.7	P-S-0.4	Si-As-0.2
Si-Se-0.6	P-Se-0.3	Ge-P-0.3
Si-Te-0.3	P-Te-0.0	Ge-As-0.2
Ge-O-1.7	As-O-1.5	
Ge-S-0.7	As-S-0.5	
Ge-Se-0.6	As-Se-0.4	
Ge-Te-0.3	As-Te-0.1	

Oxide Glasses Characterized by:

$$- O - M_1 - O - M_2 - O$$

Non-Oxide Chalcogenide Glasses Characterized by:

$$- X - M_1 - X - M_2 - X$$

or

$$- X - M_1 - M_2 - X$$

The differences listed in Table XXI reveal not only the covalent nature of the bonding between the group IVA and group VA elements with the chalcogens, but also the possibility of bond formation between the IVA and VA elements. Oxide glasses are always characterized by metal-oxygen-metal bonds, (referring to the group IVA and VA elements as metals) while the other chalcogenide glasses may contain covalent metal-metal bonds. Because of oxygen's low electronegativity, the metal-oxygen bond is always more stable thermodynamically than the metal-metal covalent bonds.

Covalent bonding in itself does not produce weak solids. The physical constants for silicon are those of a hard, strong, high melting solid. But to break down the amorphous chains and rings and form a strong three-dimensional network structure, the bond energy between other elements combined with sulfur, selenium, or tellurium must be greater than the elemental covalent bond energies.

G. Location of Glass-Forming Composition Regions in IVA-VA-VIA Ternary Systems

The boundaries of a glass-forming region in a ternary system represent a composition region so favorable to formation of crystallites that the resultant material takes on the nature of a crystalline material. This suggests that the glasses in the molten state are composed of a mixture of different stoichiometric molecules. If the concentration of one specific composition becomes great enough, nucleation occurs rapidly during the quench, and a crystalline-like material results. Therefore, the larger the number of molecules that can form between three specific elements, the larger the glass-forming composition region. A ternary system may be considered as the mixture of three binary systems: IVA-VA, IVA-VIA, and VA-VIA. The molecules from the three binaries act as a diluent for each other, preventing crystallization and promoting the formation of amorphous materials.

The mixed molecular approach to IVA-VA-VIA glass formation is supported by experimental data. The simplest case is the mixture of two binaries; no compound formation is possible in the third binary. The Si-Sb-Se system is typical of this case. The glass-forming region and pertinent compounds are

shown in Figure 33. The binary compounds are taken from two standard sources.[18,19] A line is drawn from the compound $SiSe_2$ toward an increase in the percentage of Sb. Composition points along this line represent compositions in which the correct ratio between silicon and selenium is maintained for the formation of $SiSe_2$. Along this line the $SiSe_2$ melt is diluted with antimony. The same may be said for the line drawn from the compound Sb_2Se_3 in the direction of an increase in the percentage of silicon. The glass-forming area for the Si-Sb-Se system lies within the area enclosed by these two lines. Compositional points close to the compound boundaries produce crystalline-like materials. Similar results are obtained for the Si-Sb-S system (Figure 34), the Ge-Sb-Se system[20] (Figure 35), and the Si-P-Te system (Figure 36). The dotted line in Figure 36 marks the boundary of the Si-Te eutectic occurring at 85 atom-percent tellurium.[21] A eutectic around 85 atom-percent tellurium also occurs in the Ge-Te binary,[18] Al-Te,[18] Au-Te,[18] Hg-Te,[18] InTe,[18] and probably many others. In tellurium-based glasses, the Te-IVA eutectic marks the boundary of the glass-forming regions of high chalcogenide compositions.

In the second case of interest, at least one compound is formed between the IVA and VA elements. Typical of this case is the Ge-P-Te system (Figure 37), the Ge-P-Se system (Figure 38) and the Ge-P-S system (Figure 39). The glass-forming composition regions are somewhat symmetrically located about this composition line. Generally, the glass regions still lie within the area set off by the lines of the IVA-VA compounds and the IVA-VIA compounds. The Ge-P-S system is extended somewhat past this boundary, probably because of the solubility of unreacted phosphorus in the molten Ge-P-S glasses.

The third case is one in which more than one IVA-VA compound formed. Typical are the Ge-As-Se system[5] (Figure 40), the Ge-As-Te system (Figure 41), and the Si-As-Te system (Figure 42). The second compound formed between the IVA and VA elements removes the barrier to glass formation represented by the VA-VIA compound line. The glass-forming region is effectively double that expected if there were no IVA-VA compound formation.

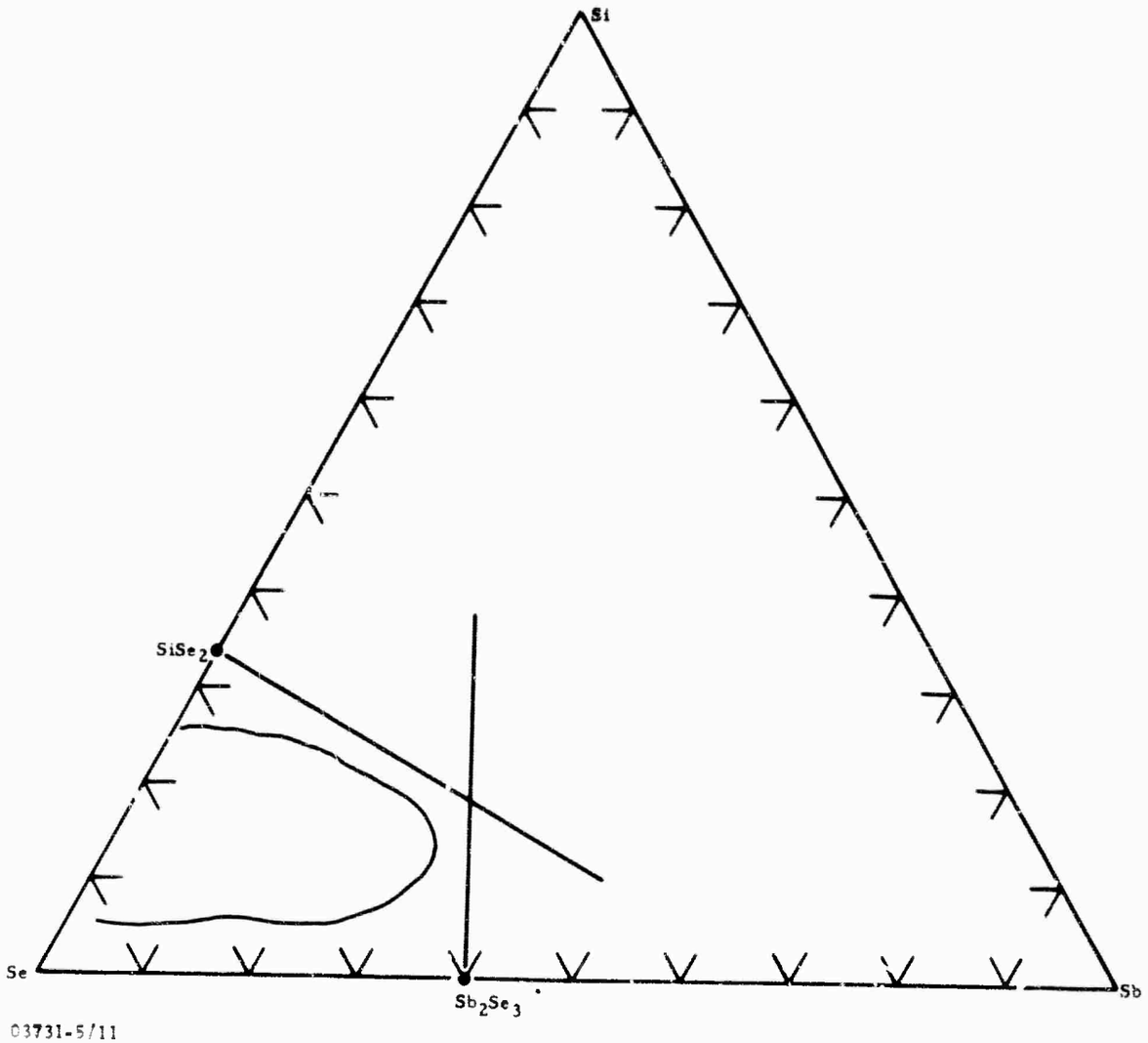

Figure 33 The Si-Sb-Se System

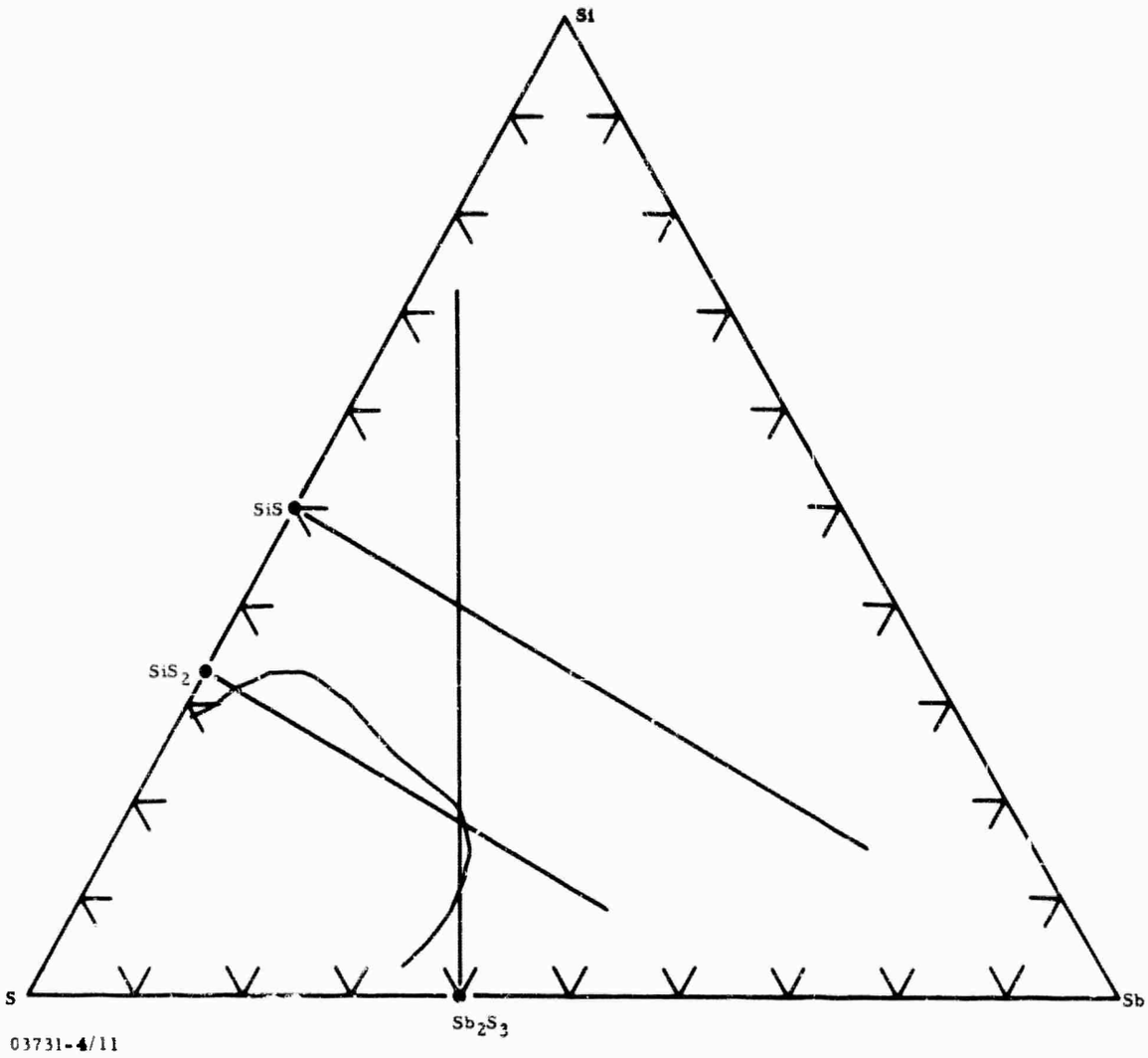

Figure 34 The Si-Sb-S System

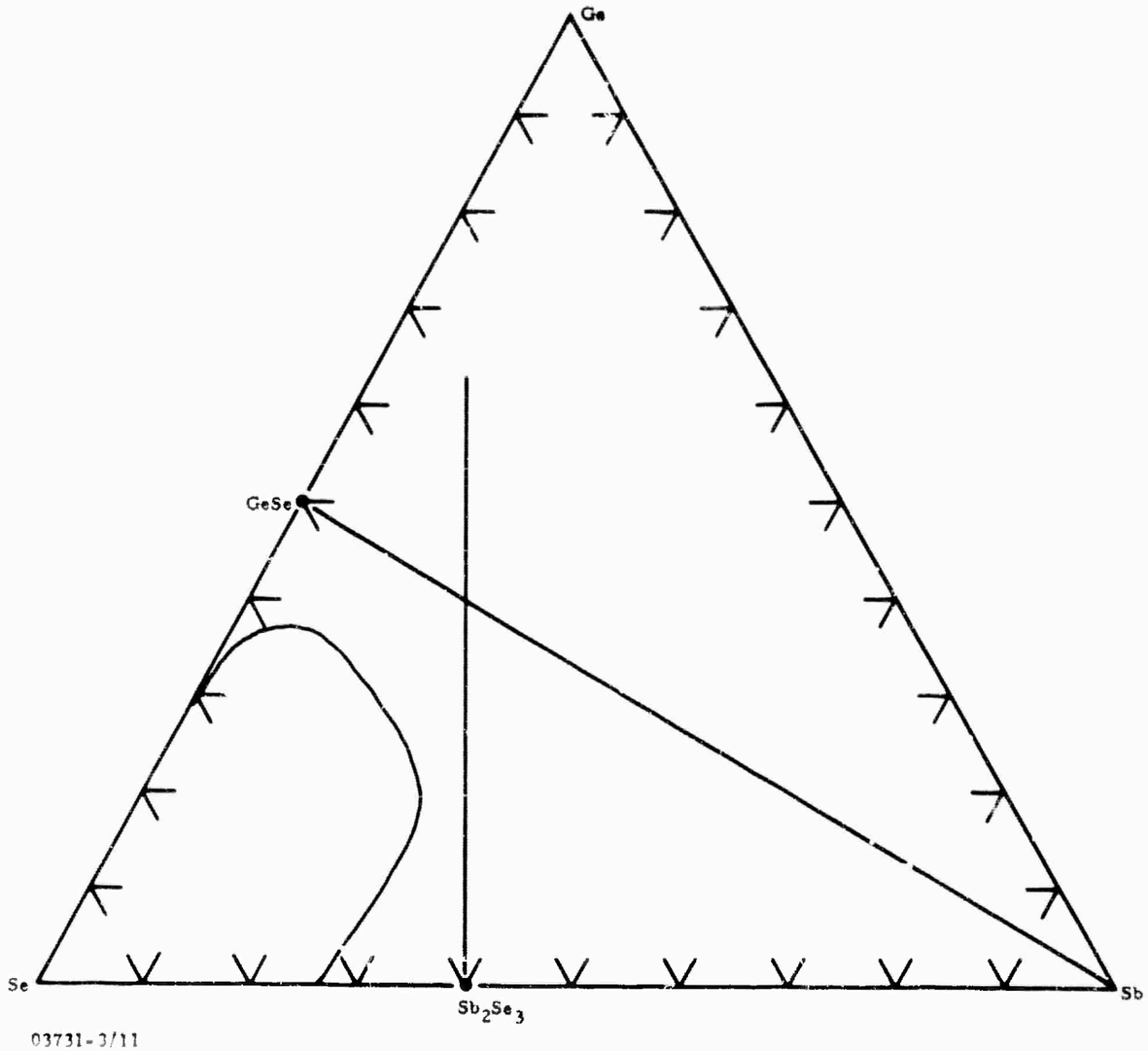

Figure 35 The Ge-Sb-Se System[20]

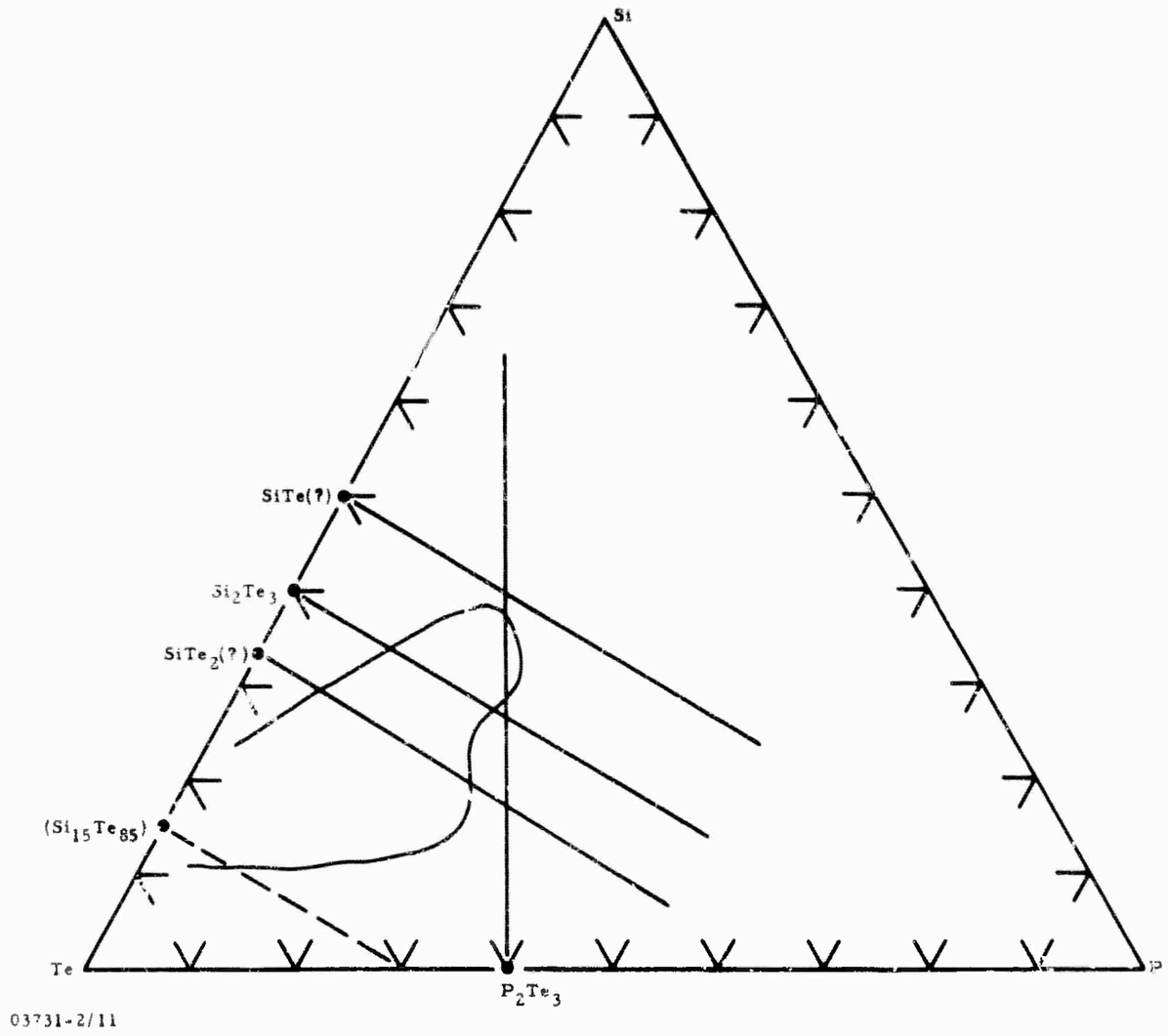

Figure 36 The Si-P-Te System

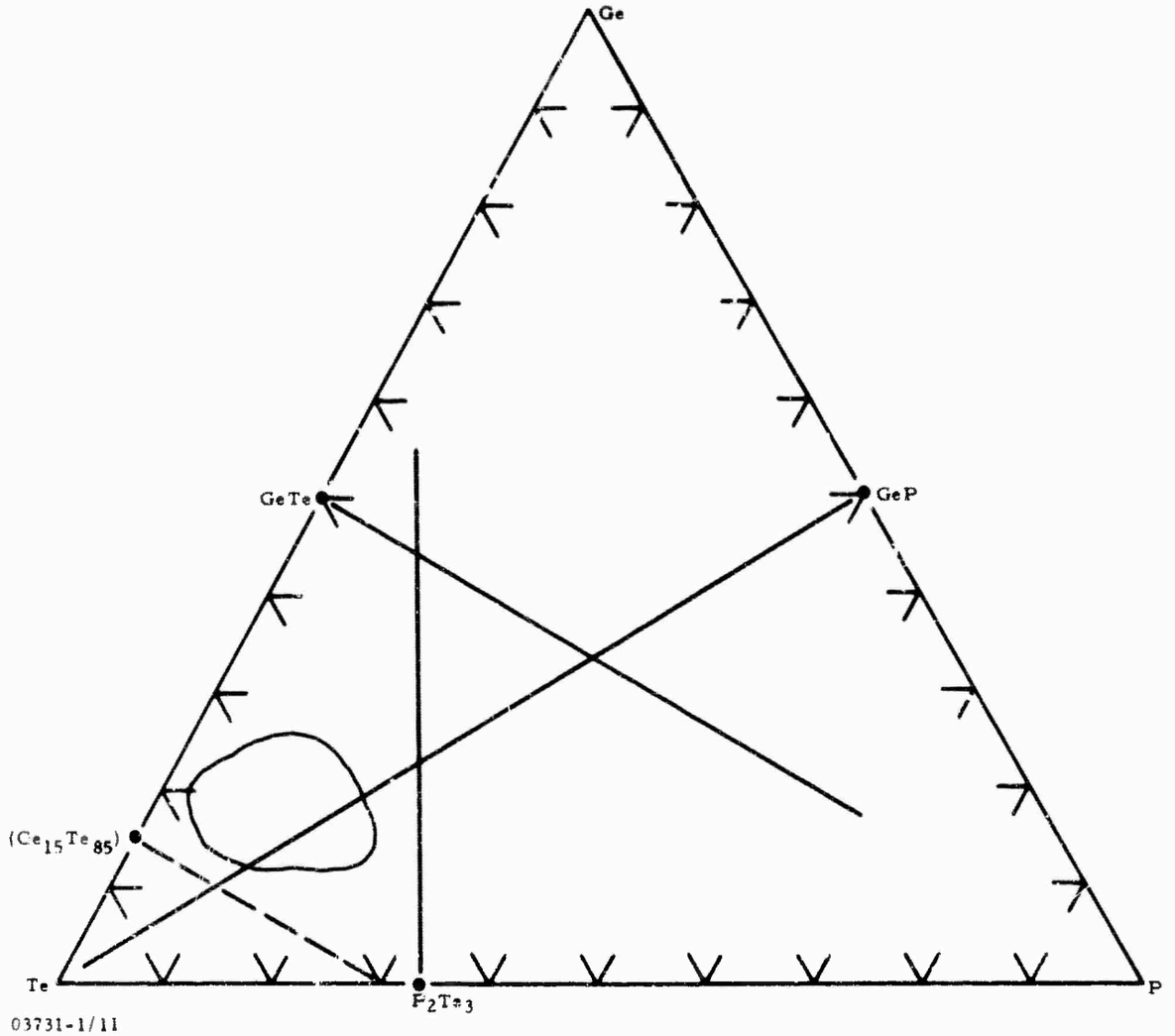

Figure 37 The Ge-P-Te System

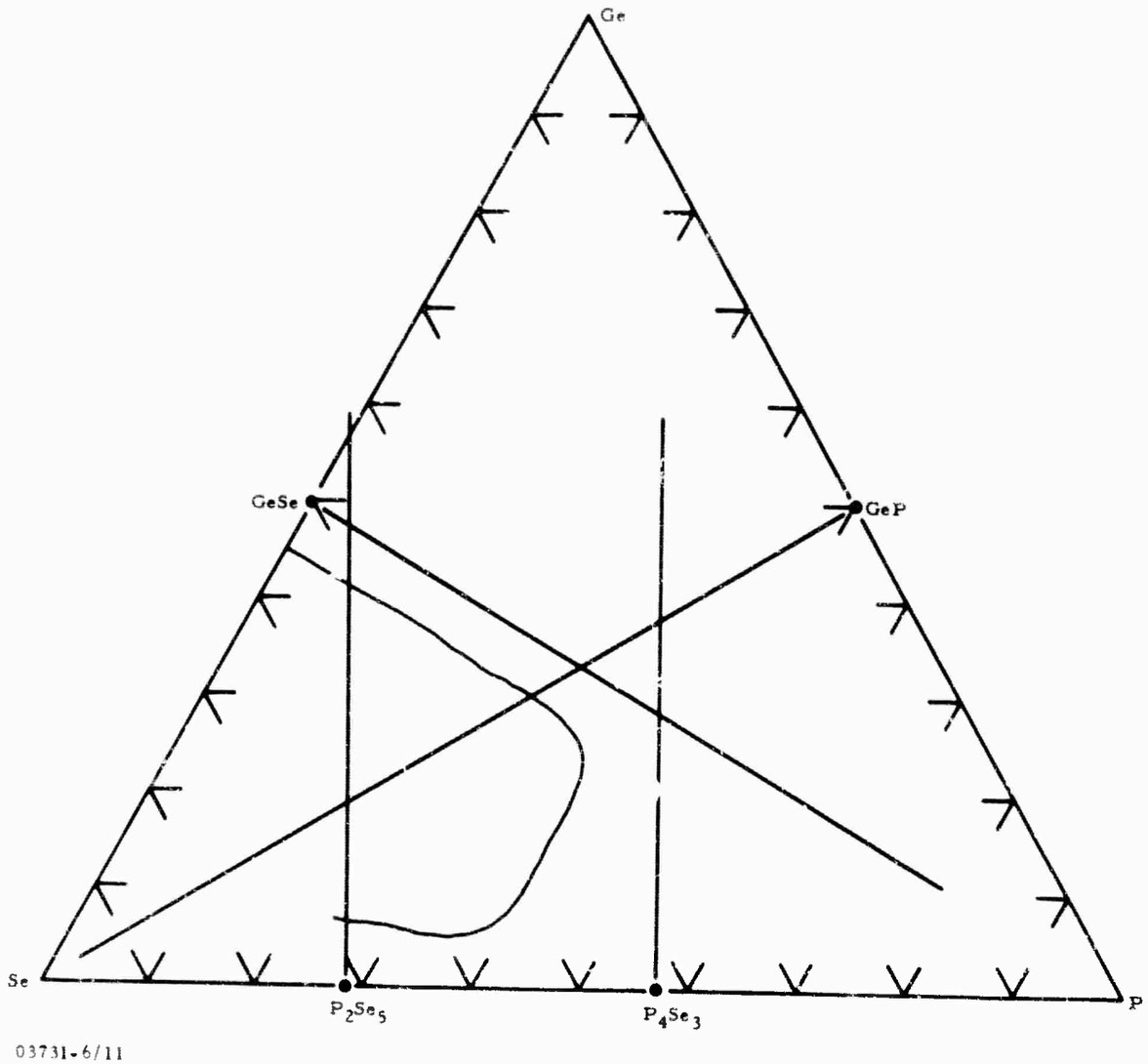

Figure 38 The Ge-P-Se System

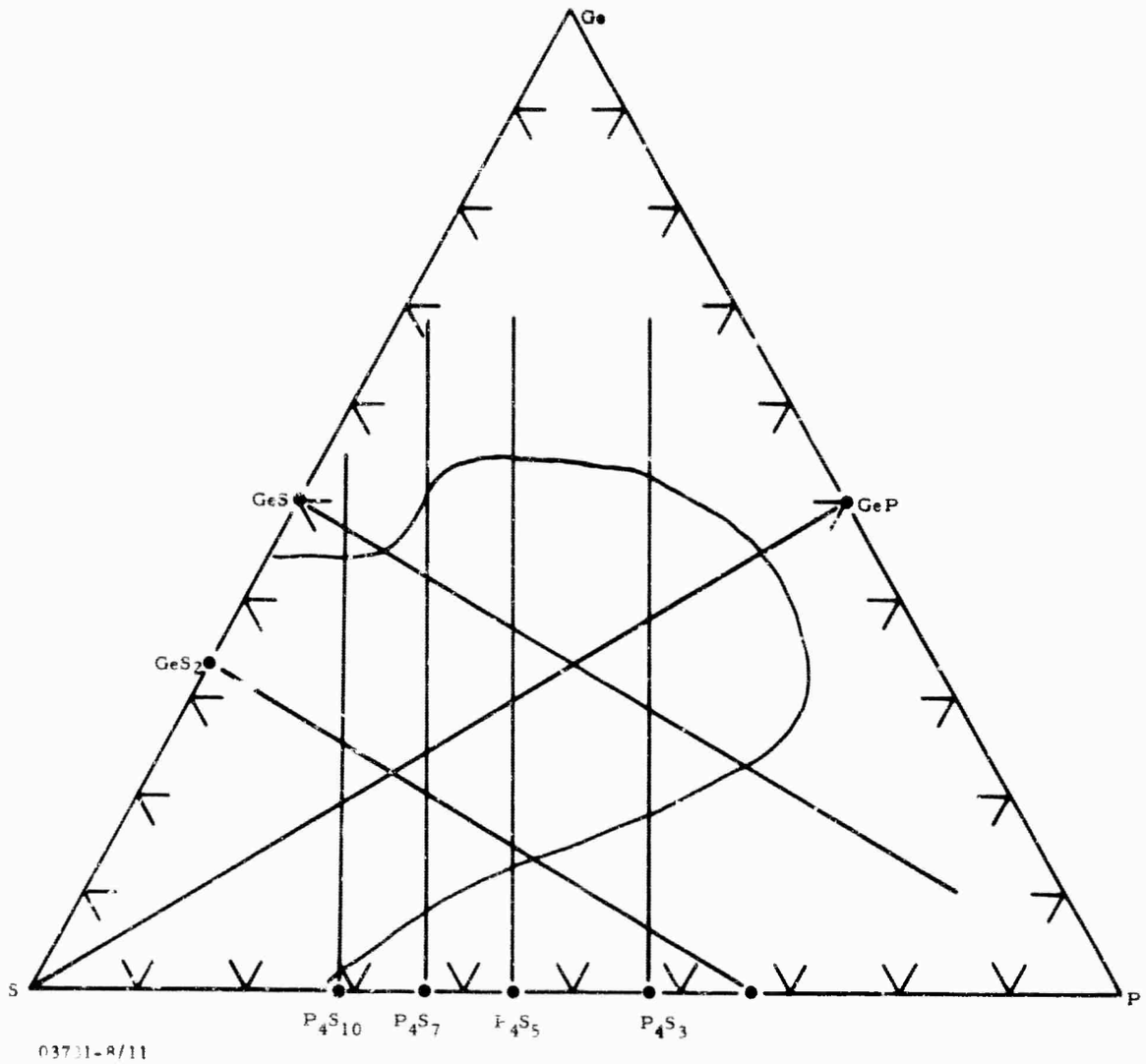

Figure 39 The Ge-P-S System

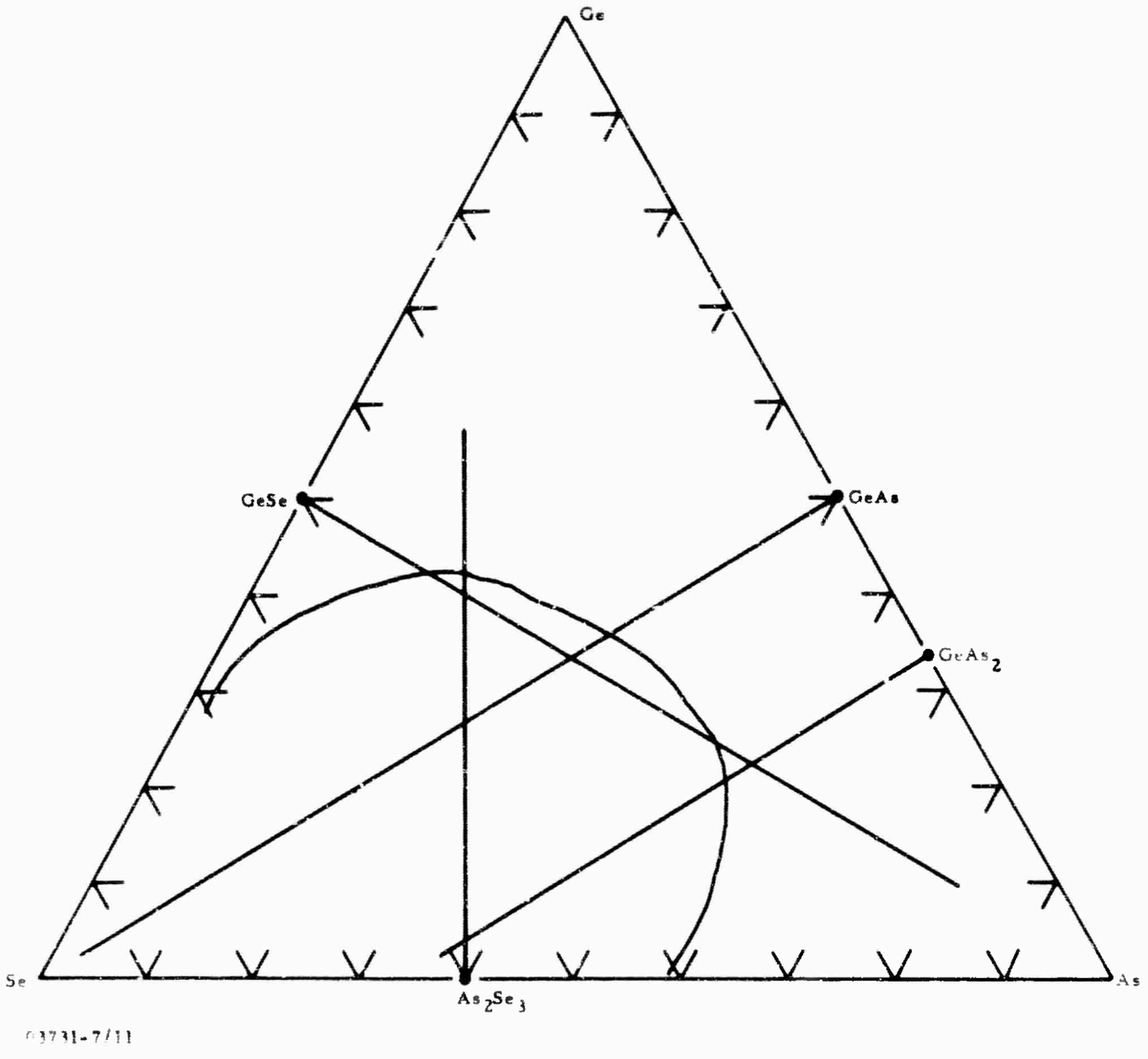

Figure 40 The Ge-As-Se System[5]

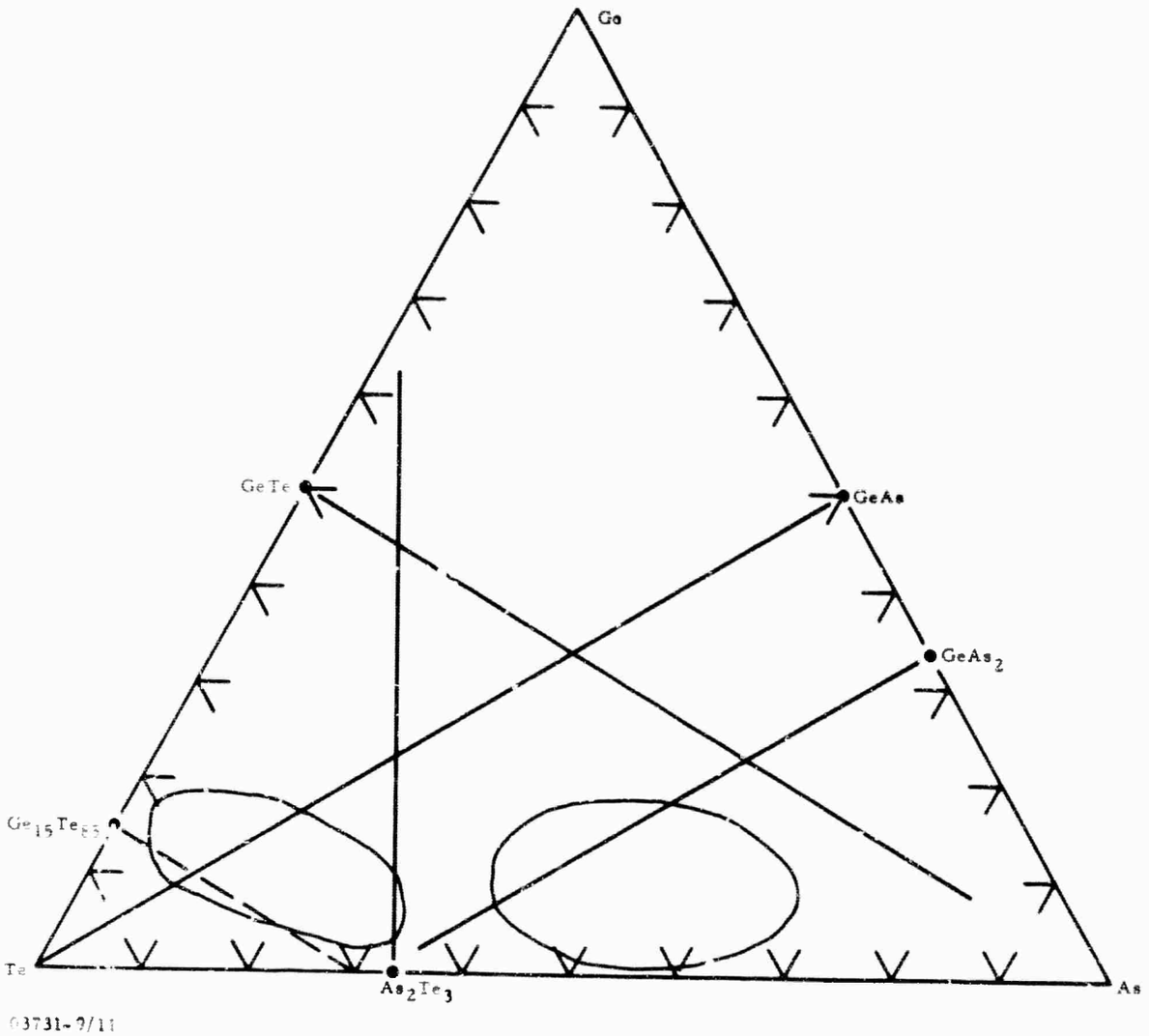

Figure 41 The Ge-As-Te System

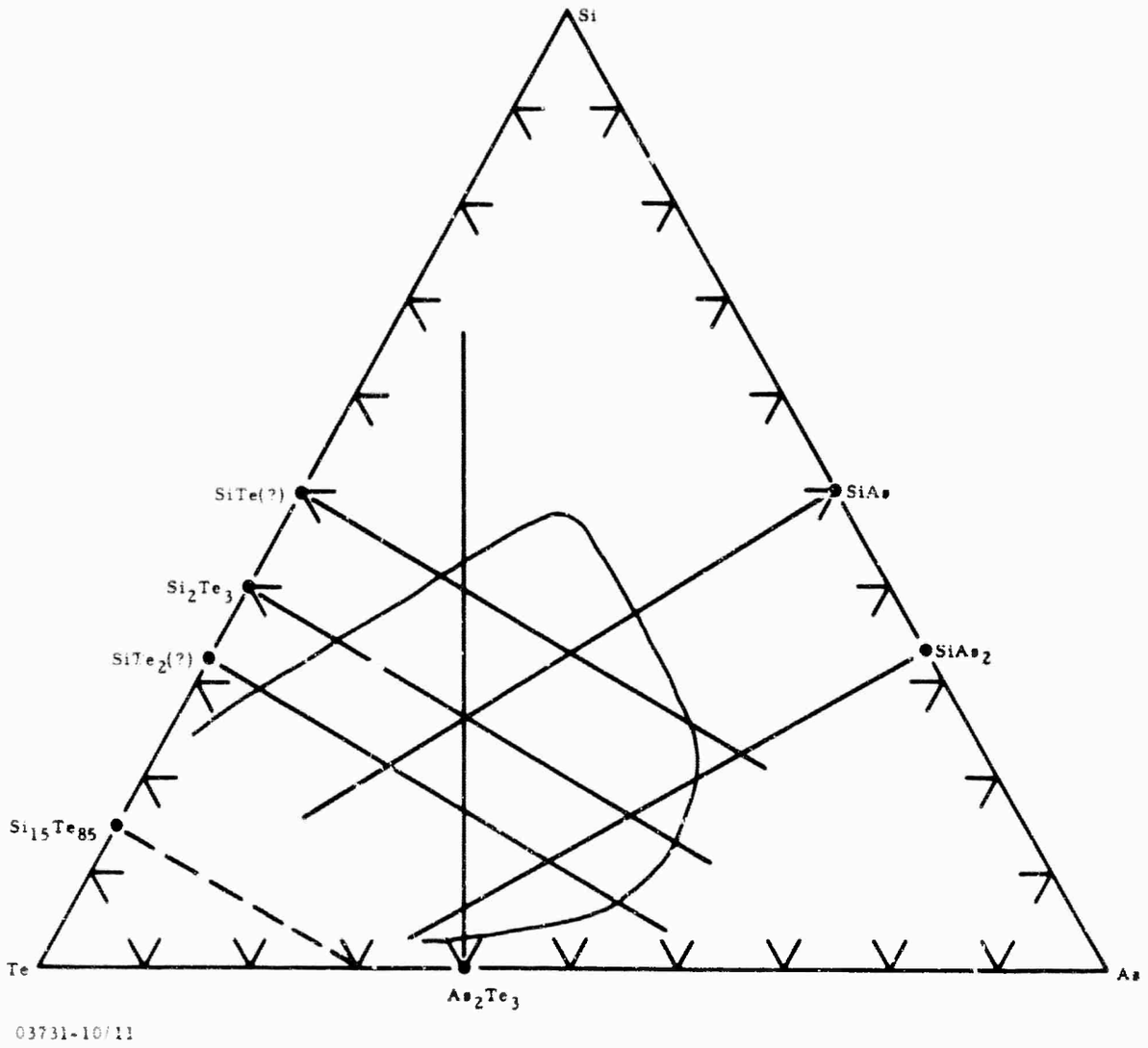

Figure 42 The Si-As-Te System

Information gained from studying the areas of all these systems can be formulated into a set of rules that can be stated as follows: The location of the composition region that produces amorphous materials in a IVA-VA-VIA ternary system can be predicted from a knowledge of the compounds formed in the three binaries IVA-VA, IVA-VIA, and VA-VIA.

(1) If no compound is formed between the IVA and VA elements, the glass-forming region lies wholly within the compositional area set off by the IVA-VIA and VA-VIA compound lines.

(2) Glasses based on tellurium have an additional boundary produced by the IVA-Te eutectic occurring around 85 atom-percent tellurium.

(3) If a single compound forms between the IVA and VA elements, the glass-forming area is distributed about the IVA-VA compound line.

(4) For two or more IVA-VA compounds, the glass-forming region extends past the IVA-VIA compound boundary line and is quite large.

III. STRUCTURAL INVESTIGATIONS

A. Present State of Infrared Transmitting Glasses as Optical Materials

The pertinent physical properties of typical examples of several classes of infrared optical materials can be compared from the values listed in Table XXII. Sodium chloride (NaCl) is typical of the alkali halides, silicon is typical of the single crystal semiconductors, Kodak Irtran 2 of the hot pressed polycrystalline materials, and arsenic trisulfide (As_2S_3) of the infrared transmitting glasses. The physical constants of optical (oxide) glasses are included for comparison. The magnitude of their physical constants represents goals that, if attained, would make a non-oxide glass perfectly acceptable (from a physical properties standpoint) as an optical material.

From the values in the table, it appears that, comparatively, As_2S_3 glass is weak and soft and has a low softening point. The values of the physical constants (excluding refractive index) of As_2S_3 glass are off by a factor of from 3 to 5 from the desirable values of oxide glasses. Obviously, As_2S_3 is not the strongest, hardest, highest softening point glass that could have been chosen for the comparison. Inclusion of the group IVA elements in the composition here[15,16,20] and in other laboratories[5,8,9] has produced glasses with better physical properties. But, the improvement has been only by a factor of about 2, not 3 to 5. After about ten years of investigation using the experimental approach, no non-oxide glass has been developed that has physical properties suitable for extensive use as a high temperature external window material. Materials with satisfactory optical properties have been found, but their physical properties have not been good enough. Apparently a change in approach is necessary to dramatically improve the physical properties of these materials. For this reason our program turned toward a more fundamental investigation aimed at understanding the chemical and physical nature of these glasses.

TABLE XXII

Comparison of Physical Properties of 8-14 Micron Infrared Window Materials*

Material	Refractive Index N at 4.3μ	Young's Modulus (10^6 psi)	Knoop Hardness	Melting Point	Solubility in H_2O g/ℓ	Comments
NaCl	1.52	5.8	17.0	803	35.7	Soft, weak, hygroscopic, low index, excellent transmission
Si	3.42	19.0	1150	1420	0	Hard, strong, high index, difficult to fabricate, purity a problem, free carrier absorption. Can't be used to 1400°C
Irtran 2 (ZnS)	2.25	14.0	354	800	0	Hard, strong, moderate index, made by hot press technique, suffers from scattering, not useful to melting point
As_2S_3	2.35	2.3	109	196	0	Weak, soft, brittle, moderate index, can be cast, purity (except for oxides) not a problem
Optical Glasses	1.5	7-10	300-600	700	0	Easily cast, fabricated, non-toxic, chemically inert

* Except for the comments, this material was taken from Elements of Infrared Technology, by Paul W. Kruse, Laurence D. McGlouchlin, and Richmond B. McQuistan. John Wiley and Sons, New York, 1962, pages 140-143.

B. Infrared Studies

1. Molar Refraction

The apparent linear relationship between density and molecular weight suggests that other properties may be additive and predictable. One such property is refractive index. Refractive index is related to the molar refraction and molecular volume of a substance. Molar refraction is given by

$$R = \frac{N^2-1}{N^2+2} \cdot V = \frac{N^2-1}{N^2+2} \cdot \frac{\text{mol. wt}}{d},$$

where R is the molar refraction, N the refractive index at some reference wavelength, and V the molar volume which is equal to the average molecular weight divided by the density. This well-known relation (from the Lorentz-Lorenz equation) has been applied to the study of bonding in organic and inorganic compounds. Molar refraction is also related to the radius of the individual molecule by

$$R = 4/3\ \pi A\alpha = 4/3\ \pi A r^3,$$

where A is Avogadro's number, α is the polarizability of the atom or ion, and r is the radius of the conducting sphere formed by the molecule. The refractive index should be measured in a wavelength region well on the long wavelength side of any absorption causing an electronic transition. It should be measured in the infrared in a non-dispersive region. For a non-polar amorphous glass the molar refraction is almost equal to the molar polarization. Molar refraction has the units of volume and can be treated as a volume made up of the additive sum of the volumes of each atom (or ion) in the molecule. Such treatments have been widely used in organic and inorganic compound and applied specifically to oxide glasses.[22] For a compound of the form

$$A_xB_yC_z,$$

where x, y, and z are mole fractions of the constituent elements A, B, and C, respectively, the molar refraction can be calculated from

$$R = xR_A + yR_B + zR_C \ .$$

Here, R_A, R_B, and R_C are the atomic (or ionic) refractions resulting from the presence of the constituents A, B, and C in the molecule.

This approach was applied to the non-oxide chalcogenide glasses. In very ionic substances the values of R_A, R_B, and R_C may vary widely from compound to compound, depending on the molecular bond formed. However, in the chalcogenide glasses the bonding is so covalent that a single value may be accurate for different glasses. Obviously, the atomic refraction of each constituent in these glasses should be directly proportional to its covalent radius. Calculating the atomic refraction directly from the accepted covalent radii would yield values too low because the atomic spheres are loosely packed. Therefore, an experimental value was used to put all values on an absolute scale. From the measured density, the molecular weight, and the refractive index of amorphous selenium, a value of atomic refraction was calculated. The reference point for the refractive index was 5 microns, well out of the dispersive region for the glasses. The atomic refraction for silicon, germanium, phosphorus, arsenic, sulfur, and tellurium was calculated from the cube of each elemental covalent radius normalized with the cube of the covalent radius of selenium. From these values the molar refractions for 28 glass compositions were calculated and compared to the measured values, obtaining an agreement of ± 4.1%. The results are shown in Table XXIII. A closer fit was obtained by solving the experimental values as simultaneous equations for separate values for silicon, germanium, phosphorus, and arsenic in sulfur, selenium, silicon-tellurium, and germanium-tellurium glasses. These results are also shown in Table XXIII. The fit to the experimental data is ± 1.1%.

The values obtained for atomic refractions are shown in Table XXIV. The literature values were obtained from crystalline or amorphous values when available. Values for phosphorus and arsenic were solved from glasses using the value for amorphous selenium. The values for sulfur, selenium, silicon-tellurium, and germanium-tellurium glasses are shown in the columns. Agreement between literature values and values calculated from covalent radii is quite good. Values calculated from the individual glasses show close agreement except in the case

TABLE XXIII

Molecular Refraction of Non-Oxide Glasses

Composition	R Measured	R Calculated Literature Value	% Error	R Calculated Average Value	% Error
PS_4	7.36	8.49	+15.4	7.36	0
Ge_3PS_6	8.26	9.23	+11.7	8.27	+0.1
Ge_2S_3	8.90	9.30	+ 6.5	8.90	0
As_2S_3	9.44	9.42	- 0.2	9.44	0
Se	11.55	11.51	- 0.4	11.55	0
$P-Se_9$	11.17	11.44	+ 2.4	11.31	+1.3
PSe_4	11.35	11.35	0	11.06	-1.7
$AsSe_9$	11.85	11.52	- 2.9	11.62	-1.9
$AsSe_4$	11.55	11.54	- 0.1	11.68	+1.1
$Si-Se_9$	11.65	11.31	- 2.9	11.65	0
$Ge_{16}As_{47.3}Se_{36.7}$	11.33	11.56	+ 2.0	11.36	+0.3
$Ge_{15}As_{45}Se_{40}$	11.45	11.54	- 0.3	11.39	-0.8
$Ge_3P_3Se_{14}$	10.70	11.36	+ 6.2	10.70	0
$Ge-Se_9$	11.23	11.49	+ 2.3	11.23	0
$SiAsTe_2$	13.42	14.55	+ 8.4	13.53	+0.8
Si_2PTe_7	16.05	15.96	+ 0.4	15.21	-5.2
Si_3PTe_{16}	16.55	16.76	+ 1.3	15.77	+1.3
$Si_3As_2Te_5$	13.70	14.43	+ 5.3	13.70	0
$Si_3As_3Te_4$	12.95	13.74	+ 6.1	13.23	+2.2
$Si_2As_3Te_5$	13.90	14.66	+ 5.5	13.90	0
$GeAs_4Te_5$	14.07	15.09	- 7.3	14.63	+4.0
$GeAs_2Te_7$	15.95	16.47	+ 3.2	15.87	-0.5
$Ge_3P_4Te_{13}$	15.83	15.90	+ 0.4	15.81	-0.1
$Ge_3As_{10}Te_7$	13.40	14.03	+ 4.7	13.58	+1.3
$GeAs_{10}Te_9$	14.30	14.75	+ 3.1	14.52	+1.5
$GeAs_{12}Te_7$	13.65	14.05	+ 2.8	13.96	+2.3
$Ge_3As_2Te_{15}$	16.25	16.77	+ 3.2	15.83	-2.6
$Ge_2As_3Te_{15}$	16.15	16.79	+ 4.0	16.02	-0.8
		Average	± 4.1		± 1.1

TABLE XXIV

Atomic Refraction Values

Element	R Calculated from Literature Values	R Calculated from Covalent Radii	R Calculated for S Glasses	R Calculated for Se Glasses	R Calculated for Si-Te Glasses	R Calculated for Ge-Te Glasses
Si	9.45	10.1		12.5	9.6	
Ge	11.35	13.4	9.7	8.3		9.9
P	10.6†	8.8	3.3	9.1	13.8	15.0
As	11.6‡	12.5	11.0	12.2	11.6	12.2
S	7.95	7.85	8.4			
Se	11.51	11.55		11.55		
Te	18.55	18.21			17.05	17.8

† From $P\text{-}Se_4$ Glass

‡ From $As\text{-}Se_4$ Glass

of phosphorus. The glasses used in these calculations contained very little phosphorus, so considerable error could result because the calculations involved taking the small difference between large numbers.

The refractive index of a non-oxide chalcogenide glass at 5 microns can be calculated within a few percent by combining the atomic refraction values from the tables with the molecular weight vs density line in Figure 26. Since

$$R = xR_A + yR_B + zR_C$$

and

$$R = \frac{N^2-1}{N^2+2} \quad \frac{\text{mol. wt}}{d},$$

the refractive index can be solved from the value of $(N^2-1)/(N^2+2)$. With this approach, the refractive index at 5 microns was estimated for 18 compositions of As-Se-Te glasses reported by Billian and Jerger.[4] Their accurately measured values and the estimated values agreed within ± 3%. The results are shown in Table XXV.

2. Infrared Absorption in the Non-Oxide Chalcogenide Glasses

There are three main sources of infrared absorption in these glasses: the absorption edge, impurity absorption, and molecular vibration of constituent elements. A fourth factor, which affects the transmission, is scattering of the radiation by occlusions of unreacted elements or a second phase. This factor is related to the preparation and perfection of a sample and for that reason will not be discussed. A fifth factor, important in the case of impure semiconductors or low band gap semiconductors at high temperatures, is free carrier absorption. This effect has not been observed in the chalcogenide glasses measured in this program, even at high temperatures.

TABLE XXV

Refractive Index of As-Se-Te Glasses[4]

Servo No.	Composition	N at 5 μ	N Calculated	% Error
1	$As_{38.7}Se_{61.3}$	2.79	2.62	- 6.0
2	$As_{27.5}Se_{72.5}$	2.65	2.59	- 2.3
3	$As_{40}Se_{35}Te_{25}$	2.88	2.90	+ 0.7
4	$As_{40}Se_{25}Te_{35}$	3.07	3.06	- 0.3
5	$As_{30}Se_{30}Te_{40}$	3.08	3.11	+ 1.0
6	$As_{20}Se_{60}Te_{20}$	2.74	2.80	+ 2.2
7	$As_{35}Se_{45}Te_{20}$	2.90	2.71	- 6.5
9	$As_{45}Se_{45}Te_{10}$	2.77	2.75	- 0.7
10	$As_{25}Se_{45}Te_{30}$	2.91	2.93	+ 0.7
11	$As_{30}Se_{60}Te_{10}$	2.76	2.71	- 1.8
12	$As_{10}Se_{60}Te_{30}$	2.73	2.89	+ 5.9
13	$As_{20}Se_{50}Te_{30}$	2.84	2.94	+ 3.5
14	$As_{20}Se_{70}Te_{10}$	2.65	2.68	+ 1.1
16	$As_{35}Se_{55}Te_{10}$	2.83	2.72	- 3.9
17	$As_{30}Se_{55}Te_{15}$	2.82	2.76	- 2.0
18	$As_{25}Se_{55}Te_{20}$	2.80	2.81	+ 0.4
19	$As_{20}Se_{55}Te_{25}$	2.64	2.84	+ 7.5
20	$As_{15}Se_{55}Te_{30}$	2.78	2.92	+ 5.0
			Average ± 2.9%	

a. Absorption Edge

The non-oxide chalcogenide glasses are semiconductors[7,12,15] and have an absorption edge just as found in crystalline semiconductors. The wavelength at which the glass begins to show bulk transmission corresponds roughly to the minimum amount of energy needed to excite carriers across the forbidden gap. The band gap of these glasses has not been of primary importance during this program and therefore has been measured on only a few samples. Most of the glasses studied begin to transmit radiation around 1 to 1.5 microns. Only a few transmit in the visible. The absorption edge does not affect transmission in the wavelength region of interest and will not be discussed further.

b. Impurity Absorption

All the elements used in making these glasses are high purity semiconductor grade materials. The impurity level should be < 100 atomic ppm for any single impurity. It is ironic that the non-oxide chalcogenide glasses were chosen over the oxide glasses because of oxide absorption, and yet the major impurity in all the glasses studied is oxygen. Oxygen can contaminate the glasses as an impurity in the reacting element or as a residual gas in the vial. It can also be extracted into the glass from the quartz as SiO (or SiO_2) or as H_2O. Once in the system, the oxygen takes the form of the most stable oxide in the melt at the molten temperature (900°-1000°C). The high temperature stable form is preserved while the glass is being quenched but may change form during annealing.

The infrared absorption bands in the wavelength region 2.5 to 25 microns observed in the systems evaluated in this program are shown in Table XXVI. Also shown are the results obtained from the many blended glasses studied. The only systems left out are the Si-Sb-S and Si-Sb-Se, which were not stable glasses. The bands are rated as to intensity by weak (w), very weak (vw), medium (m), and strong (s). A bracket indicates the band sometimes is not present in a system. Its absence may be due to composition ratios or some unknown reason. The possible cause for a band is indicated in the last column. The word possible is used because it is extremely difficult to say exactly what causes an absorption in a glass system.

TABLE XXVI

Infrared Absorption in Non-Oxide Chalcogenide Glasses

vw = very weak w = weak m = medium s = strong R = By Reflection

A = Absorption in a Glass Sample KBr = Absorption in a KBr Pellet

TlBr = Absorption in a TlBr Pellet CsI = Absorption in a CsI Pellet

P = Absorption in a Polyethylene Pellet [ ] = Sometimes not present

System	Absorption (Microns)	Absorption (cm^{-1})	Strength	Observed by	Possible Cause
Si-As-Te	[9.5]	1050	vw	A	Si-O (Surface)
	10.4	960	w	A	Si-O
	14.5	690	m	A	Te-O
	20	500	m	A	Mg-O
	25	400	m	A	Te-O
	32.5	307	s	R	Si-Te
	31.0	323	s	TlBr	Si-Te
Si-P-Te	10	1000	vw	A	Si-O
	[11.5]	870	w	A	Ge-O
	14.5	690	m	A	Te-O
	20	500	m	A	Mg-O
	32.5	307	s	R	Si-Te
Si-Te	9.5	1050	vw	A	Si-O
	14.5	690	m	A	Te-O
	20	500		A	Mg-O
	25	400		A	Te-O
	32.5	307	s	R	Si-Te
	30.5	328	s	TlBr	Si-Te
Ge-As-Te	[11.5]	[865]	vw	A	Ge-O
	[13.8]	[725]	vw	A	Te-O,As-O
	25	400	m	A	Te-O
	55	182	s	R	Ge-Te
	54	185	s	P	Ge-Te

TABLE XXVI
(continued)

System	Absorption (Microns)	Absorption (cm^{-1})	Strength	Observed by	Possible Cause
Ge-P-Te	25	400	m	A	Te-O
	37	270	m	CsI	?
	47	212	m	CsI	Ge-Te
	55	182	s	R	Ge-Te
Ge-As-Se	13	770	m	A	As-O
	21	476	m	A	Ge-Se Overtone
	42	238	s	R	Ge-Se
Ge-P-Se	[4.5]	[2220]	vw	A	H_2Se
	10	1000	m	A	P-O
	14.2	703	m	A	?
	16.0	625	m	A	Se-O
	20.5	490	m	A	Ge-Se Overtone
	40	250	s	R	Ge-Se
Ge-P-S	[4]	2500	vw	A	H_2S
	13	770	m	A	Ge-S Overtone
	18	555	m	A	P-S
	28	356	s	R	Ge-S
Ge-As-S	[4]	2500	vw	A	H_2S
	13.7	730	s	A	As-O
As-S	[4]	[2500]	vw	A	H_2S
	8.7	1150	vw	A	?
	9.5	1050	vw	A	Si-O
	10.3	965	vw	A	?
	14.8	675	s	A	As-O

TABLE XXVI
(continued)

System	Absorption (Microns)	Absorption (cm^{-1})	Strength	Observed by	Possible Cause
As-S (continued)	22	454	s	A	S-S
	26	374	m	KBR	?
	32	313	s	TlBr	As-S
	33	300	s	R	As-S
As-Se	12.8	780	m	A	As-O
	37	270	w	TlBr	As-Se
	44	226	s	TlBr	As-Se
	46	217	s	R	As-Se
	51	196	w	TlBr	?
	40	250	w	TlBr	As-Se
Ge-S	[4]	[2500]	vw	A	H_2S
	9.2	1090	w	A	Si-O
	13.1	765	s	A	Ge-O
	18	555	m	A	Ge-O
	20	500	m	A	S-S
	22	454	m	A	S-S
	24	416	w	TlBr	?
	27	370	s	TlBr	Ge-S
	28	357	s	R	Ge-S
Ge-Se	8	1250	w	A	?
	13	769	s	A	Ge-O
	18	555	m	A	Ge-Se Overtone
	42	238	s	R	Ge-Se
Si-Se	25.5	392	s	TlBr	Si-Se
	39	256	m	TlBr	Se-Se

TABLE XXVI
(Continued)

System	Absorption (Microns)	Absorption (cm^{-1})	Strength	Observed by	Probable Cause
Se	39	256	w	TlBr	Se-Se
P-S	14.1	710	s	R	P=S
	18.5	535	m	TlBr	P-S
	19.3	518		A	S-S
	21.1	473		A	S-S
	27	370	m	TlBr	?
P-Se	25	400	w	TlBr	?
	27.5	363	s	TlBr	P-Se
	32	313	w	TlBr	?
	39	256	w	TlBr	Se-Se

The thermodynamic stability of the oxides in the melt at the compounding temperature (900-1000°C) determines, in part, which oxide bonds will form and remain stable in the melt. The other factors that affect the results are the relative ratios between the elements. The thermodynamic stability of different oxides is shown in Figure 43, with the free energy plotted on the left. The greater the negative value, the more stable the oxide. In the compounding temperature range the relative stability of oxides is

$$Si\text{-}O > P\text{-}O > C\text{-}O > Ge\text{-}O > S\text{-}O > As\text{-}O > Te\text{-}O > Se\text{-}O.$$

If a glass composition is cooled below 900°C to the annealing temperature range (300 - 400°C), there are some changes in the relative stability of oxide, and the order becomes

$$Si\text{-}O > P\text{-}O > Ge\text{-}O > C\text{-}O > As\text{-}O > S\text{-}O > Te\text{-}O > Se\text{-}O.$$

Heating a glass at low temperatures for long periods of time, then, can change the impurity absorption bands.

Infrared absorption bands of the pertinent oxides are shown in Table XXVII. The results were obtained using KBr pressed pellets. Assigning a particular absorption band in a glass to a particular oxide is complicated by several factors. First, the high dielectric field of the glass ($\epsilon \approx n^2$) shifts the frequency of the molecular vibration to lower frequency. This shift is usually attributed to simple electrostatic interaction of an oscillating dipole to its surrounding of dielectric constant ϵ.[23] Absorptions of oxides observed using the pressed KBr (or other low dielectric materials) pellets may occur at slightly shorter wavelengths than in the glasses. Second, the frequency may be shifted because of chemical bonding with the surroundings by the molecular gro···

The stretching frequency of the Si-O band in SiO_2 occurs at 9.3 microns, 9.3 microns for SiO_2 in KBr pellets, 9 microns for interstitial oxygen in silicon,[24] and 10 microns for amorphous Si-O.[25] The 9.5-10.4 absorption in Si-P-Te, Si-Te, and Si-As-Te glasses could conceivably be caused by this absorption. The mass of the silicon atom is not too large relative to the oxygen atom (28 to 16).

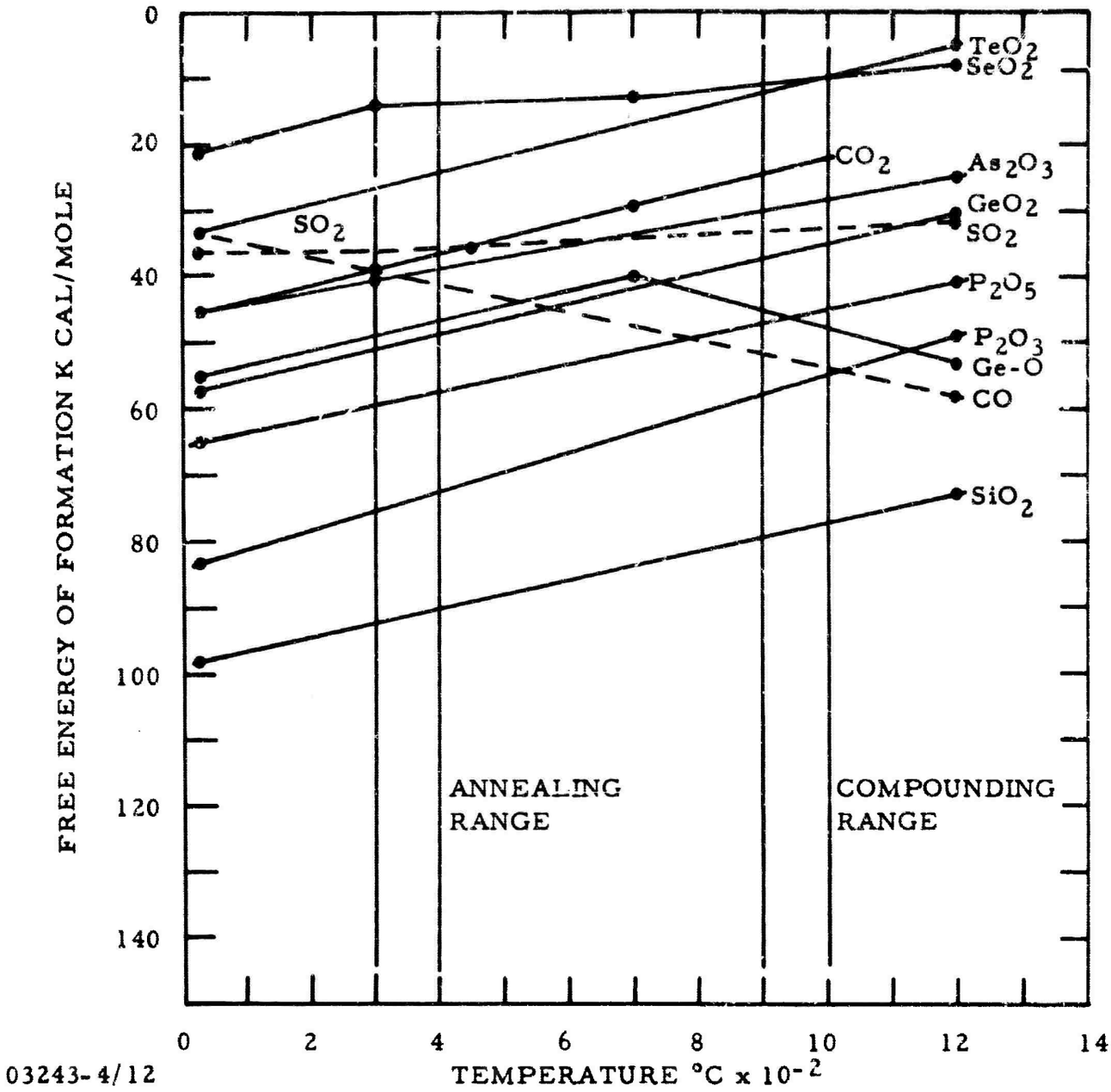

Figure 43 Thermodynamic Stability of Pertinent Oxides as a Function of Temperature *

*From The Thermochemical Properties of Oxides and Fluorides to 2500°K, by Alvin Glassner. Argonne National Laboratories ANL-5750.

TABLE XXVII

Infrared Absorption of Pertinent Oxides in the Wavelength Range 2.5-25 Microns

(Data Obtained from KBR Pellets)

Oxide	Bands (μ)				
* SiO_2	9.3 (s)	12.7 (m)	21.6 (s)		
* GeO_2	11.5 (s)	18.4 (m)			
TeO_2	13.9 (s)	17.3 (s)	(22-25) general		
As_2O_3	9.5 (vw)	12.5 (s)	16.8 (m)	21.0 (m)	
SeO_2	3.8 (s)	6.2 (w)	9.3 (s)	11.8 (s)	16.2 (s)
P_2O_5	6 (vw)	8 (m)	9.2-10 (s)	11 (w)	20.8 (s)
*MgO	20 (s)				
*Al_2O_3	17.3 (s)	22.5 (s)			
*Cu_2O	16.3 (s)				
*Fe_2O_3	17.4 (s)	21.8 (s)			

* Impurities observed in 10-100 ppm range in starting materials.

If an oxygen atom is bonded to a silicon atom which is bonded to a very heavy atom, the Si-O stretching vibration will shift to lower frequency. Thus, the Si-O stretching frequency for the O-Si-Te molecular groups found in Si-Te glasses (atomic mass of Te = 127.6) would be shifted to lower frequencies. In the case of the Ge-O stretching vibration, absorption for GeO_2 in KBr occurs at 11.5 microns, while interstitial oxygen in germanium occurs at about the same wavelength, 11.7 microns.[24] The mass of the germanium atom is already large relative to the oxygen atom (72.6 to 16). The bonding of germanium to tellurium to form the molecular species O-Ge-Te has little effect on the Ge-O vibrational frequency. The 11.5 bond is observed in Ge-As-Te glasses. Thus, many factors must be considered in deciding the origin of an absorption. After a detailed study, Servo Corporation[5] has shown that the 12.8 micron band in As-Se and Ge-As-Se glasses is the result of As-O absorption.

According to the stability of the oxides, Ge-O can form about as easily as As-O and produce a band at 11.5 and perhaps at 18.4 microns. A look at the stability order of the oxides shows that carbon should reduce Ge-O and As-O but not Si-O. This is observed. Silicon glasses that show the Si-O band still show it when they are compounded in carbon-coated tubes. Ge-As-Te glasses compounded in carbon-lined tubes or in tubes merely containing carbon do not show these bands. In Ge-As-Te glass small amounts of metals such as boron and aluminum, which form very stable oxides, are also effective in removing the bands in tellurium. High purity arsenic commonly contains magnesium, silicon, copper, and iron, while semiconductor-grade silicon contains aluminum and magnesium. It is highly probable that these trace impurities are present as oxides and thus either produce undesirable absorption in the glasses themselves or act as oxide sources for other elements. The infrared absorption of these oxides in KBr is included in Table XXVII for reference.

As mentioned earlier, the infrared absorption of Si-O and Ge-O in crystalline silicon and germanium[24,26] has been studied. Here, the level of oxygen is of the same order as that in the glasses, 50-100 ppm by weight. The magnitude of the absorption coefficient at 9 microns for silicon containing 15 ppm by weight oxygen is 5 cm^{-1}.[26] The same order of magnitude is observed for the 10.4 band

in the Si-As-Te glasses. As shown in Figure 29, the absorption coefficient at 10.4 microns in $SiAsTe_2$ glass is 3.5 cm^{-1}. The source of the oxides in the glasses may be the semiconductor-grade materials used in sample preparation. Mass spectrographic and emission spectrographic analyses carried out in our laboratory show trace impurities (10-100 ppm by weight) of germanium, silicon, aluminum, and magnesium are commonly present.

c. Molecular Vibrations of Constituent Atoms

Infrared spectroscopy has proved quite useful to study bonding in amorphous oxide systems, and with much time and effort many infrared reflection and absorption bands in a single oxide glass system can be identified and assigned. The infrared spectra of crystalline compounds of similar composition are useful in identifying the origins of the vibrations in the glasses. The task in the non-oxide chalcogenide glasses is much more difficult. The intensity of the absorptions is not great because of the very covalent nature of the bonds. There are no crystalline analogs of known structure to help, and there is even reasonable doubt about what chemical bonds form. It appears only the simplest vibrations can be identified. These would correspond to the simple bond stretching vibrations between the major constituent atoms. The stretching vibration should be the most intense.

Strong absorption due to the vibration of constitutent atoms that are infrared active can be observed by infrared absorption of extremely thin samples, absorption of pressed pellets containing a small amount of the glass, or infrared reflection. The reflection method has been applied before in studying glass structures[27] and is quite convenient. A very strong absorption can affect the reflectivity, producing a reflection peak. In crystalline solids such reflection bands are called reststrahlen bands and are used for radiation band separation.

Normal reflectivity is calculated from

$$R = \frac{(n-1)^2 + k^2}{(n+1)^2 + k^2},$$

where

n is the refractive index and

k is the extinction coefficient.

It is related to the absorption coefficient (α) by

$$\alpha = \frac{4\pi k}{\lambda},$$

where λ is the wavelength of the absorption. Normally k^2 is quite small relative to the refractive index so that it is not included in calculating reflectivity (especially if the material is transparent). When k becomes quite large, the value of n begins to drop (the optical constants are interdependent, not independent), producing first a minimum in reflection (on the short wavelength side of the maximum absorption) and then a rapid rise to a maximum value. The reflectivity then falls asymptotically to a value slightly higher than the constant value that occurs before the reflection band.

Reflection bands obtained from several glass samples are shown in Figure 44. The bands are found to show the expected shape. In a reflection band the peak of reflectivity, the maximum absorption wavelength, and harmonic oscillator frequency do not occur at the same wavelength because of the interrelationship of the optical constants. The wave number of the harmonic oscillator (ν_o) and the wave number of the maximum absorption (ν_{max}) were calculated using the method of Moss.[17] The values needed for the calculation are the magnitude of maximum reflectivity, the wavelength location of the maximum and minimum of the reflection band, and the short wavelength refractive index. The results obtained for several samples are shown in Table XXVIII. In some cases only absorption spectra were available. The values obtained are given in the brackets in the last column. The absorptions were measured using pressed pellets of KBr, TlBr, CsI, and polyethylene. The reflection spectra were favored in determining the frequency of a particular vibration. Assignments were made comparing the spectra of different glasses. For example, the Si-Te vibration was identified by comparing the spectra of Si-As-Te, Si-P-Te, and Si-Te glasses.

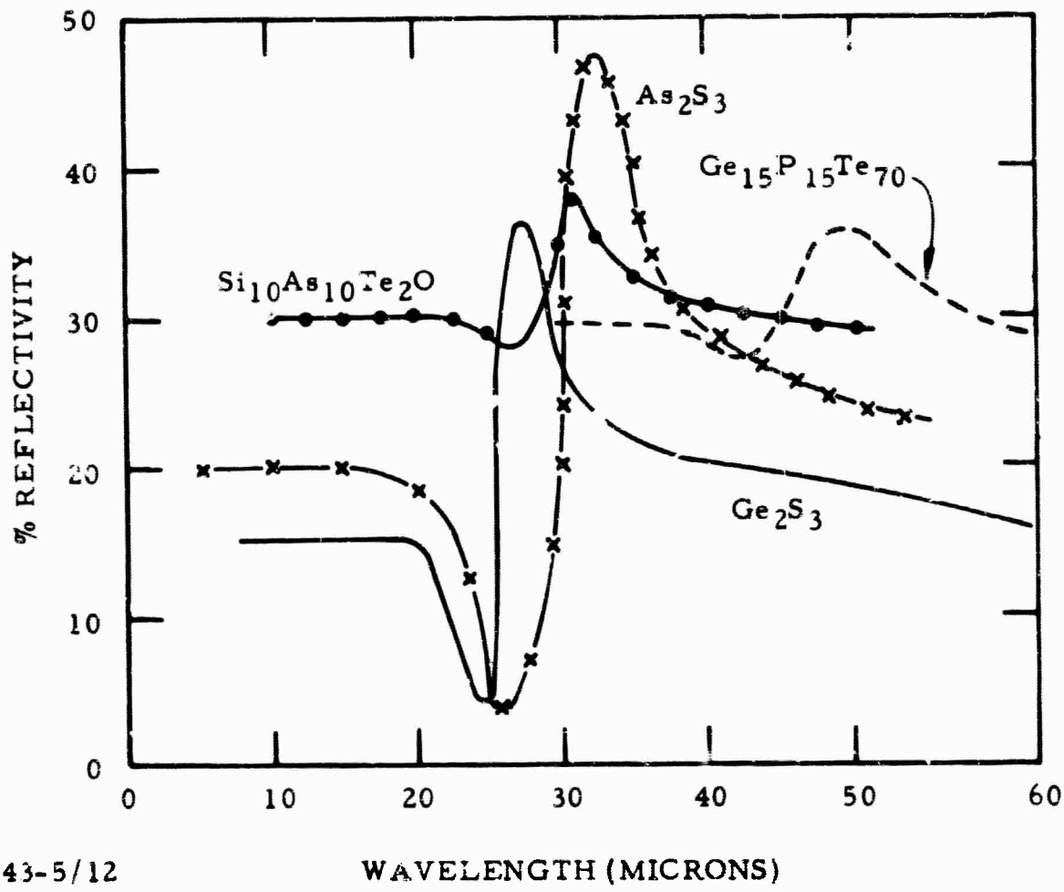

Figure 44 IR Reflection of Some Non-Oxide Chalcogenide Glasses

TABLE XXVIII

Calculated Wavelength of Infrared Absorption in Glasses
As a Result of the Vibration of Constituent Atoms

System	Constituent Atoms Involved	Wavelength of Reflection Max. (microns)	Wave Number of Calculated Harmonic Oscillator Frequency ν_o (cm^{-1})	Wave Number of Calculated Maximum Absorption Frequency ν_{max} (cm^{-1})
As-S	As-S	32	291	307 [313] TlBr
Ge-S	Ge-S	27.5	349	360 [370] TlBr
Ge-S-Te	Ge-S	28	342	355 ---
Ge-P-S	Ge-S	27	358	366 ---
Si-As-Te	Si-Te	31	307	322 [323] TlBr
Ge-P-Te	Ge-Te	50	196	205 [212] TlBr
Si-Se*	Si-Se	--	382	--- [392] TlBr
Ge-Se	Ge-Se	40	234	250 ---
As-Se	As-Se	44	217(†)	--- [226] KBr
P-Se	P-Se	--	350(‡)	--- [363] KBr
P-S	P-S	--	525(‡)	--- [535] KBr
Ge-As-Te	Ge-Te	50	196	205 ---
Ge-P-Se	Ge-Se	39	244	255 ---
Ge-As-Se	Ge-Se	41	233	247 ---
P-S	P=S	14.7	675(†)	--- [710] KBr

* Obtained from absorption data only

(†) Obtained by inspection of reflection curve

(‡) Obtained from absorption curve

[ ] Obtained by absorption

The two constituent atoms responsible for the vibration are given in the second column in Table XXVIII. In cases where only absorption data were available, the maximum of absorption was taken to be 10 cm^{-1} greater than the wave number of the oscillator.

The force constants for the vibrations are calculated easily from

$$\nu_o = \frac{1}{2\pi C} \sqrt{k/\mu},$$

where ν_o is the wave number of the resonant frequency of the harmonic oscillator, k is the force constant, and μ is the reduced mass. If it is assumed that the absorptions are due to a simple diatomic vibration, an estimate of the equilibrium interatomic distance can be obtained from Gordy's rule and the calculated force constant. Gordy's rule[28] is

$$k = 1.6N\left(\frac{X_A X_B}{d_{AB}^2}\right)^{3/4} + 0.30,$$

where k is the force constant in units of dyne cm^{-1} ($\times 10^{-5}$); N is the bond order (taken as 1, in this case); X_A, X_B the Pauling electronegativities of the atoms A and B; and d_{AB} the equilibrium distance between atoms A and B.

Next, the interatomic distances for nine tentatively identified vibrations were calculated. The distances are compared to the sum of the covalent radii in Table XXIX. Again, agreement is good. The only large discrepancy is in the bond distance calculated for As-S and As-Se glasses. Apparently, these vibrations do not fit the simple diatomic model. This fact suggests that a more detailed analysis of the infrared vibrations may yield information concerning the molecular arrangements of the constituent atoms.

The equations for calculating the frequencies of the normal vibrations for the $X\text{-}Y_2$ linear symmetric molecule, the $X\text{-}Y_2$ nonlinear symmetric molecule the XY_3 pyramidal molecule, and the $X\text{-}Y_4$ tetrahedral molecule were taken from Herzberg[23] and programmed for computer calculations. The forms of the equations

TABLE XXIX

Bond Distances Calculated from Vibration Frequencies

Bond	υ_o cm^{-1}	d Å Calculated (Gordy's Rule)	d Å from Addition Covalent Radii	Δ
Ge-S	349	2.29	2.24	+ 0.05
Ge-Se	234	2.56	2.38	+ 0.18
Ge-Te	196	2.61	2.57	+ 0.04
As-S	291	2.87	2.21	+ 0.66
As-Se	217	2.89	2.35	+ 0.54
Si-Te	307	2.35	2.46	- 0.11
Si-Se	382	2.15	2.27	- 0.12
P-S	525	2.02	2.08	- 0.06
P-Se	350	2.42	2.22	+ 0.20

assuming valence forces were used. The expressions involve atomic masses, bond lengths, bond angles, and two force constants, k and kδ. The first constant, k, is a measure of the restoring force in the line of the valence bond. The second, kδ, is the measure of the force opposing a change in the angle between two valence bonds. The magnitude of kδ is about 10% of k[23] and was assumed to be this value in all calculations. Interatomic distances were taken as the sum of the covalent radii. With these equations and Gordy's rule, the vibrational frequencies for molecular gases typical of the four molecular configurations were calculated and compared with the observed frequencies. Agreement between calculated and observed values was poor except for the $X\text{-}Y_3$ pyramidal case.

A method more suitable for polyatomic force constant prediction has been developed by Somayajulu.[29] This method utilizes the elemental covalent force constants and electronegativity to predict force constants. The expression is

$$k_{AB} = (k_{AA} \cdot k_{BB})^{\frac{1}{2}} + \Delta,$$

where k_{AB} is the force constant between the elements AB, k_{AA} and k_{BB} are elemental force constants, and Δ is an ionic contribution calculated from the electronegativity difference between elements A and B,

$$\Delta = | X_A - X_B |^{\frac{1}{2}}$$

Tables for elemental force constants are given by Somayajulu.[29] Different values for single, double, and triple bonds are given for the elements (when possible) as well as constants for hybridized orbitals such as sp^3. Thus, for elements such as silicon and germanium, two single bond force constants are given, one for the normal single bond and one for the tetrahedral bonding found with sp^3 hybrid orbital formation.

Calculation using Somayajulu's method yielded much better agreement between calculated and observed values for all cases but the $X\text{-}Y_3$ pyramidal. Gordy's rule was used for this case. The results obtained for the gases CO_2 ($X\text{-}Y_2$ linear), SO_2 ($X\text{-}Y_2$ non-linear), $AsCl_3$ ($X\text{-}Y_3$ pyramidal), and $SiCl_4$ ($X\text{-}Y_4$ tetrahedral) are given at the bottom of Table XXX. This table shows

TABLE XXX

Calculated Wave Numbers of the Normal Vibrations of Pertinent Molecular Groups

Molecular Group	Obs. Freq. (cm^{-1})	Calculated Diatomic X-Y	Calculated Linear Symm. $X-Y_2$			Calculated Nonlinear Symm. $X-Y_2$			Calculated Pyramidal XY_3				Calculated Tetrahedral XY_4				Assignment
			υ_1	υ_2	υ_3	υ_1	υ_2	υ_3	υ_1	υ_2	υ_3	υ_4	υ_1	υ_2	υ_3	υ_4	
Si-Te	307	350	149	116	473	*337	98	397	253	92	401	58	158	55	445	70	307(-8.9%) υ_1 XY_2 NL
Si-Se	382	420	215	136	554	*402	139	470	296	122	454	80	228	79	522	99	382(-5.0%) υ_1 XY_2 NL
Si-S	-	530	363	161	656	504	221	576	389	174	534	127	385	133	629	157	- - -
Ge-Te	196	238	144	75	305	*227	90	263	181	80	264	55	156	54	296	66	196(-13.7%) υ_1 XY_2 NL
Ge-Se	234	300	208	91	370	*286	127	326	226	101	309	74	224	78	362	91	238(-16.7%) υ_1 XY_2 NL
Ge-S	349	420	350	117	480	*403	195	441	335	137	401	115	378	131	483	140	352(-12.7%) υ_1 XY_2 NL
As-Te	-	241	147	76	308	230	92	266	187	82	271	57	147	51	276	62	- - -
As-Se	217	315	219	95	387	299	133	341	*235	104	318	77	219	76	350	89	217(-7.7%) υ_1 XY_3
As-S	291	445	373	124	507	428	207	467	*349	142	415	119	373	129	472	137	291(-16.7%) υ_1 XY_3
P-Te	-	322	142	106	432	309	93	363	259	97	408	61	142	49	383	62	- - -
P-Se	350	430	228	138	564	*411	147	480	306	128	464	84	228	79	502	98	350(-15%) υ_1 XY_2 NL
P-S	525	556	390	167	682	*528	236	602	408	182	552	134	390	135	618	158	525(-0.6%) υ_1 XY_2 NL
Si-As	-	366	191	118	481	350	123	409	281	116	427	76	204	71	457	88	- - -
Ge-As	-	262	184	788	322	249	111	284	216	96	293	71	200	69	317	81	- - -
P=S	675	728	511	219	894	*692	309	789	427	190	578	141	511	178	810	206	675(-2.5%) υ_1 XY_2 NL
CO_2	1337 667 2349	1697	1111 *	521 *	2127 *	1111	998	2127	440	187	465	1124	1111	385	1915	459	υ_1 = 1337(-17%) υ_2=667(-22%) υ_3 = 2349(-9.5%)
SO_2	1151 524 1361	1171	957	331	1353	1089 *	558 *	1266 *	367	935	473	726	957	332	1253	358	υ_1 = 1151(-4%) υ_2=524(+6.5%) υ_3 = 1361(7%)
$AsCl_3$	410 193 370 159	468	386	132	538	467	208	476	397 *	180 *	412 *	174 *	386	134	499	143	υ_1 = 410(-3%) υ_2 =193(-7%) υ_3 = 370(+1[illegible]%) υ_4 =159(+9%)
$SiCl_4$	424 150 608 221	594	395	182	741	564	243	648	404	180	562	129	395 *	137 *	668 *	162 *	υ_1 = 424(-6%) υ_2=150(-9%) υ_3 = 608(+10%) υ_4=221(-36%)

* Calculated value used for comparison to assigned values

calculated vibrational frequencies for the pertinent molecular species which may be present in the glasses studied. The wave number of the observed frequency for the infrared active vibration attributed to each molecular group is given in the first column.

A few remarks concerning the vibrational frequencies of each molecular group are in order. All the frequencies are calculated for free molecules. In the close association of the solid environment the vibrations will decrease in frequency (generally). Probably, the free molecule existence will not be maintained in the solid. It is difficult to visualize, for instance, a structural arrangement which allows a diatomic molecule to exist unbonded to the rest of the glass structure. A diatomic vibration can accurately portray the observed vibration if the diatomic molecular group is bonded to a much heavier atom in the glass molecular arrangement. The diatomic group could then vibrate independently.

A change in the electric dipole of the molecule produced by the vibrational mode is required if a particular normal frequency is to be observed by infrared absorption. Some normal vibrations that are not infrared active can be observed by the Raman effect. Both the $X\text{-}Y_2$ linear symmetric molecule and the $X\text{-}Y_2$ nonlinear symmetric molecules have three vibrational modes. In both cases the ν_1 wave number corresponds to the symmetric stretching vibration, while the ν_3 wave number corresponds to the unsymmetric stretch. The ν_2 wave number represents the frequency of the bending mode. The ν_1 vibration in the linear molecule is not infrared active because of the symmetry of the molecule (or vibration). It is Raman active.

Four wave numbers are listed for the pyramidal XY_3 molecule. The wave numbers ν_1 and ν_2 represent symmetric vibrations, while ν_3 and ν_4 are for doubly degenerate unsymmetric vibrations. All four are infrared active and all can produce strong absorption bands, depending on the masses and electronegativities of the individual atoms involved. Of the four wave numbers listed for the XY_4 tetrahedral configuration, only the triply degenerate ν_3 and ν_4 vibrations are infrared active.

The observed absorption for Si-Te, Si-Se, Ge-Te, Ge-Se, and Ge-S agrees very well with the wave number of the calculated frequency for the symmetric stretching vibration of a $X-Y_2$ nonlinear symmetric molecule. These wave numbers are marked with asterisks in Table XXX. The maximum disagreement is - 17%. Considering the fact that at least a 5% decrease in frequency is expected when the state changes from gas to solid, the fit is very good. The vibrations associated with As-Se and As-S glasses are quite different, as pointed out earlier. The observed values are closer to the calculated wave numbers for the ν_1 vibration of a pyramidal molecule than any other molecular arrangement considered. Values observed for As-Se and As-S were found in the binary glasses. The absorptions were not observed when a group IVA element was present. Surprisingly, the P-S, P=S, and P-Se vibrations fit the $X-Y_2$ nonlinear configuration rather than the pyramidal, as in the case of arsenic. This difference may be related to the chemical difference between arsenic and the other group VA elements, phosphorus and antimony. The difference was pointed when evaluating the glass forming composition regions.

The molecular arrangements considered in these calculations are simple ones that are likely to form. However, there is also good probability for more complicated, less symmetrical arrangements. For example, $X-Y_2$ linear or $X-Y_2$ nonlinear could be unsymmetrical. Vibrational frequencies and intensities would be different. The location of all the fundamentals would have to be known if a truly definitive assignment is to be made. A detailed investigation of the Raman active as well as the infrared-active species would be required.

d. Infrared Structural Conclusions

The conclusions drawn from the assignments are simple. The group IVA elements silicon and germanium form a zig-zag type chain arrangement with the chalcogenide. The arrangement for the Si-Te glasses can be visualized as

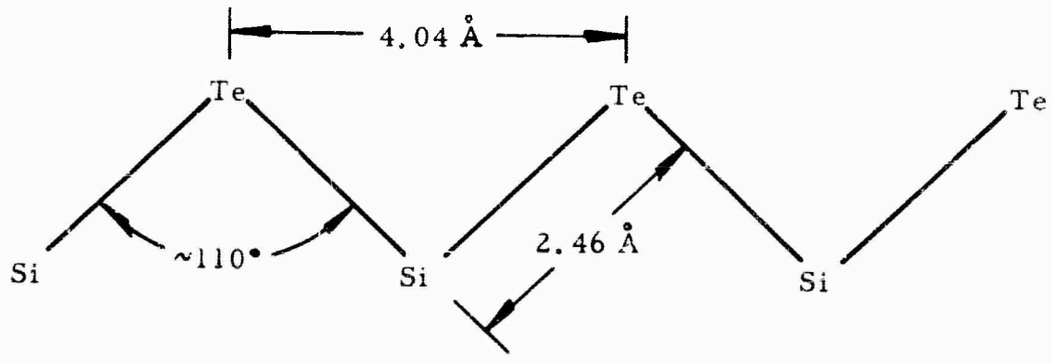

The bond distances are the sum of the covalent radii; the bond angle is about 110°. These were the parameters used in the calculations.

Infrared results for the Ge-As-Te and Ge-P-Te glasses indicate the formation of Ge-Te chains. They can be visualized as:

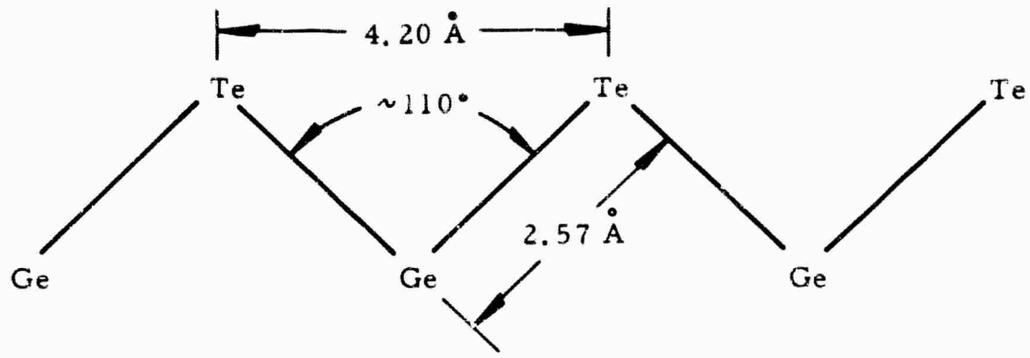

Again, the interatomic distances between the germanium and tellurium atoms are the sum of the covalent radii, and the bond angle is approximately 110°. These are the parameters used in the vibrational calculations. In both the Si-Te glasses and Ge-Te glasses, arsenic may still bond to the silicon or germanium atoms. Formation of such a bond is not sterically hindered by the two tellurium atoms. The formation of two more bonds is allowed for both silicon and germanium. The effect on the Ge-Te and Si-Te vibrational frequencies brought on by the addition of one or two arsenic atoms was not calculated.

Although the molecular arrangement of P-S is the same (from an infrared standpoint) as the Si-Te or Ge-Te, the glass structure is quite different. An appreciable percentage of P_2S_5 glass dissolved in the organic solvent CS_2.[30] The infrared absorption of the extracted mass was almost identical to that found for crystalline P_2S_5. It was concluded that small P-S molecules form in P-S

glasses and are contained in a sulfur network. For this reason these glasses show appreciable vapor pressure and are fragile, weak solids. Similar results may be expected for binaries of phosphorus and selenium. The presence of a group IVA element undoubtedly alters the structure.

The effect of the group IVA element can be illustrated best by contrasting the results obtained for As_2S_3 and Ge_2S_3 glasses. The atomic masses of germanium and arsenic are almost the same (72.6 and 74.9, respectively), their electronegativities are close (1.8 and 2.0), and their covalent radii are almost identical (1.22 and 1.19). The refractive indexes of As_2S_3 glass and Ge_2S_3 glass at 5 microns are 2.41 and 2.30, respectively. The densities are 3.21 and 3.20. The fundamental absorption edge of the two glasses occurs in the visible; both have a deep red appearance. The only real difference is their three dimensional structure. In As_2S_3 glass, the As-S absorption fits a pyramidal molecular arrangement. Undoubtedly, its structure contains many small As-S molecules trapped in a sulfur network. Its softening point is only about 200°C, and the thermal stability of the glass studied in our laboratory[31] showed many small As-S molecules were liberated from the glass when it was heated. On the other hand, the Ge-S vibration indicates a chain structure, the softening point of Ge_2S_3 glass is well over 400°C, and the glass is stable thermodynamically to above 450°C.[31] The role of the group IVA element is that of a chain former, and this role is thermodynamically favored over the formation of small VA-VIA molecules.

In the study of the Si-As-Te and Ge-As-Te glasses, no reflection bands were found that could be attributed to the As-Te vibration. The observed bands correspond to the Si-Te and Ge-Te bands in the nonlinear arrangement. The infrared absorption may be too weak to produce a reflection band. Undoubtedly some As-Te bonds form. Mass spectrometric results show high thermal stability for some of the Si-As-Te and Ge-As-Te glasses. However, glasses with high arsenic concentrations liberate arsenic quite readily. It is quite possible that part of the arsenic present in the ternary glasses is only loosely bonded to the chalcogenide and contributes very little to the long range structure. The same remarks apply to the use of phosphorus in ternary glasses.

C. Mass Spectrometric Investigation of Chemical Bonding in Non-Oxide Glasses

by Tommy George,* H. M. Klein, and A. M. Bryant

1. Introduction

A study of the vapor in equilibrium with a solid or liquid can provide information about the molecular structure of the condensed phase. In addition, measurement of the partial pressure of various equilibrium species as a function of temperature yields thermodynamic information that can be related to the binding energy of the species in the solid or liquid phase. Ideally, the partial pressure of each species in the vapor phase will equal $P_A^{\circ}X_A$, where P_A° is the vapor pressure of pure A, and X_A is the atom fraction of component A in the condensed phase. If the partial pressure of a species is measured as a function of temperature, the differential heat of solution can be obtained from the slope of a plot ℓnP vs $1/T$, where P is the partial pressure. A deviation of the slope of this plot will indicate a change in the solution process or type of association in the condensed phase.

Strong bonding in a solid, approaching that of true compound formation, means that the vapor pressure will be independent of the composition of the solid at constant temperature. The measured vapor pressure of the equilibrium species will be the dissociation pressure of the solid, and the variation of this pressure with temperature will give the dissociation energy of the solid compound.

A mass spectrometer coupled with a Knudsen cell provides a sensitive and convenient method of analyzing the equilibrium vapor over a solid material while simultaneously measuring the change in the vapor pressure with temperature. The output of the spectrometer is in arbitrary units, I. The pressure in the Knudsen cell is proportional to the absolute temperature of the cell multiplied by the intensity. If ideal behavior of the vapor in the Knudsen cell is assumed, a plot of ℓnIT vs $1/T$ will yield a straight line of slope $\Delta H_v/R$ for each species

---

* Summer Development Student in the Spectrography section of TI's Central Analytical Chemistry Facility, Summer 1965.

monitored. The value of ΔH_v measured in this way represents the heat of vaporization or sublimation, heat of solution, or dissociation energy of the species mentioned.

2 The Knudsen Cell

Figure 45 is a photograph of the Knudsen cell used in this investigation. The cell consisted of a heating block into which a quartz tube could be fitted. The sample was placed in the quartz tube. Its temperature was measured by means of a chromel-alumel thermocouple imbedded in the bottom of the tube. The top of the furnace block was a piece of tantalum foil in which a 0.01-inch diameter hole was drilled. On top of the tantalum foil and bolted to the furnace block was a smaller heater so that a 10° differential temperature could be maintained on the tantalum foil. It was necessary to maintain the foil about 10°C higher than the sample to prevent condensation of vapor on the foil, which would plug the orifice. The temperature of the foil was monitored by a thermocouple attached to the top heater block.

The entire cell and furnace arrangement was fitted into the flight tube of a Bendix TOF mass spectrometer. The vapor effusing in the form of a molecular beam was directed into the ionization region of the spectrometer. A magnetically operated shutter was placed between the Knudsen cell and the ionization source to differentiate the species originating in the Knudsen cell from the instrumental background. Only the shutter-dependent species were monitored.

To insure that the Knudsen cell would function as expected, the cell was calibrated with pure arsenic under essentially the same conditions used to study the glasses. The results of this calibration are shown in Figure 46. The value of ΔH obtained for sublimation of arsenic was 31.2 kcal. The accepted value is 31 kcal.[32]

3. Experimental Results

The mass spectrometer - Knudsen cell arrangement has been applied to the qualitative and quantitative study of five infrared transmitting glasses over

03845-2/6

Figure 45 Knudsen Cell

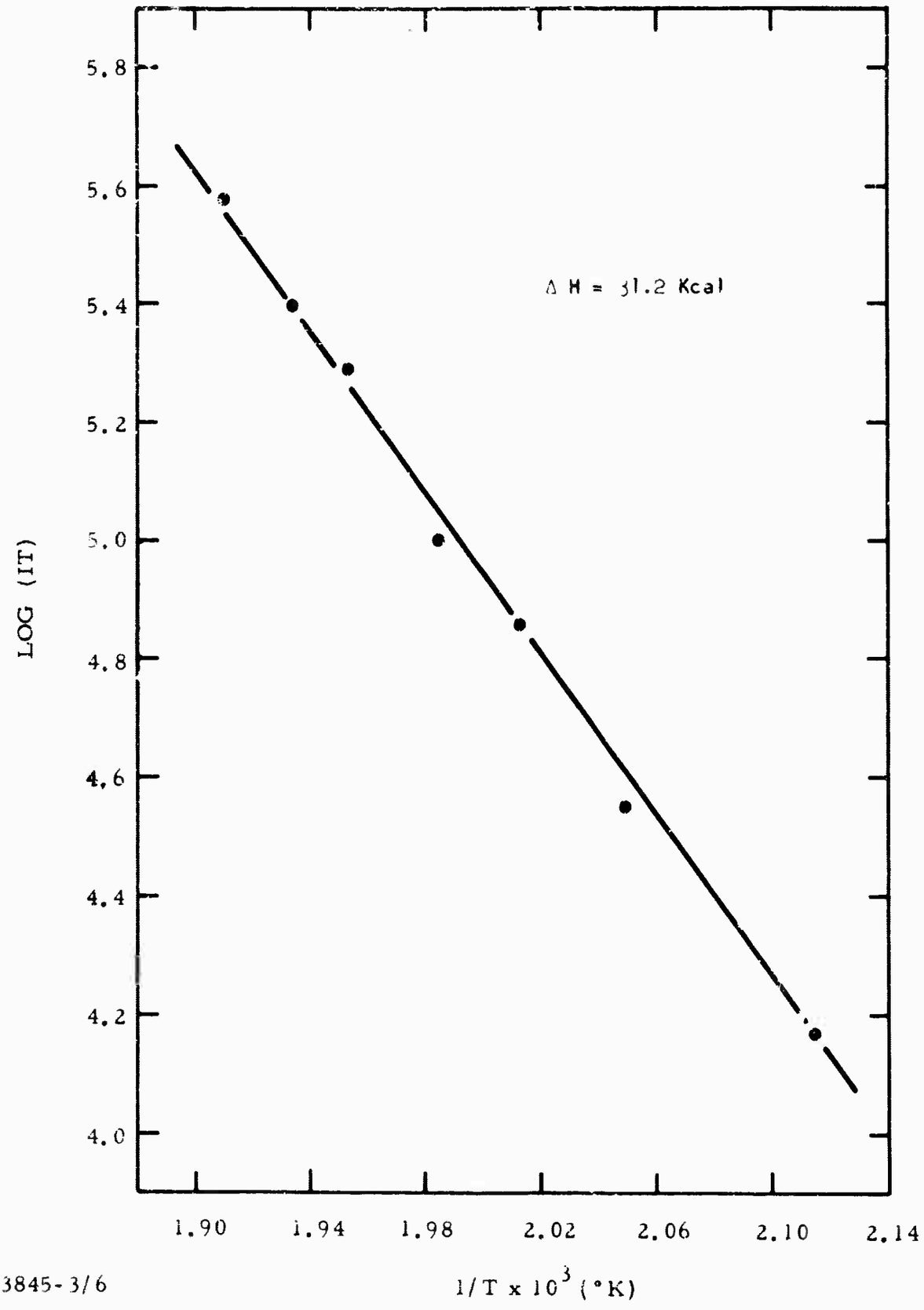

Figure 46 Arsenic Calibration of Knudsen Cell

the temperature range 25°-500°C. Over this range the pressures inside the Knudsen cell were low enough to insure that equilibrium conditions were maintained. The species evaporating from the glass were monitored, and where possible, thermodynamic studies were made to determine ΔH_v. The experimental results are summarized in Table XXXI and discussed in detail below.

a. $\underline{Si_{15}Te_{85}}$

Tellurium was observed in the vapor above about 380°C. The Te_2 peak (mass 258) was monitored up to 500°C. No other species were observed up to this temperature. Figure 47 shows a plot of the data obtained. From the slope of this line ΔH was 24 kcal for Te_2.

b. $\underline{Si_{15}As_{15}Te_{70}}$

Both arsenic and tellurium were observed. Arsenic began to appear about 290°C and was present up to 500°C. Tellurium appeared just below 380°C. Figure 47 shows results obtained for both As_4 and Te_2. Above about 360°C the partial pressure of As_4 remains relatively constant, contrary to what one would expect for simple dissociation or evaporation. The initial slope, however, yielded a value of 35 kcal for the enthalpy change of As_4. This value is only about 4 kcal higher than that found for pure arsenic.[32]

The tellurium vapor was better behaved. Analysis of the Te_2 data yielded a value for ΔH of 18 kcal. Again, this value is somewhat higher than the 12 kcal reported for pure tellurium.[32]

c. $\underline{Si_{15}As_{45}Te_{40}}$

Up to 400°C the only species present in the vapor phase was arsenic. No thermodynamic data were obtainable from this glass, however, because of the large fluctuations in arsenic partial pressure inside the Knudsen cell. These large fluctuations were observed even when the temperature was maintained constant. It was tentatively concluded that the arsenic was not evenly dispersed

TABLE XXXI

Summary of Data

	Vapor Species	Appearance Temperature (°C)	ΔH	Softening Temperature (°C)	Remarks
$Si_{15}Te_{85}$	Te	386	24 kcal	173	
$Si_{15}As_{15}Te_{70}$	As	278	35	207	Initial slope
	Te	377	18		
$Si_{15}As_{45}Te_{40}$	As	300	-	292	Arsenic inclusions
$Si_{30}As_{15}Te_{55}$	-	-	-	359	No vapor species up to 500°C
$Ge_{10}As_{20}Te_{70}$	As	262	28	178	Initial slope
	Te	386	34	-	
$Ge_{15}As_{45}Te_{40}$	As	233	36	300	Heated to 300°C

LOG (IT)

3. 3. 4. 4. 5 5 5

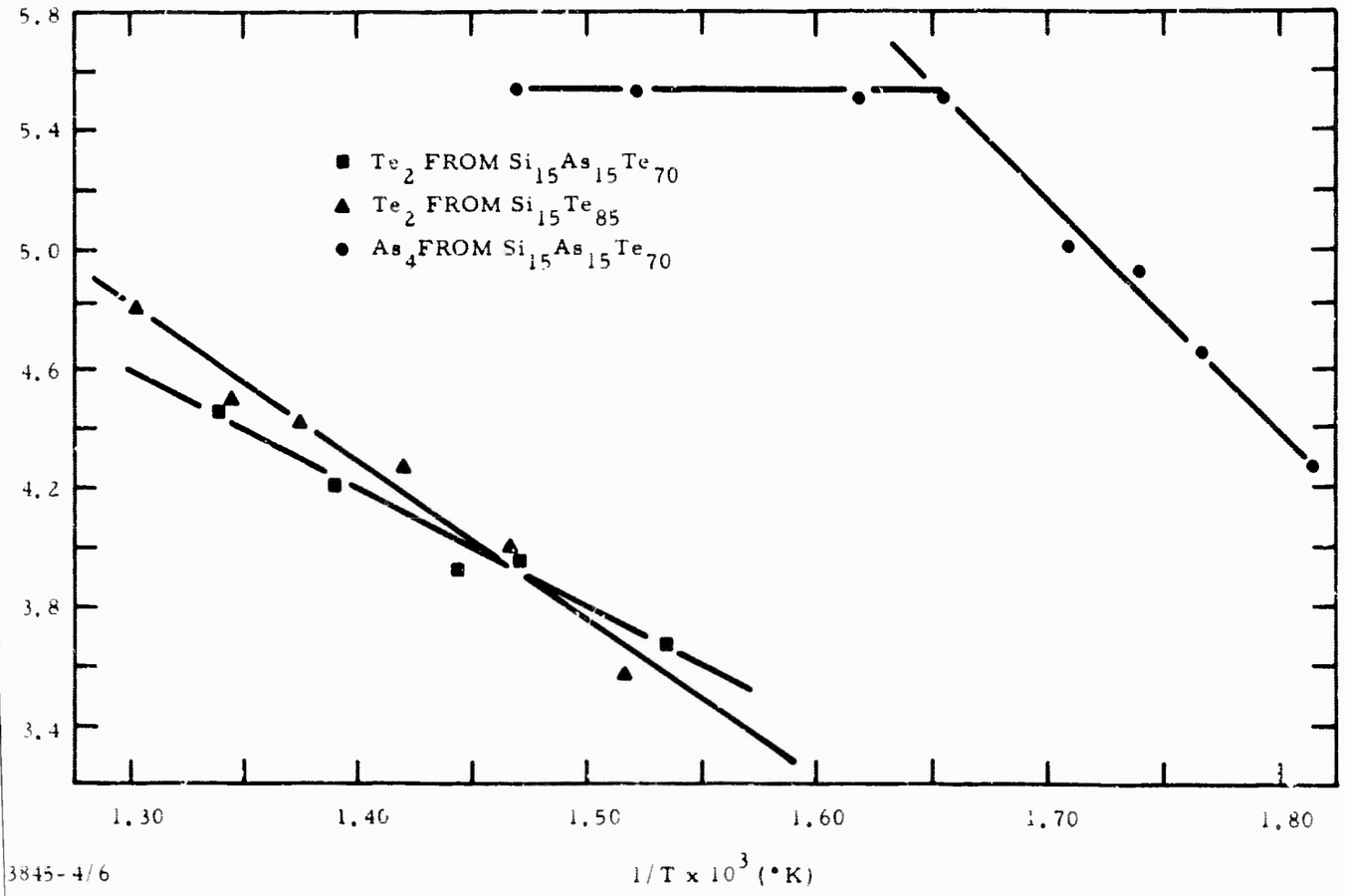

Figure 47 Clausius-Clap[illegible] Curves, Si-As-Te Glasses

in the glass, but rather was included in pockets. Visual examination of the glass after its removal from the Knudsen cell showed large holes which could have been caused by arsenic bubbling to the surface. X-ray analysis supports this picture of large quantities of arsenic inhomogeneously dispersed in the glass sample.

d. $Si_{30}As_{15}Te_{55}$

Up to 500°C this glass showed no measurable species in the vapor phase. Trace quantities of tellurium and arsenic were observed near 500°C, though no thermodynamic data could be obtained. Traces of several arsenic oxides were also observed, including AsO(91), As_3O_4(289), and As_4O_6(396).

e. $Ge_{10}As_{20}Te_{70}$

Both arsenic and tellurium were observed in the vapor. Arsenic began to appear about 260°C, while tellurium appeared about 380°C. The partial pressure of As_4 behaved much the same as in the $Si_{15}As_{15}Te_{70}$ glass. That is, above 380°C the As_4 partial pressure was independent of temperature. Below 380°C, analysis of the data yielded a value of 28 kcal for ΔH of As_4.

Measurements of the Te_2 peak between 386° and 450°C gave a ΔH of 34 kcal. Figure 48 shows results obtained for arsenic and tellurium. Figure 49 shows a scan of the spectrum of $Ge_{10}As_{20}Te_{70}$ taken above 386°C.

f. $Ge_{15}As_{45}Te_{40}$

Only arsenic was present up to 300°C. The temperature was not raised above this point because the pressure inside the Knudsen cell was approaching the point where Knudsen flow conditions no longer could be maintained. Figure 48 shows a plot of log IT vs 1/T for As_4. The slope of this plot yields a value of 36 kcal for ΔH.

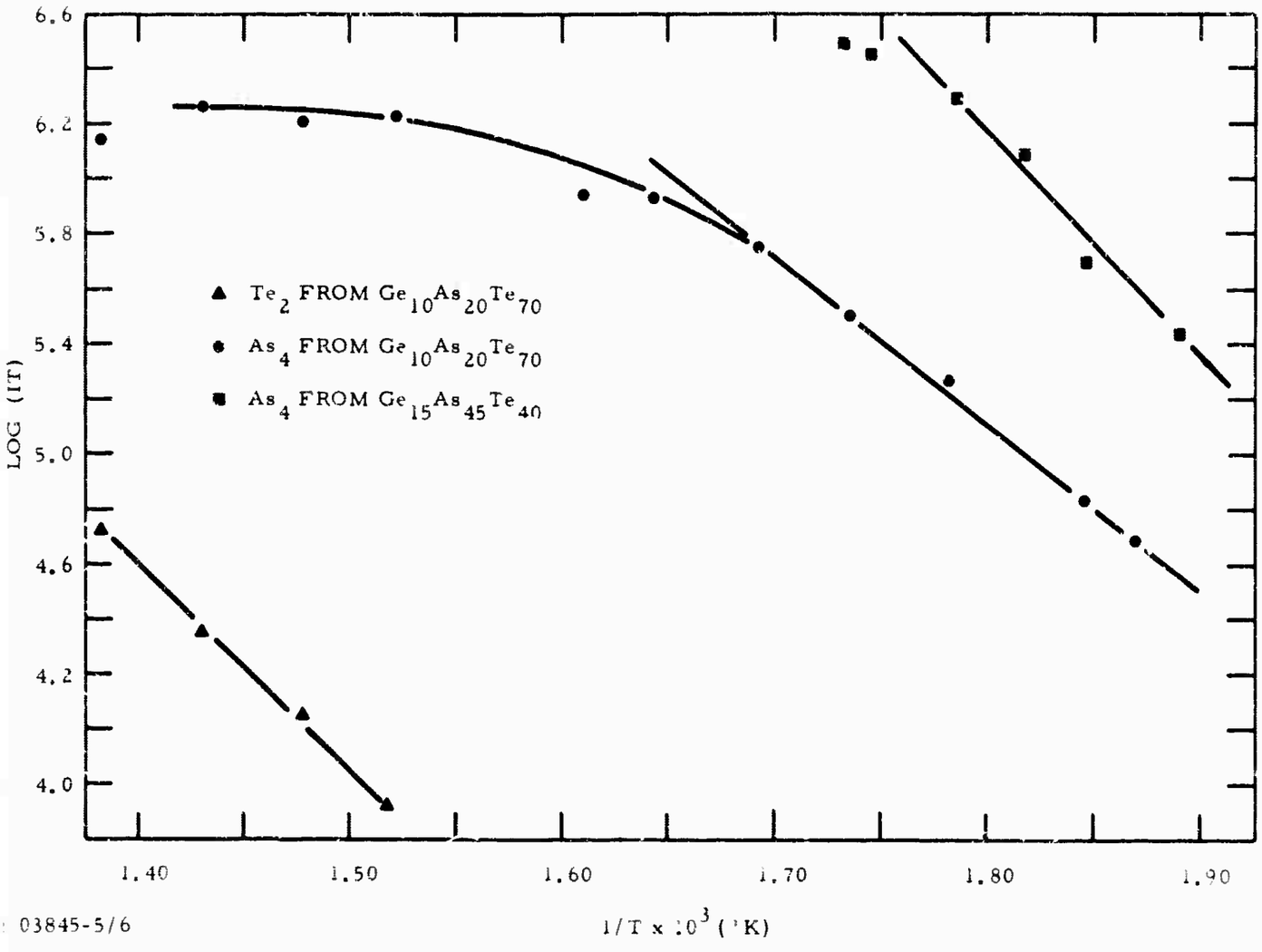

Figure 48 Clausius-Clapeyron Curves, Ge-As-Te Glasses

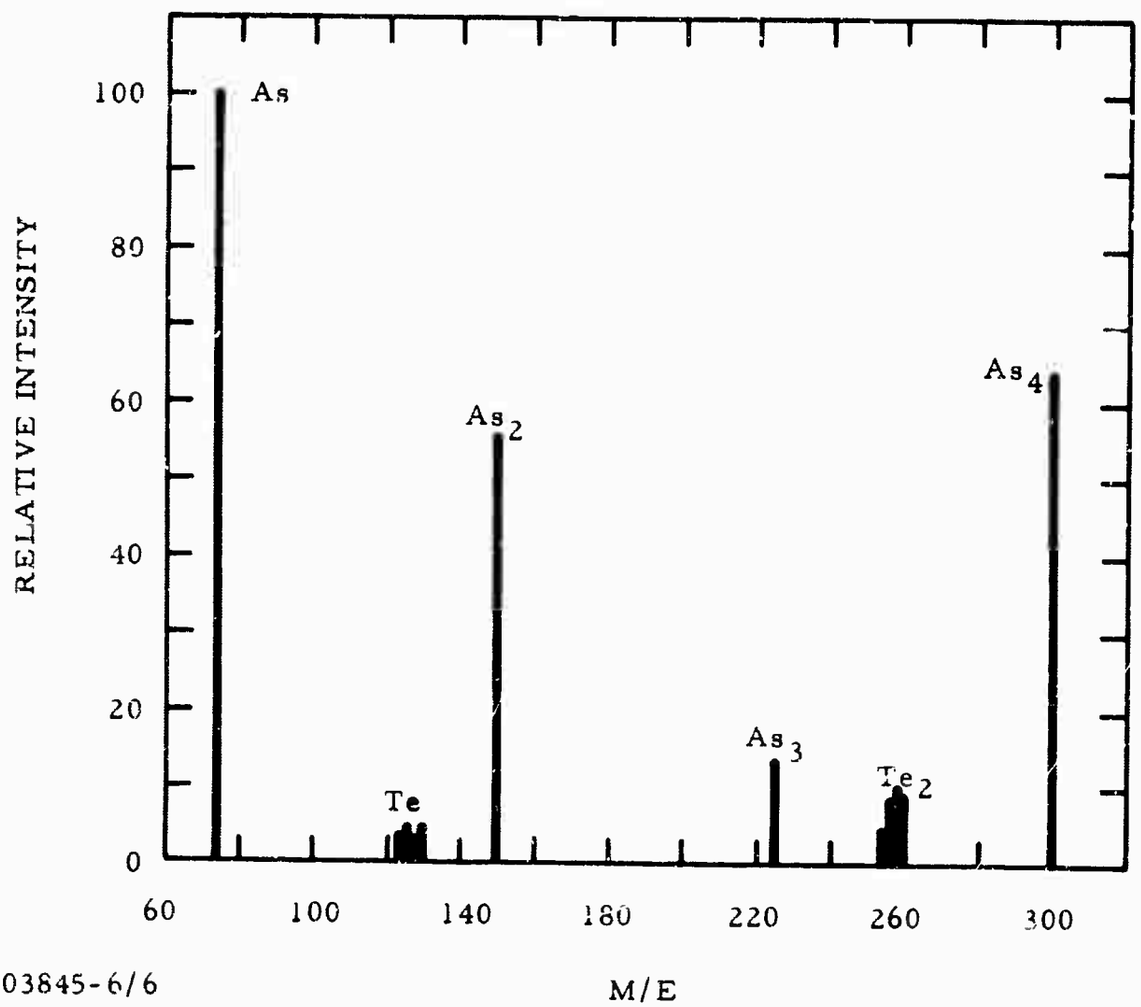

Figure 49 Mass Spectrum of $Ge_{10}As_{20}Te_{70}$

The arsenic oxide concentration was somewhat higher in this glass than in the others. Figure 50 shows the spectrum obtained for $Ge_{15}As_{45}Te_{40}$. Masses 91, 289, and 396 correspond to arsenic oxides in the glass.

4. Discussion of Results

Only one glass, $Si_{30}As_{15}Te_{55}$, failed to show any equilibrium vapor species below 500°C. All the other glass compositions showed at least one vapor species, either arsenic or tellurium. Two compositions, $Si_{15}As_{15}Te_{70}$ and $Ge_{10}As_{20}Te_{70}$, produced both arsenic and tellurium. There was no evidence of binary or ternary compositions in the vapor above the glasses. In every case arsenic was observable below 300°C. Tellurium showed a rather constant appearance temperature of about 380°C.

Heats of vaporization were measured on four of the six glasses under study. These measurements were made on both tellurium (as Te_2) and arsenic (as As_4). The values of ΔH obtained for the two species, coupled with vapor-phase behavior, have given insight into the type of bonding found in the glasses.

Two of the silicon glasses showed measurable amounts of Te_2 in the vapor phase. The heat of vaporization found for Te_2 from $Si_{15}Te_{85}$ was 24 kcal, while Te_2 from $Si_{15}As_{15}Te_{70}$ had a ΔH value of only 18 kcal. In addition $Si_{15}As_{15}Te_{70}$ gave off As_4 with an enthalpy change of 35 kcal. The difference in ΔH for Te_2 in the two glasses might be explained in terms of the arsenic. The ΔH found for arsenic indicates slightly stronger bonding than in pure arsenic. This stronger bonding probably results from some Si-As interaction which produces a considerable perturbation of the Si-Te bonding in the $Si_{15}As_{15}Te_{70}$, reducing the value of ΔH from 24 kcal to 18 kcal in the Si-Te glass.

As already noted, above 380°C the vapor pressure of arsenic above the $Si_{15}As_{15}Te_{70}$ glass was temperature-independent. Such behavior is possible if some recombination of arsenic takes place. The following sequence of equilibria offers a possible explanation.

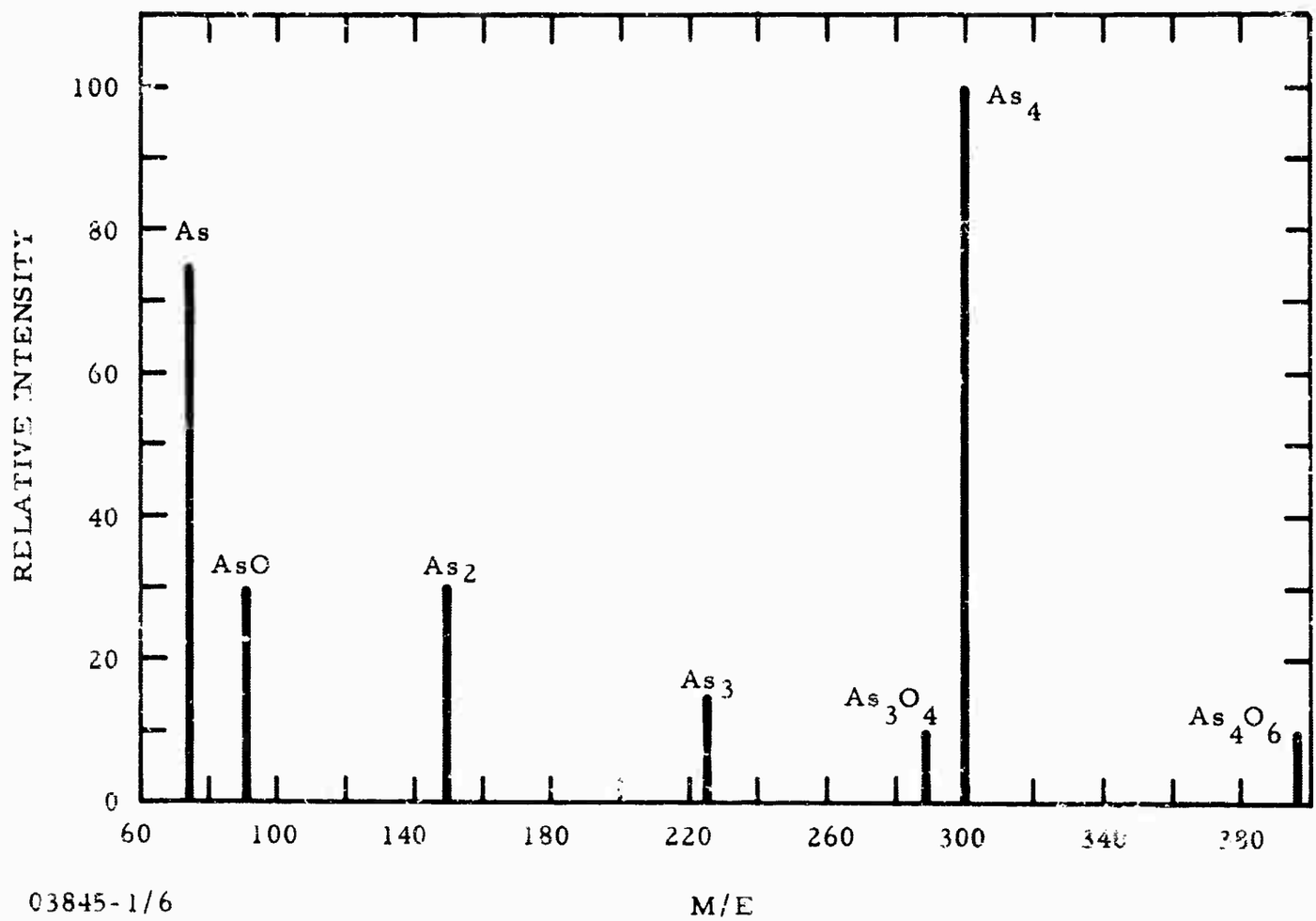

Figure 50 Mass Spectrum of $Ge_{15}As_{45}Te_{40}$

Between 275°C and 380°C the only equilibrium observable was one involving arsenic. If it is assumed that this arsenic results from arsenic in the glass, the equilibrium could be represented as

$$As_4 \text{ (trapped) (s)} \overset{< 300^\circ}{\rightleftarrows} + As_4 \text{ (g)} \quad . \qquad (1)$$

Above 380°C tellurium also exists in the vapor phase so that a second equilibrium is required.

$$2\ As_2Te_3 \text{ (s)} \overset{> 380^\circ}{\rightleftarrows} 4\ AsTe \text{ (s)} + Te_2 \text{ (g)} \quad . \qquad (2)$$

If these were the only equilibria present, the vapor pressure of both As_4 and Te_2 could be expected to increase with temperature. The fact that the vapor pressure of As_4 did not increase as expected indicates that some recombination reaction occurs.

At high temperatures Si-As bonds form. Thus the third equilibrium could be represented as

$$4\ SiTe \text{ (s)} + As_4 \text{ (g)} \overset{>380^\circ}{\rightarrow} 4\ SiTeAs \text{ (s)} \qquad (3)$$

Adding reactions 1, 2, and 3 will give an overall reaction which is dependent only on the vapor pressure of Te_2,

$$As_4 \text{ (trapped)} + 2\ As_2Te_3 \text{ (s)} + 4\ SiTe \text{ (s)} \rightarrow \qquad (4)$$

$$4\ AsTe \text{ (s)} + Te_2 \text{ (g)} + SiTeAs \text{ (s)} \qquad (5)$$

Exactly the same kind of arsenic behavior was noted in $Ge_{10}As_{20}Te_{70}$. It is probable, then, that the same sequence of equilibria is operative here as in $Si_{15}As_{15}Te_{70}$. There were, however, several significant differences in the two glasses. First, the ΔH for Te_2 was found to be 34 kcal instead of the 18 kcal previously noted, and the ΔH for As_4 was found to be a somewhat lower 28 kcal. Second, as Figure 49 shows, more arsenic than As_4 was found in the vapor. This second observation is noteworthy since in pure arsenic and each of

the other arsenic-producing glasses As_4 was the predominant arsenic species in the vapor. It must be assumed, then that the arsenic is bound the same way in $Ge_{10}As_{20}Te_{70}$ as in $Si_{15}As_{15}Te_{70}$.

The ΔH value obtained for As_4 indicates that the Ge-As interaction is somewhat weaker than in the corresponding Si-As glass. The presence of large quantities of arseric in the vapor above $Ge_{10}As_{20}Te_{70}$ indicates that arsenic is being evolved from a source other than As_4 molecules. A weak Ge-As bond could explain the results. This Ge-As bond does not have to be present in the original glass but could result from the analog of reaction (3) above.

The high ΔH value obtained for Te_2 would indicate a stronger bonding of tellurium in $Ge_{10}As_{20}Te_{70}$ than in the corresponding silicon glass. Part of the explanation may lie in the fact that germanium has vacant d orbitals available for bonding not found in silicon. These d orbitals could overlap with the tellurium orbitals, forming a considerably stronger bond than is possible with silicon.

The high value of ΔH for the evaluation of arsenic from $Ge_{15}As_{45}Te_{40}$ cannot be explained in terms chosen for the other germanium glass. The spectrum above 233°C (Figure 49) shows the presence of arsenic, with the ratio of As_4 to arsenic about equal to that found for pure arsenic. Comparison of this glass with $Si_{15}As_{15}Te_{70}$ shows a similar value of ΔH for As_4 and a similar As_4-to-arsenic ratio. Direct comparisons are not strictly applicable between $Ge_{15}As_{45}Te_{40}$ and the other glasses, however, because arsenic here is evolved much below the softening temperature (see Table XXXI). Thus, other effects probably contribute to the enthalpy change of 36 kcal.

The apparent stability of $Si_{30}As_{15}Te_{55}$ is of particular interest. Not only is the softening point relatively high (359°C), but no equilibrium vapor species were observed up to 500°C. Such properties are important in manufacturing infrared transmitting glasses. Judging from the behavior of the other

silicon-containing glasses, the presence of a large percentage of silicon causes the good stability properties. The $Si_{15}Te_{85}$ glass shows some instability with respect to tellurium. A one-to-one ratio of silicon to arsenic in $Si_{15}As_{15}Te_{70}$ shows the same instability, low softening point, and decomposition. Increasing the silicon concentration at the expense of tellurium apparently takes advantage of the strong Si-As bond and decreases interference in the formation of Si-Te bonds. A more extensive investigation will be necessary for an understanding of the exact nature of these interactions.

A more recent study of a Ge-Sb-Se glass may provide a better understanding of chemical bonding in infrared glasses. In this glass the major vapor phase species was GeSe, which began to vaporize about 450°C. Between 450 and 550°C analysis of the data yielded 44.5 kcal for the heat of vaporization of GeSe.

At 575°C, Ge disappeared from the vapor and Sb appeared. Subsequent emission spectroscopic analysis of the residue (after heating to 600°C) showed no germanium. All the germanium had been vaporized in the form of GeSe. The appearance temperature of Sb in the vapor corresponds almost exactly to the melting point of Sb_2Se_3. While there is no absolute proof that the source of antimony is Sb_2Se_3, it is felt that the appearance temperature is more than just coincidental with the melting point of Sb_2Se_3.

It was also noted that in $Si_{15}As_{15}Te_{70}$ and $Ge_{10}As_{20}Te_{70}$ the appearance temperature of tellurium corresponded roughly to the melting point of As_2Te_3. While it has not been possible to verify the existence of As_2Te_3, it appears that such a compound would provide a logical source of tellurium, whose appearance coincides with the melting point.

D. X-Ray Radial Distribution Analysis of Amorphous Materials

by R. D. Dobrott

1. General

It is well known that the molecular structure of compounds can be uniquely determined by x-ray diffraction analysis when the compound possesses a regular crystalline arrangement. However, a regular arrangement is not necessary to observe diffraction effects.

Debye[33] pointed out that one or two broad, diffuse diffraction bands were produced by liquids, glasses, resins, and unoriented polymers. These bands arise from the very small degree of local order which results because two atoms cannot be separated by a distance smaller than the sum of their radii. Therefore, in any solid amorphous substance each atom possesses permanent neighbors at definite distances and in definite directions. However, the vectorial properties relating an atom to its environment are usually not the same for any two atoms. Therefore, a radial distribution function, which specifies the density of atoms or electrons as a function of the radial distance from any reference atom or electron, is the maximum structural information that can be obtained from these broad, diffuse diffraction effects.

Debye[33] showed that the intensity in electron units scattered by an amorphous material at angle θ is given by

$$I = \sum_m \sum_n f_m f_n \frac{\sin s r_{mn}}{s r_{mn}} , \qquad (5)$$

where $s = \frac{4\pi \sin \theta}{\lambda}$,

f_m and f_n are the scattering factors of mth and nth atoms, and r_{mn} is the distance between these two atoms. The summation is taken over all pairs of atoms in the assemblage. The Fourier integral theorem can be applied in the case where there is only one kind of atom. If the number of atoms is N, equation (5) becomes

$$I = Nf^2 \sum_n \frac{\sin s r_{mn}}{s r_{mn}} , \qquad (6)$$

where it is assumed that the environment of one atom is the same as that of any other atom. Then by standard Fourier transform methods the radial distribution function can be computed by

$$4\pi r^2\rho(r) = 4\pi r^2\rho_o + 2r/\pi \int s\left(\frac{I-Nf^2}{Nf^2}\right) \sin rs\, ds, \qquad (7)$$

where $4\pi r^2\rho(r)$ is the number of atoms at distance r from any atom and ρ_o is the average density of atoms in the sample. For atoms of more than one kind the intensity equation [equation (5)] will only reduce to

$$I = N\left[\sum_m fm^2 + \sum fm \int 4\pi r^2\rho_m(r) \frac{\sin s\, r}{s\, r}\, dr\right],$$

which unlike form (6) cannot be directly inverted by the Fourier integral theorem technique, since $\rho_m(r)$ here is a function of s. An approximation using an average atom when the atomic numbers are not too widely separated does sometimes yield useful results. The main difficulty in this method consists in the exact measurement and normalization of the intensity distribution.

2. Application to Non-Oxide Glasses

X-ray intensity measurements are taken using a standard para-focusing Norelco wide range goniometer. A curved LiF crystal monochromator is used in the diffracted beam to exclude any x-radiation from fluorescence of the sample. Molybdenum radiation is used so data can be collected out to large values of s. The data are collected in air, and the air scattering is assumed to be negligible compared with the scattering by the heavy elements of these glasses. The scattered intensity was corrected for polarization by the factor

$$\frac{1 + \cos^2 2\theta' \cos^2 2\theta}{1 + \cos^2 2\theta'}$$

where θ' is the Bragg angle of the monochromator and θ is the Bragg angle of the specimen.

The incoherent scattering intensity was approximated by

$$I_{inch} = Z - (f^2/Z) \quad ,$$

where Z is the atomic number of the element and f is the normal scattering factor. The relative scattering power for different atomic pairs for Si-As-Te and Ge-As-Te glasses are given in Table XXXII. The intensity distribution was normalized by fitting the observed distribution to the theoretical coherent plus incoherent distribution from $\sin\theta/\lambda = 0.8$ to 1.1. The observed intensity distribution above $\sin\theta/\lambda = 1.1$ was discarded because it contained several false maxima.

Figure 51-55 show the radial distribution functions for the glass systems $SiTe_4$, $Si_{15}As_{15}Te_{70}$, $Si_{15}As_{45}Te_{40}$, $Si_{30}As_{15}Te_{55}$, and $Ge_{15}As_{45}Te_{40}$. All the radial distribution functions shows maxima at values of R less than 2 Å which are necessarily false. This false detail arises from series termination errors and errors resulting from the average atom technique.

The area ratio $R_I:R_{II}$ yields the most useful information. The results obtained for the glass systems studied are shown in Table XXXIII. In the $SiTe_4$ glass the 1:8 ratio can only be explained if R_I consists of as many Si-Te bonds as possible, with the excess Te forming Te-Te bonds, while R_{II} consists mainly of Te---Te interactions. This assumption would yield a high $R_I:R_{II}$ ratio, since the Si-Te interaction has only about one-fourth the scattering power of a Te-Te interaction. As shown earlier under infrared results, the radial distances correspond to an arrangement similar to

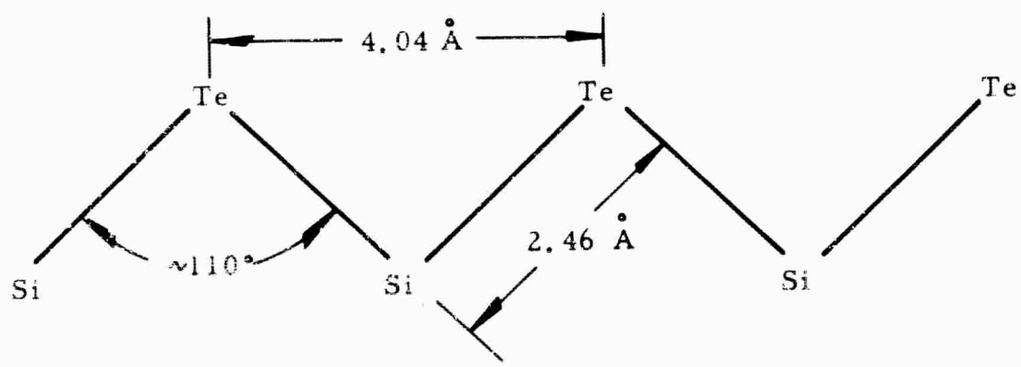

TABLE XXXII

Relative Scattering Power Between Various Atomic Interactions

	$\overline{f_i f_i}$
Si-Si	196
Si-As	462
Si-Te	730
As-As	1040
As-Te	1664
Te-Te	2700
Ge-Ge	1020
Ge-As	1060
Ge-Te	1760

TABLE XXXIII

Radial Distribution Areas for Si-As-Te and Ge-As-Te Glasses

	$\overline{R_I}$	$\overline{R_{II}}$	$\overline{R_I : R_{II}}$
$SiTe_4$	2.62 Å	4.14 Å	1:8
$Si_{15}As_{15}Te_{70}$	2.58	4.12	1:12
$Si_{15}As_{45}Te_{40}$	2.52	3.95	1:5
$Si_{30}As_{15}Te_{55}$	2.50	4.12	1:4
$Ge_{15}As_{45}Te_{40}$	2.50	4.02	1:4

Note: R_I and R_{II} are distances for nearest and second neighbor interactions from the radial distribution function. $R_I : R_{II}$ is the area ratio between nearest neighbor peak and second neighbor peak.

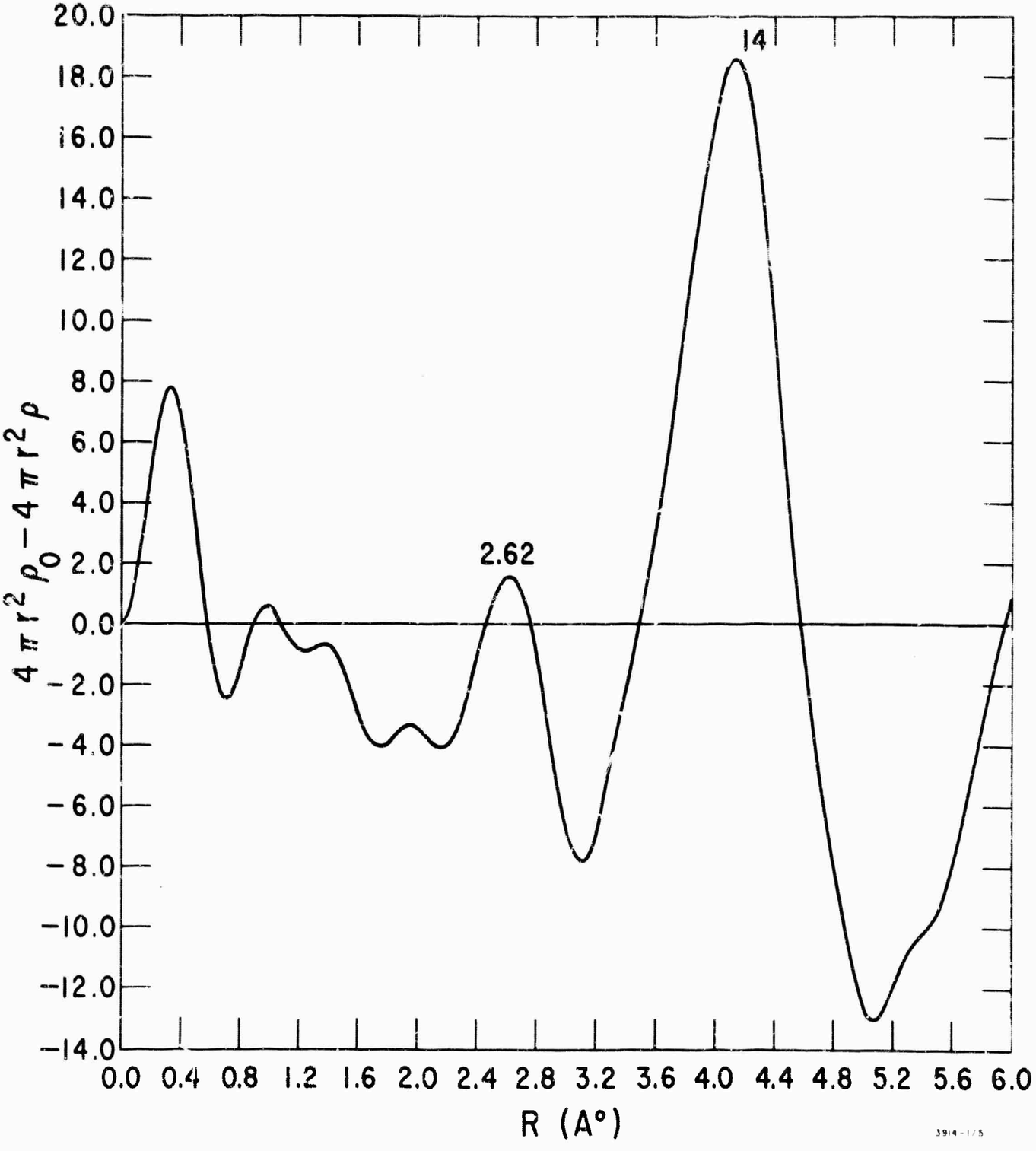

Figure 51 Radial Distribution Function of $SiTe_4$ Glass

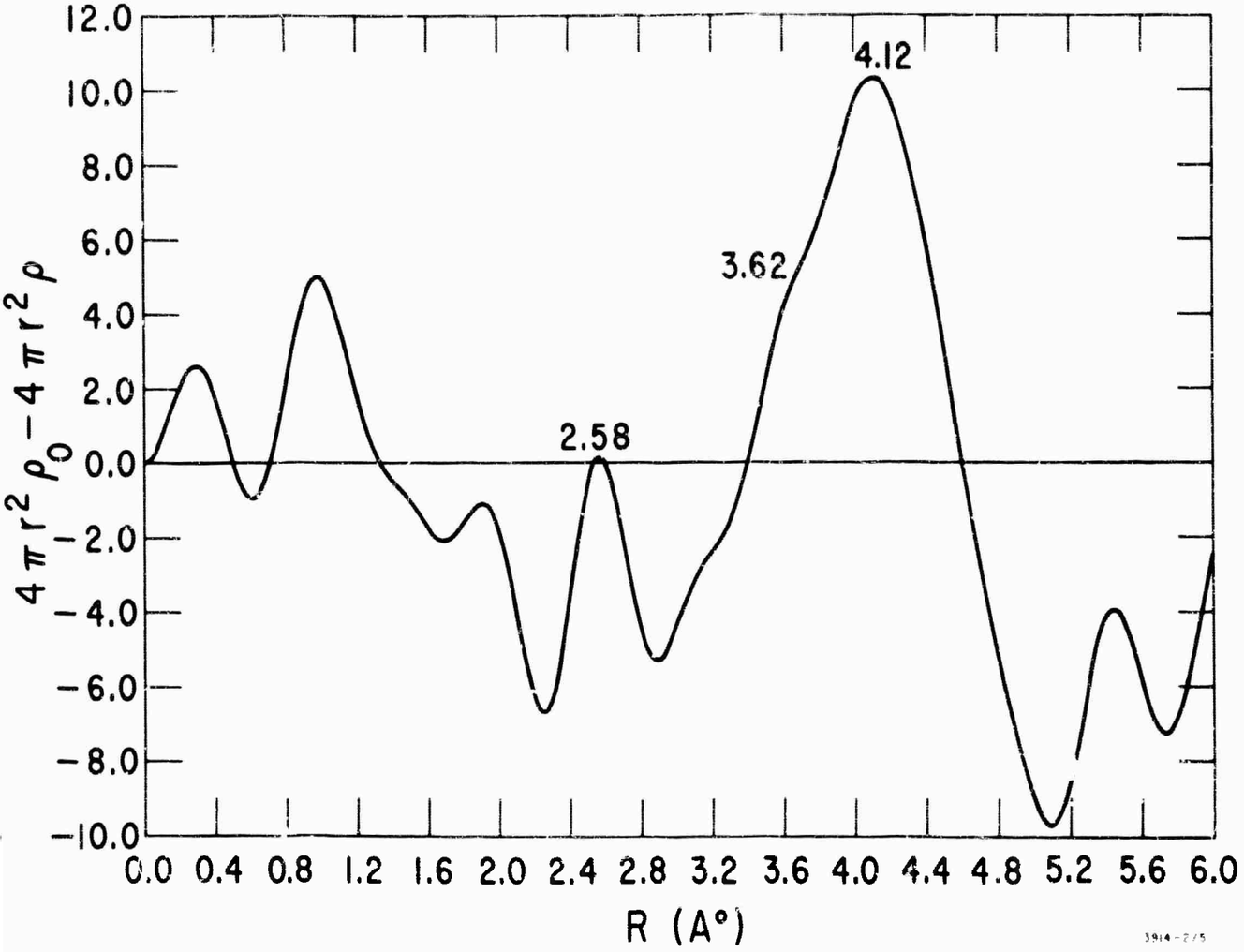

Figure 52 Radial Distribution Function of $Si_{15}As_{15}Te_{70}$ Glass

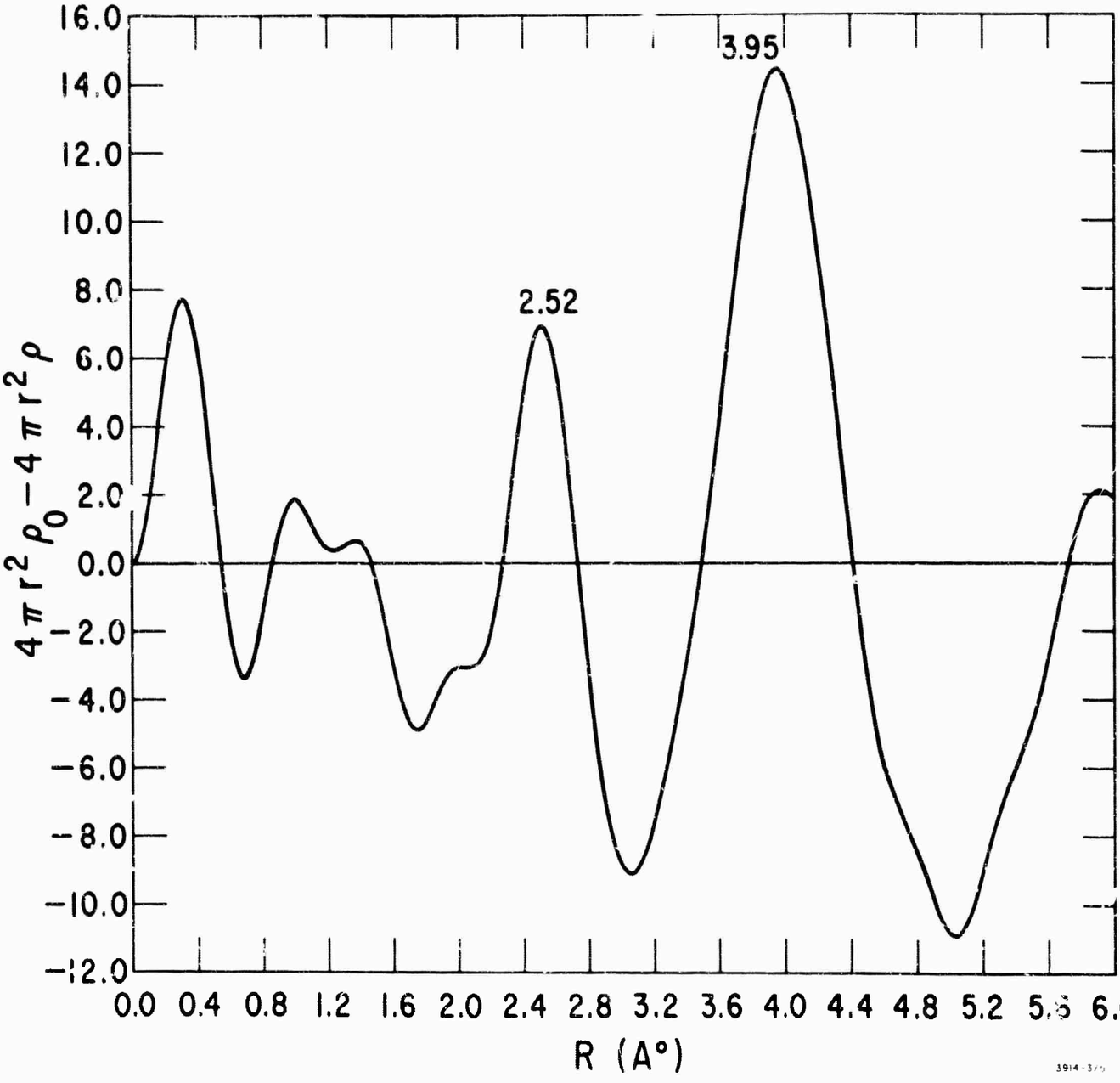

Figure 53 Radial Distribution Function of $Si_{15}As_{45}Te_{40}$

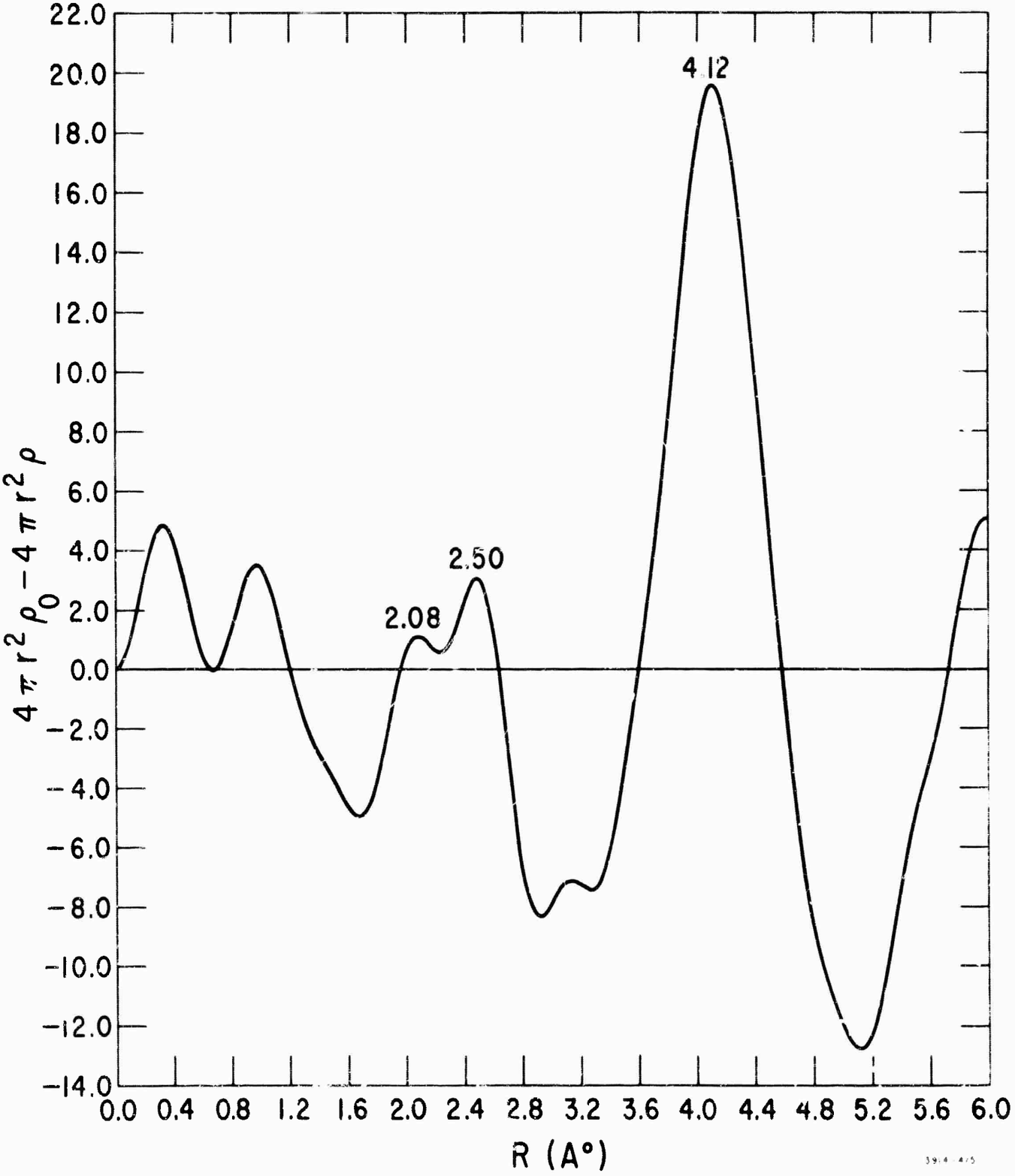

Figure 54 Radial Distribution Function of $Si_{30}As_{15}Te_{55}$

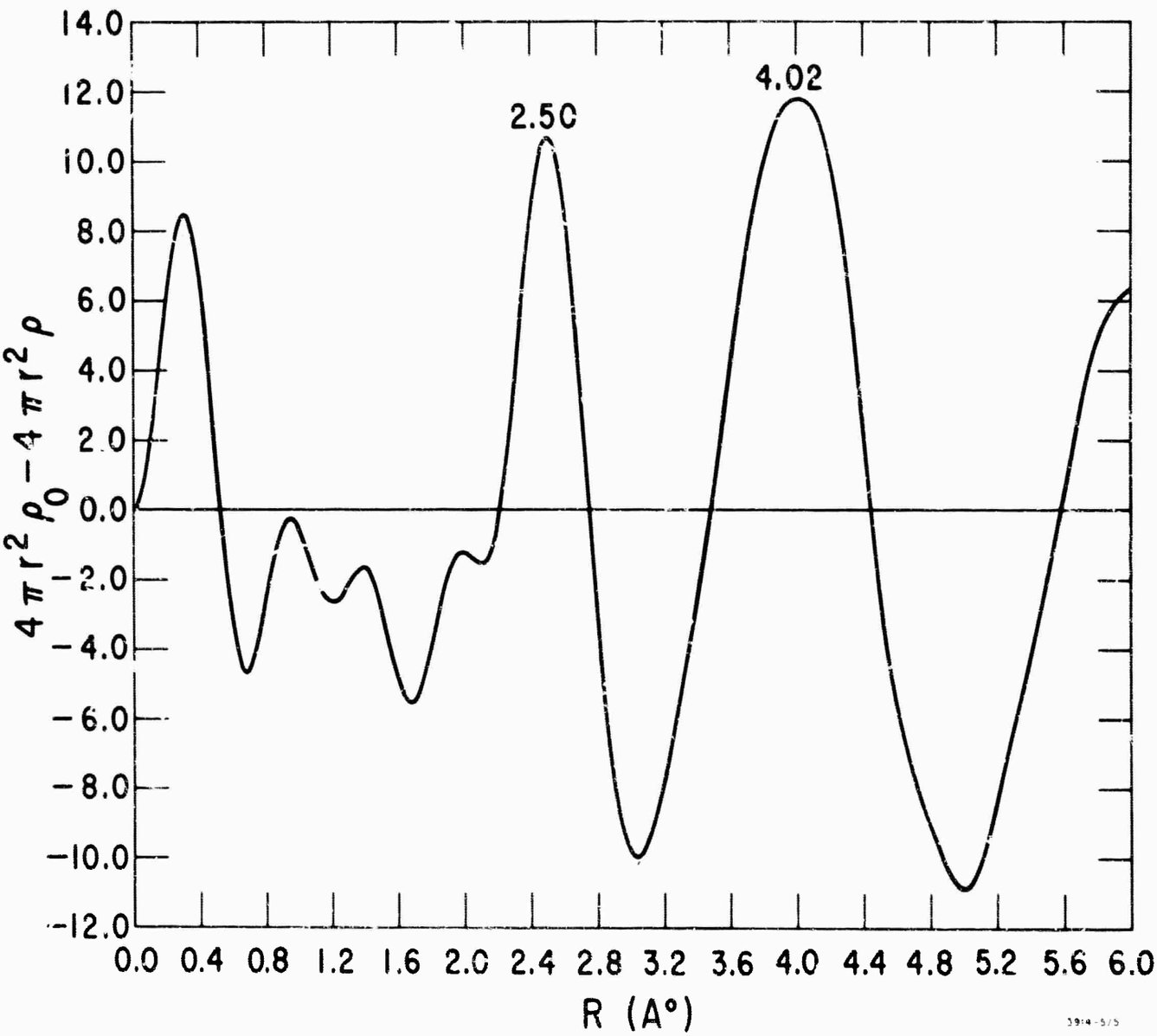

Figure 55 Radial Distribution Function of $Ge_{15}As_{45}Te_{40}$ Glass

The calculated interatomic distances used in explaining the radial distribution data are given in Table XXXIV. The Te---Te second nearest neighbor interaction is the same distance observed in crystalline Te. The $R_I:R_{II}$ ratio of 1:12 observed for the $Si_{15}As_{15}Te_{70}$ glass is evidence for the formation of Si-Te and As-Te bonds. When these bonds form, Te-Te bonds are broken, thus decreasing the amount of R_I observed. These same Te atoms, however, would still show the R_{II} scattering. Thus, the $R_I:R_{II}$ ratio decreases substantially. In addition, a shoulder appears at 3.62 Å on the second neighbor interaction, probably indicating some As---As and As---Te second neighbor interaction. The $Si_{15}As_{45}Te_{55}$ glass contains an excess of As, so the low ratio of 1:5 here indicates a fair number of As-As bonds, probably in As tetrahedra. Also, the low 1:4 ratio for the $Si_{30}As_{15}Te_{55}$ glass supports the conclusion that Te-Te bond are not present unless there is an excess of Te. This latter $Si_{30}As_{15}Te_{55}$ distribution shows a prominent peak at 2.08 Å that we are unable to explain. This peak could conceivably arise from Si-Si bonds forming, or from some contamination in the sample. The only Ge glass completed, $Ge_{15}As_{45}Te_{40}$, fits this same conclusion; Ge-Te shows a stronger scatter than Si-Te, and hence the $R_I:R_{II}$ ratio increased to 1:4.

The only structural conclusion which can be drawn from this x-ray study is that Si-Te, Si-As, and As-Te bonds are formed wherever possible in preference to Si-Si, As-As and Te-Te bonds. Many more glasses in this series must be studied before knowledge of additional structural features could be gained. At best, the results could only be qualitative, since the atomic numbers of the elements are too widely spearated to use an average atom. However, we believe the peak positions and area ratios obtained are accurate, since these results lead to the same conclusions reached by infrared and mass spectrographic techniques.

E. Summary of Structural Information

From all the facts available, the following statements can be made about the Si-As-Te and Ge-As-Te glasses.

TABLE XXXIV

Calculated Bond Distances From Covalent Radii

	Å
Si-Si	2.22
Si-As	2.30
Si-Te	2.46
As-As	2.38
As-Te	2.54
Te-Te	2.70
Ge-Ge	2.45
Ge-As	2.42
Ge-Te	2.57

1. Zigzag chains of Si-Te and Ge-Te form in Si-As-Te and Ge-As-Te glasses. X-ray and infrared data support this conclusion.

2. Three types of arsenic are found.

a. Arsenic bonded to tellurium. The appearance temperature for tellurium corresponds to the melting point of As_2Te_3. The disappearance of the R_1 (tellurium) peak when arsenic is added indicates the formation of As-Te bonds.

b. Free arsenic existing as molecules. The evolution of arsenic at the softening point of the glass supports this statement. The locations of the glass-forming regions indicate free arsenic dissolved in the molten glass.

c. Arsenic bonded to the group IVA elements silicon and germanium. The location of the glass-forming composition region is affected by the formation of Si-As and Ge-As bonds. These bonds are stable at high temperature. When the glass is quenched, they become unstable. Small amounts of heat allow dissociation and the production of unbonded arsenic in the glass. As the temperature is raised, the As-IVA bonds become thermodynamically stable again, and they reform.

3. In addition to the primary bonding found in the zigzag chains, weaker, more distant bonding interactions take place between silicon and germanium with tellurium. The interaction is stronger between germanium and tellurium than between silicon and tellurium. Evidence for this fact is that the heat of vaporization is higher for tellurium in Ge-As-Te glasses than in Si-As-Te or Si-Te glasses. Further evidence is that as a rule, Ge-As-Te glasses fall above the density vs molecular weight curve. That is, Ge-Te glasses form a bit closer, denser glass structure.

A truly quantitative structural model of a specific Si-As-Te or Ge-As-Te glass composition could be obtained by applying the now-developed structural techniques repeatedly on many different samples. Reproducibility would be en-

hanced as experimental errors were reduced or eliminated. As confidence in the results grew, refinement in the interpretation could be made. Although such a study would be satisfying from the investigator's standpoint, it would not add significantly to the molecular structure picture already obtained. As composition changes, the average structure changes. More important than a specific average structure for a specific composition is a general idea of the type of chemical bonding present and how this bonding affects the glass properties.

IV. CONCLUSIONS

1. The glasses from seven ternary systems containing elements from the IVA, VA, and VIA group were evaluated as high temperature infrared optical materials. Glasses from the Si-As-Te, Ge-As-Te, and Ge-P-Te systems show the best infrared transmission of all in the 8 to 14 micron region. Attempts to form glasses from systems based on tin or boron failed. The effects on glass properties produced by individual elements were studied using four-component glasses formed as a blend between two ternary systems. As a group of materials, the non-oxide chalcogenide glasses can be characterized as soft, weak, low softening glasses with large thermal coefficients of expansion.

2. Properties of a specific glass composition are determined by the individual constituent elements present in the composition and their relative amounts. In a ternary system the relative amount of each element that can be present is determined by the location of the glass-forming composition region. The location and size of the glass-forming region depend on the number of binary compounds that can form in the ternary system.

3. The non-oxide chalcogenide glasses are characterized by covalent bonding. By using a molar refraction approach and the covalent radius of each constituent element, one can predict the non-dispersive refractive index of a specific glass composition within a few percent.

4. Almost all the undesirable absorption for wavelengths less than 25 microns are caused by trace impurities of metal oxides.

5. Non-oxide chalcogenide glasses containing group IVA elements are harder and stronger and have higher softening points than glasses containing group VA elements. Results obtained in a structural investigation of the physical and chemical nature of the glasses using x-ray diffraction, infrared spectroscopy and mass spectrometry indicate the group IVA elements silicon and germanium

form zigzag chains with the chalcogens, while the group VA elements form small molecules which are contained within a chalcogen network. In Si-As-Te and Ge-As-Te glasses arsenic is found as unbonded arsenic and arsenic bonded to tellurium. At high temperatures, arsenic forms bonds with silicon and germanium. In glasses containing only arsenic, with no group IVA element present, pyramidal molecules form. More than one type of bond forms between tellurium with silicon and germanium.

REFERENCES

1. R. Frerichs, Phys. Rev. 78, 643 (1950).

2. R. Frerichs, J. Opt. Soc. Am. 43, 1153 (1953).

3. W. A. Fraser and J. Jerger, Jr., J. Opt. Soc. Am. 43, 332 (1953).

4. C. J. Billian and J. Jerger, Jr., Servo Corporation of America, Final Technical Report, Contract No. Nonr 3647(00), January 2, 1963.

5. J. Jerger, Jr. and R. Sherwood, Servo Corporation of America, Final Technical Report, Contract No. Nonr 4212(00), August 1964.

6. J. Black, E. M. Conwell, L. Sleigle, and C. W. Spencer, J. Phys. Chem. Solids 2, 240 (1957).

7. A. David Pearson, Modern Aspects of the Vitreous State (Buttersworth, Washington, 1964), Vol. 3, pp 29-58.

8. J. A. Savage and S. Nielsen, Physics and Chemistry of Glasses 5, 82-86 (1964).

9. S. Nielsen, Infrared Physics 2, 117 (1962).

10. J. T. Edmond, A. Anderson, and H. A. Gebbie, Proc. Phys. Soc. 81, 378 (1963).

11. J. T. Edmond and W. W. Redfearn, Proc. Phys. Soc. 81, 380 (1963).

12. The Structure of Glass, Volume 2, Proceedings of the Third All-Union Conference on the Glassy State, Leningrad, 1959 (Consultants Bureau Enterprises, New York, 1960).

13. B. T. Kolomiets, Phys. Stat. Sol. 7, 359 (1964); Phys. Stat. Sol. 7, 713 (1964).

14. R. I. Myuller, L. A. Bardakov, and Z. U. Borisova, J. Univ. of Leningrad 10, 94-101 (1962).

15. A. R. Hilton and M. J. Brau, Infrared Physics 3, 69-76 (1963).

16. A. R. Hilton, C. E. Jones, and M. J. Brau, Infrared Physics 4, 213-221 (1964).

17. T. S. Moss, Optical Properties of Semiconductors (Academic Press Inc., New York, 1959).

18. Max Hansen, Constitution of Binary Alloys, Second Edition (McGraw Hill Book Co., Inc., New York, 1958).

19. Handbook of Chemistry and Physics, 39th Edition, 1957-1958 (Chemical Rubber Publishing Co., Cleveland, Ohio).

20. Rowland E. Johnson, Robert Patterson, and Maurice J. Brau, Texas Instruments Incorporated, unpublished work.

21. Louis G. Bailey, Texas Instruments Incorporated, unpublished work.

22. W. A. Weyl and E. C. Marboe, The Constitution of Glasses: A Dynamic Interpretation (Interscience Publishers, New York, 1962), Vol. I, p. 61

23. Gerhard Herzberg, Molecular Spectra and Molecular Structure; II Infrared and Raman Spectra of Polyatomic Molecules, D. Van Nostrand Company, Inc., Princeton, New Jersey, 1956)

24. W. Kaiser, P. H. Keck, and C. F. Lange, Phys. Rev. 101, 1264 (1956).

25. A. Smakula and J. Kalnags, J. Phys. Chem. Solids 6, 46-50 (1958).

26. W. Kaiser and P. H. Keck, J. Appl. Phys. 28, 882 (1957).

27. Scott Anderson, J. Am. Ceram. Soc. 33, 45 (1950); Scott Anderson, Robert L. Bohon, and Dudley D. Kimpton, J. Am. Ceram. Soc. 38, 370 (1955).

28. Walter Gordy, J. Chem. Phys. 14, 305 (1946).

29. G. R. Somayajulu, J. Chem. Phys. 28, 814 (1958).

30. Professor Heinz Krebs, Lehrstuhl für Anorganische Chemie der Technischen Hochschule, Stuttgart, Germany (Visiting Scientist at Texas Instruments Summer of 1964), unpublished work.

31. "Fourth Semiannual Technical Summary Report for New High Temperature Infrared Transmitting Glasses," Contract Nonr 3810(00), Texas Instruments Incorporated, May 1965.

32. A. Glassner, "The Thermochemical Properties of the Oxides, Fluorides, and Chlorides to 2500°K", U. S. Government Printing Office, Washington, D. C. (ANL-5750)

33. P. Debye, Ann. Physik 46, 809 (1915).

APPENDIX I

FORMATION OF NON-OXIDE CHALCOGENIDE GLASSES*

The glass-forming composition regions for the glass system $A_x^{IVA}B_y^{VA}C_z^{VIA}$ evaluated under this contract are shown in Figures 1, 2, and 3. Also included are the Si-As-Te system evaluated prior to the contract[1] and the Ge-As-Se system reported by Jerger, et al.,[2] of Servo Corporation.

Figure 1 shows a direct comparison between the glass-forming composition ares of the system Ge-P-S, Ge-P-Se, and Ge-P-Te. The glass-forming area decreases going from S → Se → Te. A direct comparison of Si and Ge is made in Figure 2 by the systems Si-As-Te, Ge-As-Te, Si-P-Te, and Ge-P-Te. The remaining systems Si-Sb-S, Si-Sb-Se, and Ge-As-Se are shown in Figure 3. The direct comparison of As and P can be obtained by comparing the composition area of Ge-As-Se (Figure 3) to Ge-P-Se (Figure 1).

From studying these diagrams the following conclusions can be drawn.

(1) For the formation of a glass, it is normally necessary that a greater amount of the divalent element (C^{VIA}) be present.

(2) As the atomic number of the constituent elements increases in the series Si, Ge, Sn or P, As, Sb or S, Se, Te, the glass-forming composition range decreases. The element As is an exception to this rule. The conclusion concerning Sn is based on very limited data. As reported earlier[3] most Sn compositions form crystalline solids.

Similar conclusions are given in the literature concerning the glass-forming ease of these elements,[4] but the reasons for their relative order has not been given. These relationships can be explained as follows.

(1) Most of the atoms in these glasses are normally bonded together in some form of amorphous network, as directly evidenced by the relatively high softening

*Contributed by Professor Heinz Krebs, Lehrstuhl für Anorganische Chemie der Technischen Hochschule. Stuttgart, Germany. Visiting scientist at Texas Instruments, summer 1965.

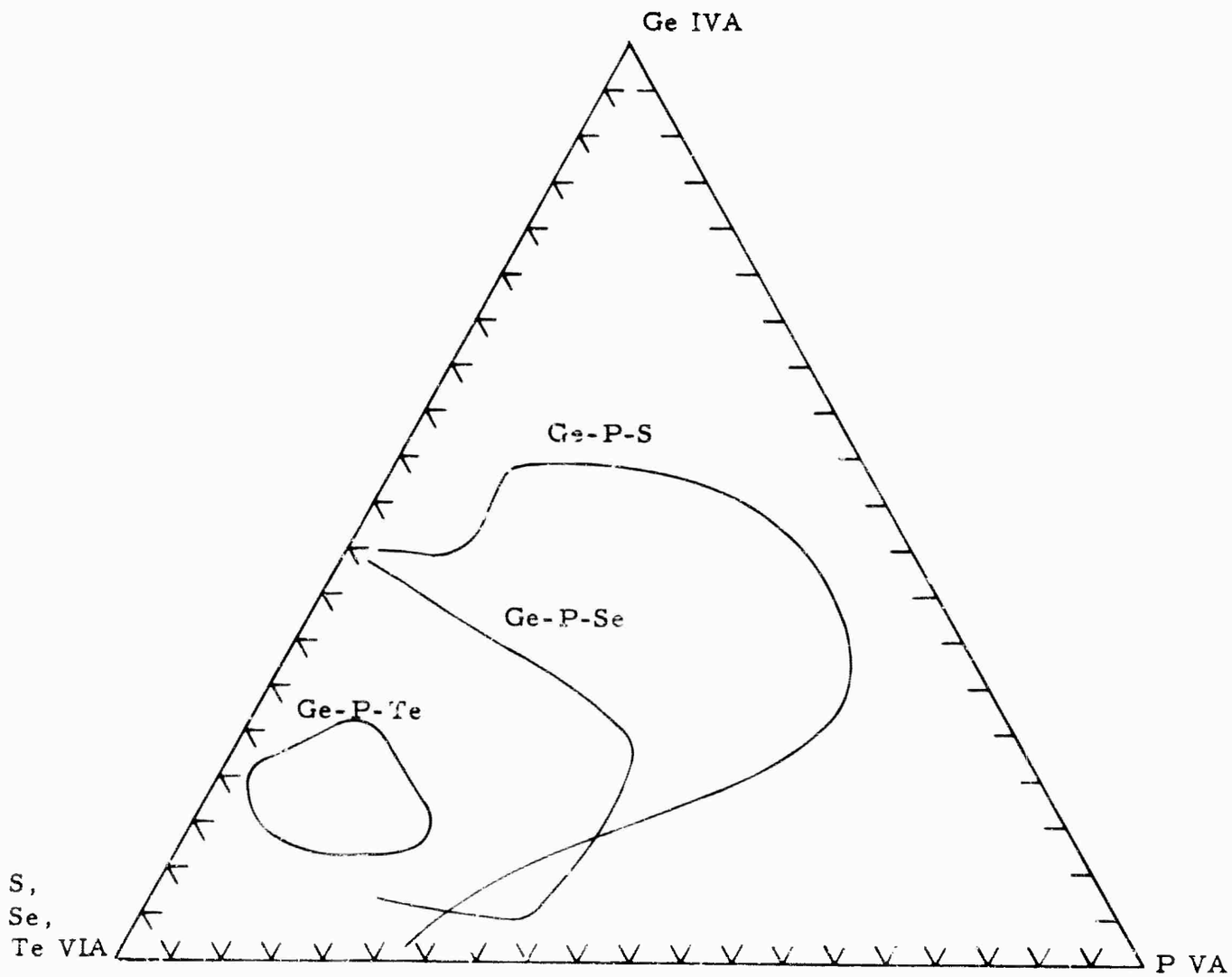

03243-12/12

Fig. 1 A Comparison of the Glass-Forming Composition Region of Ge-P-S, Ge-P-Se, and Ge-P-Te

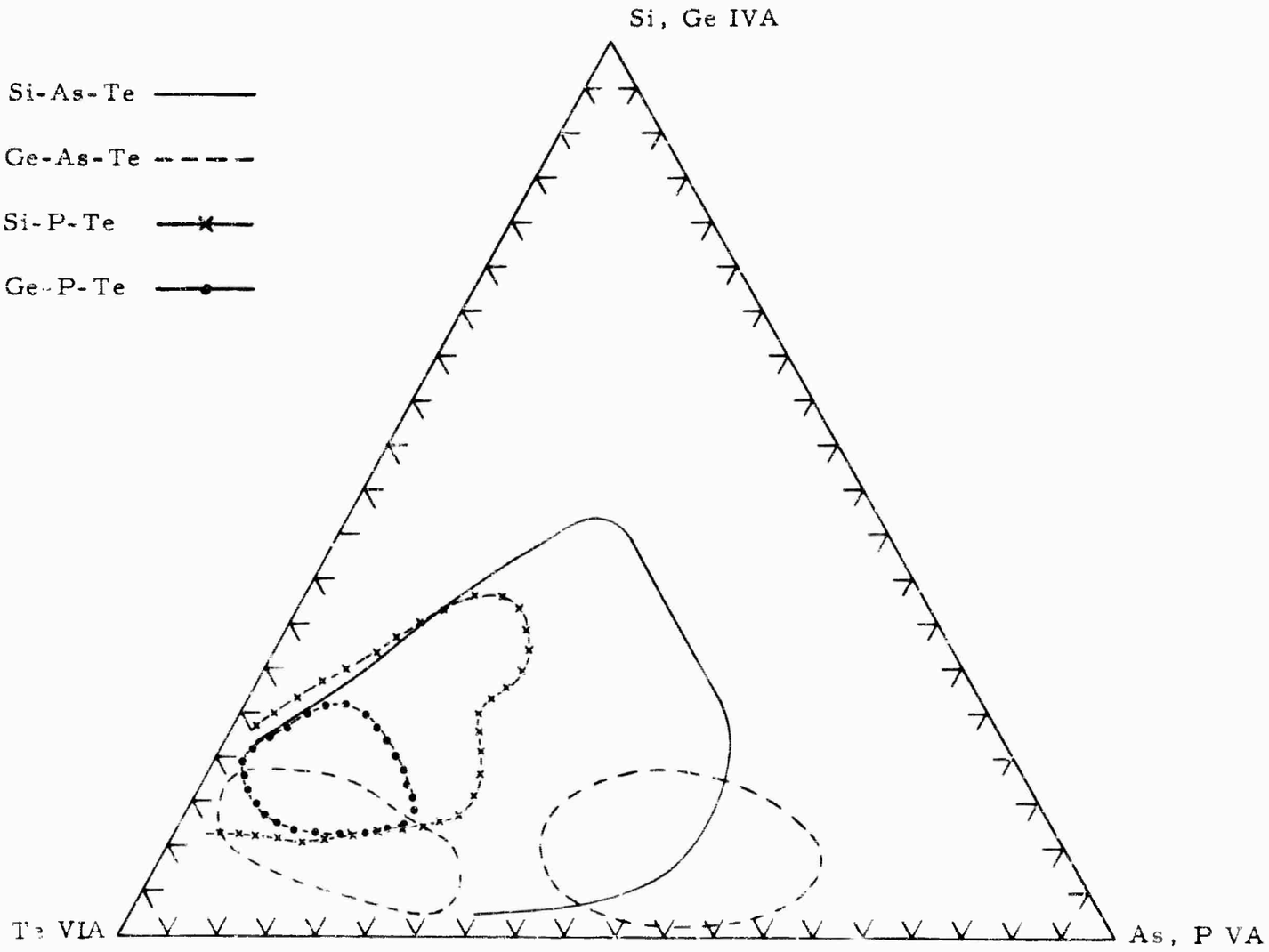

03243-10/12

Fig. 2 Comparison of the Glass-Forming Composition Regions of Si-As-Te to Ge-As-Te and Si-P-Te to Ge-P-Te

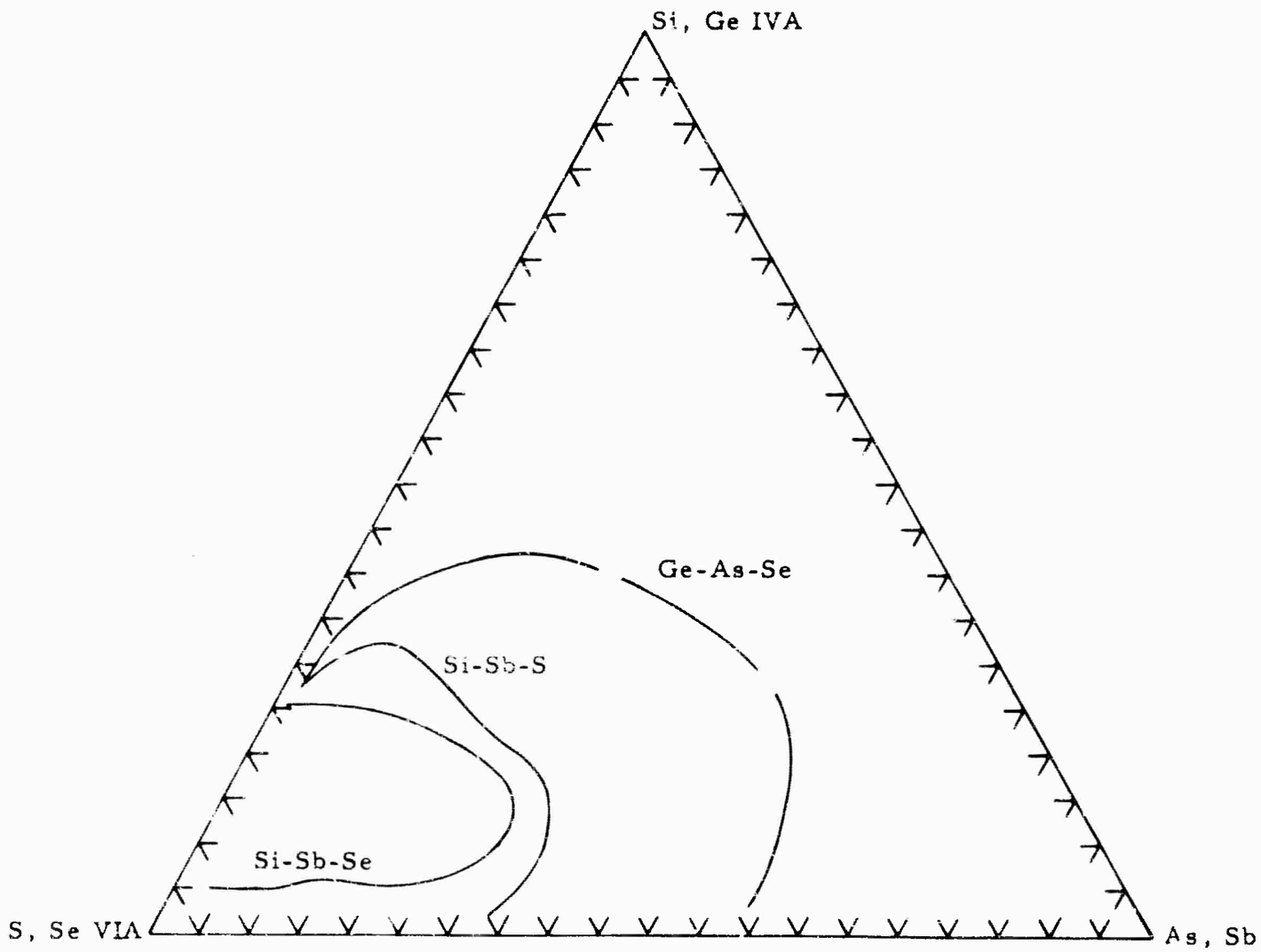

03243-11/12

Fig. 3 Glass-Forming Composition Region of the Systems Si-Sb-S, Si-Sb-Se and Ge-As-Se

points of the glasses. When the constitutent elements of the glass are light elements such as P and S, small molecules of P and S can easily form and fit into the cavities of the network. These molecules occupy positions in the glass similar to those of plasticizers in plastics. The small molecules of P_4S_3, P_4S_5, P_4S_7, and P_4S_{10} are easily formed by P and S, and they readily form crystals from the molten state. For this reason it is not possible to form a glass from P and S in th composition range about P_2S_3. In the system As and S, the formation of As_4S_4 (realgar) is well known. In glasses containing As and S, or P and S it should always be kept in mind that such molecules form and influence the properties of the glass. Small molecules will lower the softening point of the glass. As the tendency toward forming small molecules decreases, the softening point increases. The extent of small molecule formation may be decreased by holding a glass at its softening point for periods of time. At temperatures above the softening point the tendency towards small molecule formation is greater.

(2) The tetravalent elements (A^{IVA}) in the pure state do not form a glass because the bonding requirements can be fully satisfied only in a tetrahedrally ordered network (a crystalline lattice). If Ge is evaporated onto a plate, a layer of glassy Ge forms in which the valence requirements of some of the Ge atoms are not fully satisfied. These atoms may have a radical-like nature. They catalyze the transformation of the unordered network into the ordered network of the thermodynamically favored crystalline form when the temperature is raised to 400°C.[5]

The elements P, As, and Sb do not form a glass from the molten state. Glasses
b VA can be formed, as in the case of Ge, by evaporation and condensation. Normally, red P is prepared by heating white P. A polymerization of the P_4 molecules takes place, forming the highly polymerized network of red P. The red P begins to crystallize at 450°-550°C. The glassy form of As transforms into the crystalline α modification (metallic arsenic) at 270°C, and Sb transforms into the metal at room temperature.

The increased tendency toward crystallization with increasing atomic number has two causes. First, the strength of the bonds will decrease with atomic number, facilitating dissociation and resultant rearrangement and crystallization.[6] Second, as the atomic number increases, the metalloids tend to form bonds with more atoms than correspond to their normal valency; thus, their coordination number increases.

Characteristically, Sb in the non-ordered network structure (explosive antimony) as well as in the ordered crystalline network (antimony metal) has three neighbors at a short bond distance and three (or two) neighbors at a little greater bond distance (greater by ~ 20%). In this way the molecular arrangement becomes that of a distorted octahedron.[7-9] Figure 4 is a diagram of this arrangement. The short bonds (favored) are indicated by the solid lines and the longer bonds (unfavored) by the dashed line. The strength of the normal bonds decreases when additional bonds are formed in the backward direction. Because of this ability to form additional bonds, the heavier elements such as Sn, Sb, and Te can move easily from site to site in the solid as the strength of the bonds changes in different directions as a result of thermal motion of the atoms. Such a process has a very small activiation energy. The thermal energy needed for such a rearrangement process is available at relatively low temperatures. With the light elements, such as S, dissociation occurs before rearrangement is possible.

The pyramidal type arrangement of the bonds of the three valent elements (B^{VA}) does not allow much mobility of the atoms for rearrangement; therefore, the structure of the red P network or the metallic form of Sb or As is not preserved when the solid is melted. A liquid state with the same bond system form for these substances does not exist. If we melt the network of red P, depolymerization of the network occurs and P_4 molecules are formed.[6,10] Metallic Sb changes to a NaCl-type short range order[11] in which every atom is surrounded by six atoms in the form of an octahedron. The difference between the favored and unfavored bond is smeared out. In the melt, the network structure of the solid is changed to a coordination picture which reflects the metallic character of the liquid state.[8] What happens if As is melted is not known.[10]

● DISTORTED OCTAHEDRON

○ REGULAR OCTAHEDRON

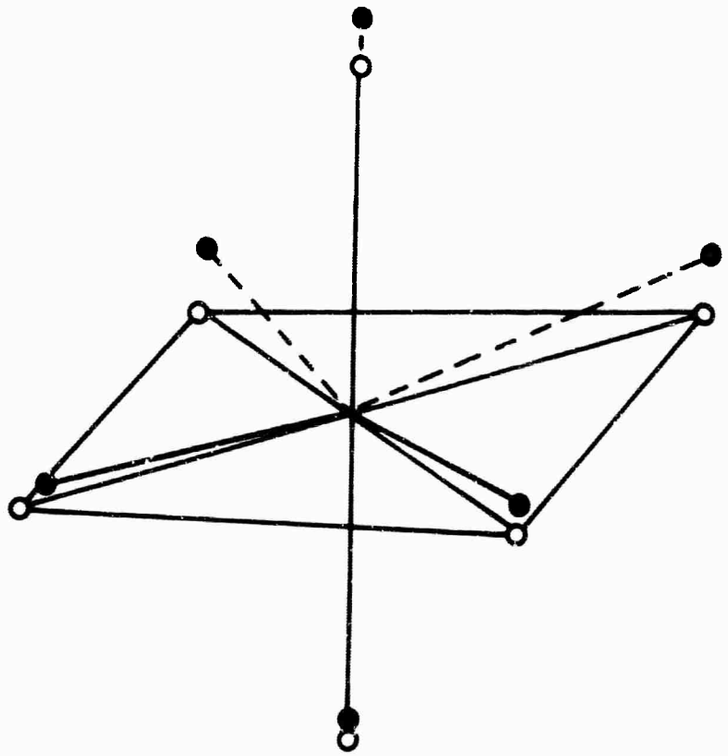

03243-9/12

Fig. 4 Distorted Octahedron Produced by Additional Bonding

Atoms of the elements S or Se are very mobile. They form only two bonds separated by the bond angle 102°-105°. In the melt, low and high molecular weight rings form.[6,12] The low molecular weight rings are mobile in the melt because of their small size. The high molecular weight rings are able to change their shape in the melt because of free rotation around each bond. Their shape is like a long fiber closed in a ring which is free to move and change its shape. The atoms are therefore mobile in both the small and the large rings. This melt of high and low molecular weight rings will form a glass when it is cooled because the rings of different sizes cannot be ordered together to form a crystal.

The bonding system of a glass will have to be essentially the same as that of the liquid from which it forms. Excluding the formation of the unfavored additional bonds of the heavy elements, the atoms of the non-oxide chalcogenide glasses must be connected so that every atom is bonded with the proper number of other atoms to satisfy its valence requirements. A melt with a sufficient amount of network-forming character is possible only if a large number of the divalent atoms are present. The divalent atoms produce the necessary mobility of atoms in the melt. This is why the non-oxide chalcogenide glasses form only when large amounts of S, Se, or Te are present. The same factors apply to glasses formed from the monovalent halogens.

From a consideration of all these factors, the decreasing glass-forming tendency in the series S, Se, Te or P, As, Sb or Si, Ge, Sn can be explained in the following way.

(1) The decrease in binding energy with increasing atomic weight makes breaking of bonds easier; therefore, rearrangement and crystallization occur more readily.

(2) The formation of additional bonds (unfavored) by the heavier elements increases the tendency toward the rearrangement reaction. In the systems P-Te, As-Te, and Sn-Te a glass will not form from the melt,[13] because the tendency for Te to form bonds in the back direction is too great. Addition of the tetravalent (A^{IVA}) network-forming atoms compensates this tendency and produces a glass.

(3) If not enough divalent atoms (C^{VIA}) are present, the atoms in the melt are forced toward higher coordination numbers. The difference between the favored and the unfavored bonds is smeared out to a certain extent. Normal octahedrons can form around the atoms, especially the heavier elements. As the melt is cooled, the regular octahedron is not stable. Rearrangement must occur, and the more favored crystalline form results.

The large area for the Si-As-Te system is surprising. It probably results from the fact that Si forms compounds with As but not with P or Sb.[14] The Si is probably not bonded to the P or Sb in the systems Si-P-Te, Si-Sb-S, and Si-Sb-Se but is only bonded to the S, Se, or Te. Thus, a network structure is more difficult to form. The ability to form Si-As bonds as well as Si-Te bonds produced a wide glass-forming composition range. The same remarks can be applied to the Ge glasses. The Ge-As-Te glass-forming composition region is much larger than that of the Ge-P-Te system.

APPENDIX REFERENCES

1. A. Ray Hilton and Maurice J. Brau, Infrared Physics 3, 69 (1963).

2. "Longwavelength I. R. Transmitting Glasses," prepared by J. Jerger, Servo Corporation of America, ASD-TDR-63-552, June 1963.

3. "Third Semiannual Technical Summary Report for New High Temperature Infrared Transmitting Glasses," Contract Nonr 3810(00), Texas Instruments Incorporated, Report No. 08-64-78, May 1964.

4. B. T. Kolomiets, N. A. Goryunova, and V. P. Shilo, Proceedings of the Third All Union Conference on the Glass State, Leningrad, 1959. Consultants Bureau, New York (1960), p. 410.

5. J. R. Parsous and R. W. Balluffi, J. Phys. Chem. Solids 25, 263 (1964).

6. H. Krebs, Angew. Chemie 65, 293 (1953)

7. H. Krebs, Acta Cryst. 9, 95 (1955).

8. H Krebs, The International Conference on Coordination Chemistry, Detroit, Michigan (1961). "Advances in the Chemistry of the Coordination Compounds," (McMillan Co., New York, 1961).

9. H. Krebs and W. Steffen, Z. Annorg. Allgem. Chemie 327, 224 (1964).

10. W. Klemm, Proc. Chem. Soc., 329 (1958). W. Klemm, H. Niemann, and H. Spitzer, Angew. Chemie 72, 985 (1960), and 75, 508 (1963).

11. H. K. F. Muller and H. Hendus, Z. Naturforsch. 12A, 102 (1952).

12. H. Krebs, Z. Naturforsch. 12B, 795 (1952).

13. N. A. Goryunova, B. T. Kolomiets and V. P. Shilo, Soviet Phys. - Tech. Phys. 3, [5], 912 (1958). Proceedings of the Third All Union Conference on the Glass State, Leningrad (1959). Consultants Bureau, New York (1960), p. 58.

14. M. Hansen, Constitution of Binary Alloys (McGraw Hill Book Co., New York, 1958) p. 1124.

APPENDIX II

CONTRIBUTORS TO THIS PROGRAM

Professionals

A. Ray Hilton
Charlie E. Jones
Maurice J. Brau
H. Michael Klein
A. Max Bryant
Tommy George[1]
Robert D. Dobrott
C. Grady Roberts[1]
Professor Heinz Krebs[2]
Edward F. Abbott
Gene F. Wakefield
Michael McNiel

Technicians

Jimmie D. Parker
Hall Jarman
Ronnie Nelms
Rod L. Doster
A. Wayne Fagan
Gene Keeney

[1] Work carried out while in Summer Development Program

[2] Visiting Scientist at Texas Instruments, summer 1964